

Durham E-Theses

Understanding cell type responses to SARS-CoV-2 coronavirus spike proteins

GRANGE, THOMAS,DANIEL

How to cite:

GRANGE, THOMAS,DANIEL (2024) *Understanding cell type responses to SARS-CoV-2 coronavirus spike proteins*, Durham theses, Durham University. Available at Durham E-Theses Online:
<http://etheses.dur.ac.uk/15600/>

Use policy

The full-text may be used and/or reproduced, and given to third parties in any format or medium, without prior permission or charge, for personal research or study, educational, or not-for-profit purposes provided that:

- a full bibliographic reference is made to the original source
- a [link](#) is made to the metadata record in Durham E-Theses
- the full-text is not changed in any way

The full-text must not be sold in any format or medium without the formal permission of the copyright holders.

Please consult the [full Durham E-Theses policy](#) for further details.

Understanding cell type responses to SARS-CoV-2 coronavirus spike proteins

Thomas Daniel Grange

Abstract: The angiotensin converting enzyme 2 (ACE2) receptor is important for the regulation of blood pressure and as an entry receptor for the SARS-CoV-2 coronavirus. ACE2 degrades the vasoconstrictive Ang II protein to assist in the maintenance of fluid homeostasis. As the entry receptor for SARS-CoV-2, ACE2 expression can predict susceptibility to infection alongside host priming enzymes including TMPRSS2. Whilst SARS-CoV-2 is largely associated with lung pathology, extrapulmonary organs including the heart, kidney and small intestine are also implicated in COVID-19. Disruption to ACE2 levels during COVID-19 is associated with exacerbated immune responses leading to the development of cytokine storms and severe disease states. In this thesis, ACE2 expression has been assessed in keratinocyte, placental and cervical carcinoma cell lines. Furthermore, the regulation of ACE2 by cytokines was also investigated. The administration of recombinant spike proteins did not alter ACE2 expression or localisation in keratinocytes, although ACE2 downregulation was indicated within placental cells, demonstrating potential cell line specific responses to SARS-CoV-2 protein. Assays were also devised to investigate downstream responses to spike proteins in HaCaT, BeWo and HeLa cell lines. The gamma, kappa and omicron spike protein variants were unable to affect the gross expression of the ACE2 receptor or cytokine responses. This thesis assesses the suitability of ACE2 antibodies for protein expression and immunofluorescence analysis and provides a basis for future investigation of SARS-CoV-2 spike responses within susceptible cell lines.

Master of Science (MSc) Thesis

**Understanding cell type
responses to SARS-CoV-2
coronavirus spike proteins**

Thomas Daniel Grange

Department of Biosciences, Durham University

June 2024

Supervisor: Professor Adam Benham

Table of contents

Section 1.0	Introduction	1
1.1	Overview of SARS-CoV-2	1
1.2	Genomic organisation of SARS-CoV-2	2
1.3	ACE2 and the RAAS	3
1.4	The SARS-CoV-2 spike protein	4
1.5	Priming of spike proteins by host factors	7
1.6	Spike-ACE2 complex formation	9
1.7	SARS-CoV-2 variants	11
1.8	SARS-CoV-2 uses ACE2 for cellular entry	15
1.9	SARS-CoV-2-mediated effects on ACE2 and the RAAS	17
1.10	Inflammatory response and cytokine storm	19
1.11	Thesis aims	20
Section 2.0	Materials and methods	21
2.1	Chemicals and reagents	21
2.2	Antibodies	21
2.3	Cell culture procedure	22
2.4	Cell treatments	22
2.5	Cell lysis	23
2.6	BCA protein assay	23
2.7	Orangu cytotoxicity assay	24
2.8	SDS-PAGE and sample preparation	24
2.9	Western blotting	26
2.10	Coomassie gel staining	27
2.11	Immunofluorescence microscopy	27

2.12 ELISA assay	28
Section 3.0 Results	30
3.1 ACE2 expression in BeWo, HaCaT and HeLa cell lines	30
3.1.1 Effects of mouse derived IFN- γ upon ACE2 expression	32
3.1.2 Human-derived IFN- γ mediates ACE2 expression	34
3.2 Synergistic effects of IFN- γ and TNF- α on ACE2 expression	37
3.3 ACE2 immunoblotting with alternative anti-ACE2 antibodies	39
3.4 Recombinant SARS-CoV-2 spike treatments do not alter ACE2 expression	40
3.5.1 ACE2 detection in HaCaT cells with immunofluorescence microscopy	42
3.5.2 ACE2 detection in BeWo cells with immunofluorescence microscopy	44
3.5.3 ACE2 detection in HeLa cells with immunofluorescence microscopy	46
3.6.1 HaCaT ACE2 localisation in response to cytokine and spike treatments	48
3.6.2 BeWo ACE2 localisation in response to cytokine and spike treatments	50
3.6.3 HeLa ACE2 localisation in response to cytokine and spike treatments	52
3.7.1 Initial assessment of cytokine and SARS-CoV-2 spike cytotoxicity	54
3.7.2 Cell viability following SARS-CoV-2 spike and cytokine treatments	56
3.8.1 SARS-CoV-2 spike treatment does not induce TNF- α production	58
3.8.2 SARS-CoV-2 spike alone does not induce TNF- α immunostimulation	60
3.9 Experimental summary	62
Section 4.0 Discussion	63
4.1 HaCaT and BeWo cell lines express ACE2	63
4.2 IFN- γ and TNF- α mediate upregulation of ACE2 expression	64
4.3 Synergistic effects of IFN- γ and TNF- α on ACE2	66
4.4 Characterisation of alternative anti-ACE2 antibodies	67
4.5 Recombinant SARS-CoV-2 spike protein does not dysregulate ACE2	68
4.6 Spike protein and cytokine treatments do not inhibit cell growth	70

4.7 SARS-CoV-2 spike variants do not affect ACE2 expression or localisation	71
4.8 SARS-CoV-2 spike protein alone is unable to stimulate TNF- α production	74
4.9 Conclusions	75
Section 5.0 References	76

List of tables and figures

Section 1.0 Introduction

Figure 1: SARS-CoV-2 virus structure and interaction with host factors	6
Figure 2: Sequence alignments for SARS-CoV-2 variant spike proteins	14

Section 2.0 Materials and methods

Table 1: Volumes of ingredients required to cast two gels for western blotting experiments	25
Table 2: Buffer solutions prepared for western blotting experiments	26

Section 3.0 Results

Figure 3: Database-derived ACE2 and TMPRSS2 expression data	31
Figure 4: ACE2 expression following murine-derived IFN- γ treatment	33
Table 3: Relative ACE2 expression for untreated (NT) and mouse IFN- γ treated (IFN- γ) cells	33
Figure 5: The effects of human IFN- γ and TNF- α upon ACE2 expression	35
Table 4: Relative ACE2 expression for untreated (NT), human IFN- γ treated (IFN- γ) and TNF- α treated cells	36
Figure 6: Cell lysate protein composition is unaffected by either IFN- γ or TNF- α treatment	36

Figure 7: Synergistic effect of IFN- γ and TNF- α on ACE2 expression	38
Figure 8: Testing alternative commercially available anti-ACE2 antibodies	38
Figure 9: SARS-CoV-2 spike protein treatments do not appear to affect ACE2 expression	41
Figure 10: Visualization of ACE2 in HaCaT cells following IFN- γ treatment	43
Figure 11: Visualization of ACE2 in BeWo cells after IFN- γ treatment	45
Figure 12: Detection of putative ACE2 in HeLa cells +/- IFN- γ	47
Figure 13: HaCaT ACE2 distribution following cytokine and spike incubation	49
Figure 14: BeWo ACE2 distribution post cytokine and spike protein treatment	51
Figure 15: HeLa ACE2 distribution after cytokine and spike protein treatments	53
Figure 16: Orangu cytotoxicity assays for cytokine and SARS-CoV-2 spike protein treatment	55
Figure 17: Cell morphology is unaffected by cytokines and the SARS-CoV-2 spike protein	57
Figure 18: Initial ELISA for SARS-CoV-2 spike induced TNF- α production	59
Figure 19: Improved ELISA for spike protein induced TNF- α secretion	61
Section 4.0 Discussion	
Figure 20: SWATH mass spectrometry workflow	73

List of frequently used abbreviations

ACE	Angiotensin converting enzyme
ACE2	Angiotensin converting enzyme 2
Ang 1-7	Angiotensin (1-7)
Ang 1-9	Angiotensin (1-9)
Ang I	Angiotensin 1
Ang II	Angiotensin 2
APS	Ammonium persulfate
ARDS	Acute respiratory distress syndrome
AT1R	Angiotensin II type 1 receptor
BCA	Bicinchoninic acid assay
BSA	Bovine serum albumin
CCL2	C-C motif chemokine ligand 2
COVID-19	Coronavirus disease 2019
DAPI	4'6-diamino-2-phenylindole
di-H₂O	Deionized water
DMEM	Dulbecco's modified eagle medium
DTT	Dithiothreitol
E	Envelope protein
ECL	Enhanced chemiluminescence solution
ELISA	Enzyme linked immunosorbent assay
ER	Endoplasmic reticulum
FBS	Foetal bovine serum
FCS	Furin cleavage site
FP	Fusion peptide

GAMPO	Goat anti-mouse polyclonal antibody
HC-10	Histocompatibility complex 10
hCoV	Human coronavirus
HRP	Horseradish peroxidase
IF	Immunofluorescence
IFN	Interferon
IFN-γ	Interferon gamma
IgG	Immunoglobulin G
IL-10	Interleukin 10
IL-1β	Interleukin 1 β
IL-4	Interleukin 4
IL-6	Interleukin 6
IL-8	Interleukin 8
ISG	Interferon stimulated gene
JAK-STAT	Janus kinase/signal transducers and activators of transcription
M	Membrane protein
mAb	Monoclonal antibody
MAPK	Mitogen-activated protein kinase
MEM	Minimum essential medium
MES	2-(N-morpholino)-ethanesulfonic acid
MHC	Major histocompatibility complex
MS	Mass spectrometry
N	Nucleocapsid protein
NF-κB	Nuclear factor kappa B
NSP	Non-structural protein
NT	No treatment (untreated)

NTD	N-terminal domain
ORF	Open reading frame
pAb	Polyclonal antibody
PBMC	Peripheral blood mononuclear (cells)
PBS	Phosphate buffered saline
PFA	Paraformaldehyde
PVDF	Polyvinyl difluoride
RAAS	Renin-angiotensin aldosterone system
RBD	Receptor binding domain
RBM	Receptor binding motif
RIG-I-MAVS	Retinoic acid-inducible gene 1-mitochondrial anti-viral signalling
S	Spike protein
S₁	Spike protein subunit 1
S₂	Spike protein subunit 2
sACE2	Soluble ACE2
SARPO	Swine anti-rabbit polyclonal antibody
SARS-CoV	Severe acute respiratory syndrome coronavirus
SARS-CoV-2	Severe acute respiratory syndrome coronavirus 2
SDS	Sodium dodecyl sulphate
SDS-PAGE	Sodium dodecyl sulphate-polyacrylamide gel electrophoresis
SP	Signal peptide
SWATH	Sequential window acquisition of all theoretical fragment ion spectra
TBS	Tris-buffered saline
TBST	Tris-buffered saline-Tween 20
TEMED	N,N,N',N'-Tetramethylethylenediamine
TGS	Tris-glycine-sodium dodecyl sulphate

TLR2	Toll-like receptor 2
TMB	3,3',5,5'-Tetramethylbenzidine
TMPRSS2	Transmembrane serine protease 2
TNF-α	Tumour necrosis factor alpha
VOC	Variant of concern
VOI	Variant of interest
VUI	Variant under investigation
WHO	World Health Organisation
δ-ACE2	Delta (truncated) ACE2 isoform

Acknowledgements

I would firstly like to thank my supervisor, Professor Adam Benham for his endless help and encouragement during this project, even in the most challenging of times. I would also wish to thank Jamie Thomas, Lucy Dan, Stephen Bell, and all the rest of the Lab 8 team who took time out of their days to teach and support me.

To my wonderful family and friends, thank you for believing in me and helping me in so many ways- I really cannot thank you enough.

Finally, I would also like to thank IBM for funding the consumables used during my project.

Statement of copyright

The copyright of this thesis rests with the author. No quotation from it should be published without the author's prior written consent and information derived from it should be acknowledged.

Declaration

I declare that the full content and all data presented in this thesis, is the result of my own work. No part of the material offered has previously been submitted for a higher degree. This body of work was achieved under the supervision of Prof. Adam M. Benham.

Thomas Grange, June 2024

Section 1.0 Introduction

1.1 Overview of SARS-CoV-2.

In December 2019, the emergence of pneumonia cases with unknown etiology in Wuhan, China represented the first cases of severe acute respiratory syndrome coronavirus 2 (SARS-CoV-2). This novel, highly pathogenic betacoronavirus is the causative agent of coronavirus disease 2019 (COVID-19) which has developed into a worldwide pandemic. SARS-CoV-2 primarily affects organs of the respiratory system, causing flu-like symptoms including a cough, fever, loss of taste or smell, fatigue and in severe cases, lung failure, septic shock, and death (Zaim et al. 2020). Surges of COVID-19 cases have led to global lockdowns, major economic damage, and a heavy human toll. As of March 19th 2023, over 760 million positive cases have been diagnosed in 228 countries and territories, with over 6.8 million deaths reported (WHO 2023).

The predominant cause of death during COVID-19 is from acute respiratory distress syndrome, ARDS (C. Huang et al. 2020). ARDS is characterised by the rapid onset of pulmonary inflammation causing a build-up of fluid within the lungs (Han and Mallampalli 2015). This prevents oxygen from reaching the lungs and subsequent hypoxemia develops. Systemic hyperinflammation resulting from exacerbated production of pro-inflammatory cytokine and chemokine signalling molecules can also lead to the development of ARDS and multiple organ failure in severe cases of disease (Ragab et al. 2020). The COVID-19 pandemic represents the 3rd severe epidemic caused by a β -coronavirus in the previous two decades, after the SARS-CoV and MERS-CoV epidemics in 2003 and 2012 respectively. This demonstrates the global threat of viral zoonotic transmission to human populations, especially within the *Coronaviridae* family.

Controversy surrounds the proximal origins of the SARS-CoV-2 virus, although there is a scientific consensus that the emergence is a result of animal-to-human interspecies transfer (J. Xu et al. 2020). The detection of an early cluster of cases linked to the Huanan market in Wuhan supports the possibility of zoonotic transfer from an animal source at this location (Andersen et al. 2020). Phylogenetic analyses have shown that the SARS-CoV-2 viral genome is closely related to that of SARS-CoV, with up to 79.5% base pair similarity (R. Lu et al. 2020). However, the SARS-CoV-2 virus exhibits greater human-to-human transmission than SARS-CoV. Structural differences in surface protein composition and the kinetics associated with viral load may be responsible for this increased transmissibility (Cevik et al. 2020). This property, combined with a relatively long average incubation time of 5.8 days, has hampered human efforts to limit viral spread (Mcaloon et al. 2020).

1.2 Genomic organisation of SARS-CoV-2.

As with related coronaviruses, the genetic material of SARS-CoV-2 is organised into a positive single-stranded RNA genome with a 5' cap and a 3'-poly-A tail. SARS-CoV-2 possesses one of the largest known RNA genomes, consisting of approximately 30,000 nucleotides (Naqvi et al. 2020). The SARS-CoV-2 genome comprises five major open reading frames (ORF's) and a number of accessory genes which encode for 29 viral proteins. The genetic arrangement of ORF's within SARS-CoV-2 is highly similar to both the SARS-CoV and MERS-CoV viruses (Naqvi et al. 2020). Of the 29 SARS-CoV-2 proteins, 16 are non-structural proteins (nsp's), 9 are accessory and 4 have structural functions (Bai, Zhong, and Fu Gao 2022). Two-thirds of the RNA genome is occupied by two overlapping ORF's located at the 5' end- ORF1a and ORF1b, which encode two polypeptides that are proteolytically processed into the 16 nsp's required for RNA replication and transcription (Troyano-Hearnese, Reinososa, and Holguín 2021).

The 3' end of the SARS-CoV-2 genome encodes for the four major structural proteins- the spike (S) glycoprotein, membrane (M) protein, envelope (E) protein and nucleocapsid (N) protein. The molecular arrangement of SARS-CoV-2 is displayed in Figure 1. The spike, membrane and envelope proteins constitute the viral envelope whilst the nucleocapsid protein binds to viral RNA to assist in genome packing against the internal envelope surface (Xiang et al. 2020). The membrane and envelope proteins are important for viral assembly, budding and virus morphogenesis (Kumar et al. 2020). The spike protein has a major role in binding host cellular receptors via spike-receptor fusion to stimulate viral infection. Together, these structural proteins confer stability to the complete viral particle and are responsible for pathogenicity of the complete virus.

The 3' end of the SARS-CoV-2 genome also encodes the nine accessory proteins which are understood to have roles in virulence and host interaction (Xiang et al. 2020). ORF3b, ORF6, ORF7a, ORF8 and ORF9b proteins function to assist immune evasion by interfering with type I IFN action and by inhibiting cytokine secretion (Redondo et al. 2021). ORF9b also inhibits the RIG-I-MAVS antiviral signalling pathway which may contribute to worsening infections (Wu et al. 2021). Despite their high sequence similarity, accessory proteins are poorly conserved between SARS-CoV-2 and SARS-CoV. Accessory proteins are also less well characterised than other SARS-CoV-2 proteins, possibly because they are not essential for viral replication (Hassan et al. 2022). As such, they present less potent targets for the development of therapeutic interventions. However, the manipulation of the host immune system through interference in inflammatory cytokine production suggests that accessory proteins may have a greater role in SARS-CoV-2 pathogenicity than initially believed.

1.3 ACE2 and the RAAS.

In mammals, the *ACE2* gene encodes for angiotensin converting enzyme II (ACE2), a type I cell surface glycoprotein with a molecular weight of 110kDa (Devaux, Rolain, and Raoul 2020). This membrane-bound protein is expressed in a range of tissue types, and consists of a C-terminal transmembrane anchor, N-terminal signal peptide region and a metalloprotease motif with catalytic activity (Samavati and Uhal 2020). Although ACE2 acts as the primary receptor for SARS-CoV-2 entry, the standard function of ACE2 in humans is the regulation of the renin-angiotensin aldosterone system (RAAS). The RAAS is required for maintaining blood pressure and systemic vascular resistance (Fountain and Lappin 2022). The RAAS is composed of two counter-regulatory arms, the classical arm and the alternative anti-inflammatory arm. The classical arm comprises the ACE/Angiotensin II (Ang II)/AT1 receptor (AT1R) axis, whilst the anti-inflammatory arm involves the ACE2/Angiotensin 1-7 (Ang 1-7)/Mas receptor system (Lanza et al. 2020).

ACE protein exhibits 42% sequence homology with ACE2 and is more ubiquitously expressed in human cell types (Donoghue et al. 2000). Despite the shared structural constitution, these enzymes perform divergent functions. ACE catalyses the conversion of physiologically inactive angiotensin I (Ang I) into the potent vasoconstrictor Ang II (Guang et al. 2012). Ang II then binds to AT1R receptors expressed in the adrenal cortex, brain and kidney, stimulating release of aldosterone (Benigni, Cassis, and Remuzzi 2010). ACE also degrades peptides required for vasodilation including bradykinin and substance P (Sturrock and Acharya 2021). Overall, these actions result in vasoconstriction and an increase in blood pressure.

ACE2 plays a major physiological role within the RAAS by counterbalancing the function of ACE, the human homolog of ACE2, to maintain fluid homeostasis (Sparks et al. 2014). ACE2 converts Ang I into Ang 1-9 (Angiotensin 1-9) through cleavage of a single C-terminal leucine residue. ACE2 also produces the vasodilator Ang 1-7 by degradation of Ang II (Burrell et al. 2004). Although ACE2 degrades both Ang I and Ang II in-vivo, it preferentially metabolises Ang II. Indeed, ACE2 displays a 400-fold higher catalytic efficiency for Ang II than for Ang I (Polak, Speth, and Faha 2021). The bipartite regulation of Ang II levels by ACE and ACE2 allows angiotensin metabolism to be closely controlled. Together, the enzymatic actions of ACE and ACE2 modulate the balance of vasodilators and vasoconstrictors to control fluid homeostasis. Relatively high overall ACE2 expression within mammals favours Ang 1-7 over Ang II, giving ACE2 a cardioprotective role through the Ang 1-7/Mas signalling pathway (Wong 2016). The RAAS also assists in regulation of cell proliferation and the immune-inflammatory response which occurs during infection (Mascolo et al. 2021). The RAAS is a delicate balance between the counter-regulatory arms, with dysregulation resulting in severe clinical consequences including hypertension, cardiovascular disease and strokes (T. K. W. Ma et al. 2010).

1.4 The SARS-CoV-2 spike protein.

The mechanism of viral entry into susceptible host cells is a crucial component of the infection pathway of all viruses. All human coronaviruses (hCoVs) express surface crown-like spike proteins on the exterior of the viral particle to allow these viruses to penetrate susceptible cells (Verma and Subbarao 2021). The SARS-CoV-2 spike protein is responsible for the recognition of appropriate host receptors and as such, is a major determinant for viral tropism. Attachment of the virion to the cell surface precedes the fusion of host and viral membranes which leads to viral invasion.

The SARS-CoV-2 virus requires surface expression of ACE2 for infecting host cells. HeLa cells that transiently express ACE2 protein are susceptible to infection by SARS-CoV-2 although ACE2-deficient HeLa cells are not, demonstrating the importance of receptor expression (P. Zhou et al. 2020). The ACE2 protein is also characterised as the functional entry receptor for the closely related SARS-CoV and the alphacoronavirus HCoV-NL63 (W. Li et al. 2003). Association of the homotrimeric SARS-CoV-2 spike protein with surface ACE2 is the initial step for invasion of susceptible host cells (Figure 1). These spike proteins protrude from the surface of mature viral particles and mediate cellular invasion of the host cells through binding to ACE2 (Y. Huang et al. 2020). Receptor recognition by β -coronaviruses is a key determinant for infectivity, pathogenesis, and host selection (Shang et al. 2020). Prior to receptor binding, spike proteins adopt a metastable pre-fusion conformation that is enzymatically cleaved to allow cell entry (Figure 1).

The SARS-CoV-2 S protein consists of two subunits, S₁ and S₂ which perform distinct roles in the infection process. The S₁ subunit is located at the membrane distal tip of the spike glycoprotein and contains the receptor binding domain (RBD, 319-541 residues) and an N-terminal domain (NTD, 14-305 residues) (Dejnirattisai et al. 2021). An N-terminal signal peptide (SP) located in the S₁ subunit helps guide the S protein to the cell membrane (Hoffmann, Hofmann-Winkler, and Pöhlmann 2018). The S₂ subunit is required for mediating the fusion of host and viral membranes to allow viral entry.

During viral replication inside infected cells, modification of nascent spike proteins through attachment of N-linked glycans results in the production of complete spike glycoproteins (Bagdonaite and Wandall 2018). The exterior envelope of a SARS-CoV-2 particle displays 66 N-linked glycosylation sites, enabling extensive glycosylation to occur (Petrović, Lauc, and Trbojević-Akmačić 2021). This glycosylation can mask the SARS-CoV-2 virus from detection by the host immune system. By presenting a so-called 'glycan shield' to the exterior of the viral particle, neutralising antibodies of the host can be prevented from recognising key viral epitopes (Casalino et al. 2020). This form of immune evasion is effective for promoting pathogenicity. Shielding of S proteins with a polysaccharide coat is observed for a wide range of viral glycoproteins, including those of SARS-CoV, influenza and HIV-1. This glycosylation assists in immune evasion by masking immunogenic surface proteins (Watanabe et al. 2020). The emergence of novel SARS-CoV-2

variants exhibiting additional or altered glycosylation sites has been reported (Newby et al. 2023). These mutations may give rise to greater immune escape through additional masking of viral antigens from host antibodies or by altering the wider antigenic structure beyond this site.

The RBD of the S₁ subunit is a critical component as this presents the interacting surface for binding with ACE2 receptors. Furthermore, the RBD of the spike protein is thought to be one of the most variable sections of the SARS-CoV-2 genome (P. Zhou et al. 2020). Crystal structures of SARS-CoV-2 spike proteins have elucidated that the RBD is composed of a core region and a receptor binding motif (RBM), the latter of which mediates the direct contact with ACE2 (Shang et al. 2020). There is significant sequence homology (76%) between SARS-CoV-2 and SARS-CoV spike proteins, with the RBD's also displaying 74% sequence similarity (Jaimes et al. 2020).

Cryo-electron microscopy analysis has confirmed that the SARS-CoV-2 spike protein adopts multiple conformations with individual functions. Prior to infection, the S protein exists as an inactive trimer on the surface of the virus. However, as the SARS-CoV-2 virus interacts with the host cell, the spike protein transitions from a pre-fusion to a post-fusion state. These structural changes facilitate the invasion of susceptible host cells. The initial binding of SARS-CoV-2 spike proteins to the host receptor results in conformational changes that cause dissociation of the S₁ subunit from ACE2. This process prompts the S₂ subunit to adopt a post-fusion state which subsequently enables membrane fusion to occur (Kirchdoerfer et al. 2018; Lan et al. 2020). The conformational transitions that occur within the spike protein during cellular invasion are crucial for coronavirus pathogenicity. Stabilising mutations which prevent the structural shift from pre-fusion to post-fusion states can inhibit viral entry and thus eliminate the infectivity of SARS-CoV and SARS-CoV-2 (Kirchdoerfer et al. 2018). Additional enzymatic actions on exposed regions of the spike protein also assist in the viral infection pathway. This activation of the spike protein through proteolytic processing is called 'priming'.

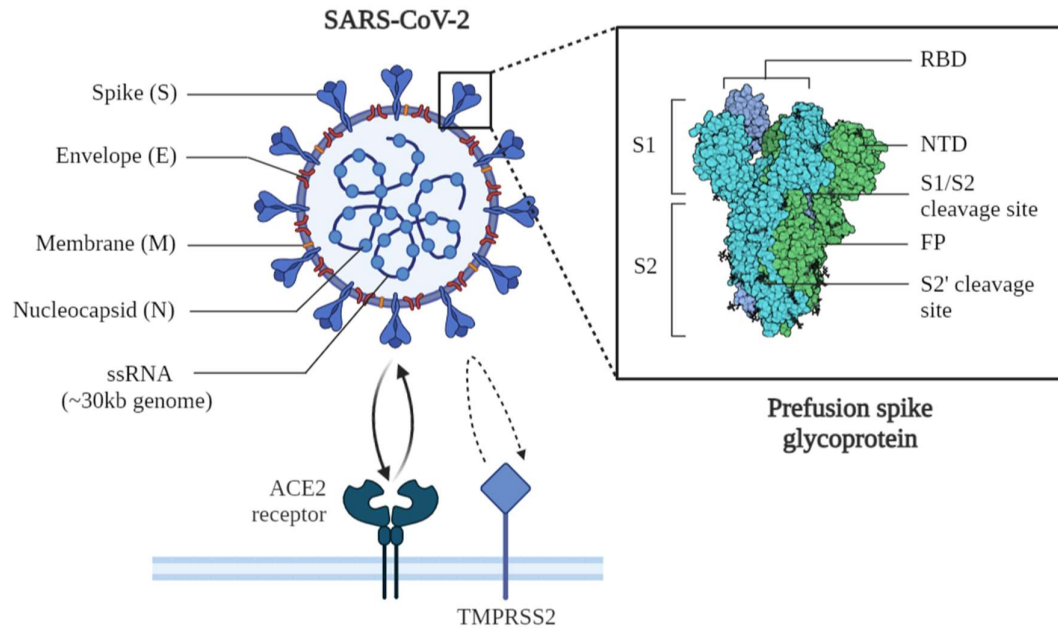


Figure 1: SARS-CoV-2 virus structure and interaction with host factors.

The prefusion spike glycoprotein consists of subunits 1 and 2 (S_1 and S_2), with a receptor binding domain (RBD), N-terminal domain (NTD), S_1/S_2 cleavage site, fusion peptide (FP) and S_2' cleavage site. Interaction of the spike protein with host ACE2 precedes cellular invasion, with TMPRSS2-mediated priming of S also required for viral entry.

1.5 Priming of spike proteins by host factors.

Following binding of the spike protein to ACE2, host proteases can cleave the S protein into individual S₁ and S₂ subunits, activating the spike and allowing subsequent viral entry (Y. Huang et al. 2020). Host proteases are utilised by all members of the *Coronaviridae* family to ‘prime’ spike glycoproteins through cleavage at specific sites. A polybasic cleavage site located at the boundary between the S₁ and S₂ subunits contains multiple arginine residues (RRAR). This region is able to be cleaved by the subtilisin-like host enzyme furin along with other proteases and as such, is described as a furin cleavage site (FCS). The presence of polybasic cleavage sites within spike protein subunits is not unusual for β -coronaviruses, with the human infecting OC43, HKU1 and MERS-CoV viruses all expressing these motifs (Sternberg and Naujokat 2020).

Processing of the spike protein at these cleavage sites plays an important role in the pathogenesis of β -coronaviruses (Chan and Zhan 2022). Whilst SARS-CoV possesses a monobasic cleavage site at the S₁/S₂ boundary, SARS-CoV-2 contains a unique polybasic FCS at this region (Winstone et al. 2021). The presence of a polybasic FCS has been suggested to contribute to the greater infectivity of SARS-CoV-2, as furin or furin-like human proteases are necessary for activation of the spike protein (Sternberg and Naujokat 2020). These enzymes are ubiquitously expressed in humans, providing ample priming to the SARS-CoV-2 spike. The critical importance of priming by host proteases has led to these enzymes being proposed as possible targets for antiviral intervention (Hoffmann, Hofmann-Winkler, and Pöhlmann 2018). Furthermore, investigations into deletions of the FCS at the S₁/S₂ boundary have demonstrated that this region is important for viral entry, with modified SARS-CoV-2 particles restricted to low pH compartments (Winstone et al. 2021).

Priming of the spike protein by the host protein transmembrane serine protease 2 (TMPRSS2) is required for viral entry of SARS-CoV-2 (Figure 1). TMPRSS2 is widely expressed on the surface of many susceptible human tissues including the lungs, thyroid, gastrointestinal tract, pancreas, kidney and liver (Piva et al. 2021). In addition to the polybasic FCS site at the S₁/S₂ boundary, the cleavage site S₂' must also be processed to allow viral invasion (Jackson et al. 2021). This site has been identified as the KPSKR sequence at residues 810-815 in the spike (Essalmani et al. 2022).

The S₂' site is situated within the S₂ subunit and is thus inaccessible to external proteases in the pre-fusion state. However, engagement of ACE2 with the S₁ subunit enacts conformational changes which expose the S₂' cleavage site for processing (D. Ma et al. 2020). Cleavage of S₂' induces additional structural rearrangements within the spike glycoprotein that bring the viral and cellular membranes into close contact. This assists in the creation of a fusion pore, allowing insertion of viral genetic material into the host cell. TMPRSS2 is one of multiple host enzymes that proteolytically cleave residues within the S₂' site to enhance viral entry (Yi et al. 2020).

Additional cleavage sites within the SARS-CoV-2 spike protein also exist. Additional host serine proteases and cathepsins such as furin and cathepsins B and L may also act upon these cleavage sites to liberate the S₂ fusion peptide (FP) and instigate membranal fusion (Bollavaram et al. 2021; Peacock et al. 2021). The cathepsin B/L dependent auxiliary activation pathway is especially prevalent during infection of cells lacking expression of TMPRSS2. The cysteine protease cathepsin L is predominantly located within endolysosomal vesicles where it degrades protein antigens produced by pathogen endocytosis (Müller, Dennemärker, and Reinheckel 2012). However, during COVID-19 infection, cathepsin L is excessively secreted into circulating plasma where it may cleave between residues Thr696 and Met697 to cause dissociation of the S₁ and S₂ domains at the subunit boundary (Gomes et al. 2020). The concentration of cathepsin L is also correlated with disease severity in patients suffering from COVID-19 (Zhao et al. 2021). This suggests that cathepsin L may contribute to acute disease states by assisting the processing of the SARS-CoV-2 spike protein.

The TMPRSS2 enzyme also primes the spike proteins of other coronaviruses including the pathogenic human viruses MERS-CoV and SARS-CoV, resulting in virus-cell membrane fusion (Iwata-Yoshikawa et al. 2019). This ability to utilise a range of host proteases for activation of entry proteins provides multiple routes for SARS-CoV-2 invasion. A number of serine protease inhibitors have been developed as potential therapeutic agents following the discovery of their importance within the SARS-CoV-2 infection pathway. The use of potent TMPRSS2 inhibitors, such as camostat mesylate have proven effective in inhibiting SAR-CoV-2 activation and reducing cellular entry *in vitro* (Hoffmann et al. 2021). Human trials have also been performed on COVID-19 patients with mixed results. Whilst studies have reported viral load reductions, the clinical improvement of hospitalised patients may be unaffected by camostat mesylate (Chupp et al. 2022; Tobback et al. 2022; Kinoshita et al. 2022). Due to the exploitation of numerous host enzymes for priming spike proteins, absolute suppression of viral entry through protease inhibition is unfeasible. However, limitation of SARS-CoV-2 pathogenicity through therapeutic means may be effective in preventing severe disease. The development of prophylactic medicines to protect against acute COVID-19 has also involved priming proteinase inhibitors (Rahbar Saadat et al. 2021).

1.6 Spike-ACE2 complex formation.

The presence of suitable membrane-bound receptors and the expression of viral surface proteins with complementary binding sites contributes to the success and pathogenicity of β -coronaviruses. The molecular interactions and binding affinity between the host receptor and viral entry proteins can therefore play a major role in determining the outcomes of infection. For this reason, extensive characterisation of the complex formed between the SARS-CoV-2 spike protein and the ACE2 receptor has been completed. Whilst isoforms of ACE2 exist, including the truncated form δ -ACE2, only full length ACE2 acts as the receptor for SARS-CoV-2 (Onabajo et al. 2020).

The structure of the SARS-CoV-2 RBD-ACE2 complex has been elucidated using X-ray crystallography. The interface of this complex represents the initial interaction between SARS-CoV-2 and ACE2 on the surface of susceptible host cells. The receptor binding motif (RBM) is a region of the SARS-CoV-2 spike protein RBD (residues 438-506) containing the majority of contacting residues required for binding to ACE2 (Yi et al. 2020). ACE2 contains an N-terminal peptidase domain consisting of two lobes, the smaller of which interacts with the RBM region of the viral spike (Lubbe et al. 2020). This RBM consists of short β -5 and β -6 strands twisted together to present a concave interacting surface towards the N-terminal helix of ACE2 (Lan et al. 2020). The surface area of this interface is maximised through 'cradling' of the N-terminal α -helix by the exterior surface of the spike RBM, resulting in 17 RBD residues being in close contact with 20 residues of ACE2 (Lan et al. 2020).

There are six amino acid residues within the SARS-CoV-2 spike RBD that are crucial for interaction with ACE2- L455, F486, Q493, S494, N501 and Y505 (Andersen et al. 2020). Of these six residues, five are distinct from the SARS-CoV genome. Although the RBM is the major functional motif of the RBD, the remaining regions are important for maintaining structural integrity of the RBD-ACE2 complex (Yi et al. 2020). Amino acid alignment investigations have determined that the sequence similarity of the RBD region between SARS-CoV and SARS-CoV-2 is 74% (R. Lu et al. 2020). However, RBM similarity is only 47%, highlighting the variability of this binding region (Jaimes et al. 2020). Interestingly, the overall mode of SARS-CoV-2 RBD-ACE2 binding is determined to be nearly identical to that of SARS-CoV RBD-ACE2, despite the low amino acid identity.

Interactions between ACE2 and SARS-CoV-2 S proteins have been determined both in-vitro and with computer simulations. A network of hydrophilic interactions is a prominent feature of the RBD-ACE2 interface, with 2 salt bridges and 13 hydrogen bonds strengthening formation of this complex (Lan et al. 2020). Independent of the RBD, the SARS-CoV-2 spike protein also expresses a single lysine residue, Lys417, that forms a salt-bridge interaction with the ACE2 residue Asp30 (Lan et al. 2020). This contact is absent within SARS-CoV spike-ACE2 interaction. Presence of the salt-bridge contributes to a greater electrostatic complementarity for SARS-CoV-2 than SARS-CoV binding

ACE2 (Yingjie Wang, Liu, and Gao 2020). These minor differences in spike-ACE2 binding between SARS-CoV and SARS-CoV-2 may contribute to the overall difference in spike-ACE2 affinity. Indeed, an investigation using surface plasmon resonance analysis has determined that overall binding affinity for the spike RBD-ACE2 complex is greater for SARS-CoV-2 than SARS-CoV, 15nm and 40nm respectively (Shang et al. 2020). Surface area of the binding interface is also greater for SARS-CoV-2, with additional amino acid residues contributing to this interacting region (Sternberg and Naujokat 2020).

The significance of the association between the SARS-CoV-2 spike RBM and ACE2 can be observed through the effects of altering the interacting surface. Mutations within key residues of the RBD, such as Lys353, have a significant impact upon enhancement of the binding interaction (Y. Huang et al. 2020). This residue forms a strong hydrophobic interaction with Tyr505, which is required for stabilising the binding surface (Du et al. 2021). If the conserved Lys353 residue is mutated to histidine, then the RBD-ACE2 complex exhibits weaker binding (Lupala et al. 2020). Simulations of molecular dynamics also show how mutations within non-RBM regions can alter the structure of the RBD and influence its interaction with ACE2 (Du et al. 2021). Although mutations within the RBD can be deleterious for binding ACE2, there are a substantial number which are well-tolerated or lead to enhanced binding (Starr et al. 2020). Enhancement mutations may be selected for if they provide greater SARS-CoV-2 infectivity. Therefore, surveillance of viral mutations and the functional annotation of these is important for tracking the evolution of the SARS-CoV-2 virus and for identifying possible new variants of concern (VOC's).

The RBD and NTD of the S₁ subunit are important immunogenic regions which promote immune responses. The RBD in particular constitutes the principal target for binding of neutralising antibodies (Hoffmann, Hofmann-Winkler, and Pöhlmann 2018). Due to the critical importance of the RBD within the viral life cycle, it has been designated a major site for antibody-induced inhibition of viral entry (Jackson et al. 2021). Whilst all sub-regions of the spike protein can elicit an immune response, antibodies produced against the RBD have the highest affinity (Ravichandran et al. 2020). Interestingly, neutralising antibodies against the SARS-CoV RBD may exhibit cross-binding to the SARS-CoV-2 RBD (Lok et al. 2021). This is the result of partly shared RBD sequence homology, although cross-neutralisation of live SARS-CoV-2 virus with SARS-CoV antibodies is limited (Lv et al. 2020). SARS-CoV-2 therapeutics also target exposed regions required for successful viral invasion and replication. The central helix and HR1 domain of the S₂ subunit stimulate immune responses as these are exposed on the stem region of spike protein trimers (J. Zhang et al. 2021). Identification of these immunogenic regions, along with an understanding of the interactions occurring during spike-ACE2 association, can provide insights into key targets of monoclonal antibody therapy.

1.7 SARS-COV-2 variants.

The efficient transmissibility of SARS-CoV-2, along with the emergence of asymptomatic variants has led to high viral success. This is demonstrated by the rise in global infections, especially in re-infected individuals. The majority of mutations that arise are deleterious and are soon purged from the gene pool. However, if a mutation occurs which heightens transmissibility, assists in immune evasion or otherwise improves host-pathogen interactions, then this may be selected for. An increase in frequency of a particular variant suggests that the present mutations confer a competitive advantage in the phenotype (Lauring and Hodcroft 2021). This advantage may be expressed as a greater capacity for intrinsic replication, increased viral loads within the host or greater immune evasion contributing to increased transmissibility (Yurkovetskiy et al. 2020).

A single mutation conferring a significant phenotypic advantage can result in the dominance of a variant across the globe. Indeed, the D614G substitution first observed in March 2020 causes increased interhuman transmission and has become ubiquitous among highly transmissible SARS-CoV-2 variants (Plante et al. 2021). Compared to the beginning of the COVID-19 pandemic, there are now heightened selection pressures affecting the evolution of the SARS-CoV-2 genome. Mass vaccination and widespread infections have changed the immune profiles of susceptible human populations, protecting individuals against disease. This selection pressure may have contributed to the emergence of SARS-CoV-2 variants that are more effective in escaping the neutralising antibodies present after vaccination or primary infection (L.-F. Wang et al. 2022). Additionally, variant-dependent effects of the SARS-CoV-2 virus upon the host immune response may exist. Possible dysregulation of cytokine and/or ACE2 levels during infection may negatively influence host responses during COVID-19, contributing to greater viral pathogenicity.

The rise of asymptomatic variants has been observed during the course of the COVID-19 pandemic, with reductions in lethality and greater infectivity becoming more predominant in recently identified variants (Hu et al. 2021). Highly contagious and asymptomatic viruses with an extended incubation period (such as SARS-CoV-2) are difficult to track, which makes the identification of positive cases difficult. However, the identification of many SARS-CoV-2 mutations and possible links with pathological changes is critical for understanding viral evolution and responding effectively to the emergence of dangerous variants (Cheng et al. 2022).

Publicly available genomic epidemiology data has allowed for global characterisation of variant subtypes, with those greatly influencing viral transmissibility and antigenicity labelled as ‘Variants of Concern’ (VOC’s) by the World Health Organisation (WHO). As of 22nd March 2023, five VOC’s have been characterised by the WHO- the alpha, beta, gamma, delta, and omicron SARS-CoV-2 variants (WHO 2023). In addition to this, ‘Variants Under Investigation’ (VUI’s) and ‘Variants of

Interest' (VOI's) have also been designated, representing recently discovered lineages and those with genetic changes affecting viral transmissibility or immune escape.

The most important mutations acquired within the SARS-CoV-2 genome occur within the regions encoding for the spike protein (Gusev et al. 2022). This is likely due to the importance of the spike protein for cellular invasion, as well as being a major target for neutralising antibodies during the host immune response. Mutations within this region can significantly alter pathogenicity and virulence or impede the efficacy of vaccines in preventing infections. Enhancement of the binding affinity between the SARS-CoV-2 spike and the ACE2 receptor may also result in greater viral entry, improving efficiency of infection. The evolution of SARS-CoV-2 spike proteins appears to select for mutations that increase ACE2 binding and allow for greater evasion of host neutralising antibodies (Saville et al. 2022).

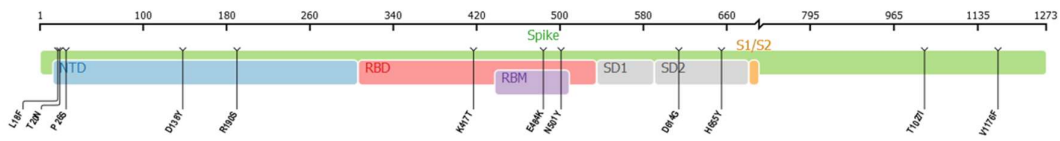
The kappa (κ) variant (B.1.617.1) was first detected in India in October 2020 with identification of this variant coinciding with a resurgence of COVID-19 cases in the country (W. Ren et al. 2022). Eight mutations are determined within the κ -spike protein (Figure 2). The E154K mutation occurs within an exposed loop of the NTD, likely affecting the propensity of antibody binding to this region (Saville et al. 2022). After the RBD, the N-terminal domain is the region targeted most by anti-SARS-CoV-2 neutralising antibodies (McCallum et al. 2021). The L452R mutation is a substitution within the RBD which may contribute to greater binding affinity to ACE2, increasing the efficiency of cellular invasion (Tchesnokova et al. 2021). L452R also contributes to immune escape, potentially leading to increased transmissibility and pathogenicity (Motozono et al. 2021). The E484Q mutation, as with L452R, reduces susceptibility of the κ -spike to monoclonal antibodies (Verghese et al. 2021). Interestingly, these two mutations are not synergistic for antibody evasion, as sensitivity to neutralising antibodies is reportedly similar for L452R and E484Q alone when compared to the presence of both mutations in κ -spike protein (Ferreira et al. 2021). The P681R mutation is present immediately prior to a FCS at residues 682-688. Substitution here enhances cleavage and activation of the spike by furin and furin-like proteases (Saito et al. 2021). Thus, P681R results in enhanced viral tumorigenicity and transition of the spike protein into a post-fusion state (Saville et al. 2022). P681R mutations are also present in the delta variant (also of the B.1.617.2 lineage) with significantly increased pathogenicity (Dhawan et al. 2022).

The gamma (γ) variant (lineage P.1) first appeared in Brazil in December 2020 where it contributed to a surge in COVID-19 cases in the city of Manaus (Naveca et al. 2022). Several mutations within the γ variant are not present within the original SARS-CoV-2 virus genome (Figure 2), including N501Y, also present within α and β SARS-CoV-2 (Y. Liu et al. 2022). N501Y increases the affinity of the viral spike for ACE2, enhancing the binding interaction (F. Tian et al. 2021). Convergent evolution of the N501Y mutation in several lineages suggests this substitution confers a major

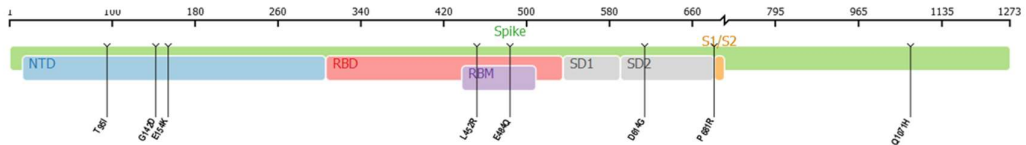
phenotypic advantage. E484Q is also observed within the γ -spike, as with the κ variant (Jangra et al. 2021). Substitution of glutamic acid at residue 484 is also shared by spike proteins of the β , δ and \omicron variants, with reductions in antibody neutralisation conferred in each case (Wise 2021; Khateeb, Li, and Zhang 2021). This highlights the importance of E484Q for viral success as mutations robustly increase reproductive fitness.

The current COVID-19 pandemic is predominated by cases of omicron (\omicron , lineage B.1.1.529), a VOC first reported in South Africa in November 2021 and has since developed into many sub-lineages (BA.1-BA.5) (D. Tian et al. 2022). The initial SARS-CoV-2 omicron variant displays 32 mutations within the spike protein (Figure 2) (Shrestha et al. 2022). Three mutations in the proximity of the FCS at the S_1/S_2 boundary facilitate cellular invasion (Lubinski, Jaimes, and Whittaker 2022). A multitude of substitutions within the RBD, such as S371L, S375F, G446S, S447N and T478K assist in increasing spike-ACE2 affinity (J. Zhang et al. 2022; D. Tian et al. 2022). Vaccine efficacy is also reduced by NTD and RBD mutations, as neutralising antibodies are unable to bind due to considerable RBD modification. The reduced immunogenicity conferred by the \omicron -variant has contributed to a wave of re-infections after primary infection or vaccination (Pilz et al. 2022). Structural analysis of the omicron variant has demonstrated that ACE2 binding, whilst improved, is similar to the Alpha variant first detected in November 2020 (Mannar et al. 2022). However, the increased transmissibility of omicron is a result of a heightened ability to evade neutralisation by host antibodies (Zepeng Xu, Liu, and Gao 2022). The combination of enhanced ACE2 binding and greater immune escape explains the dominance of novel variants across the globe. It is inevitable that mutations within the SARS-COV-2 genome will continue to arise, presenting a constant epidemiological need for genetic monitoring to identify novel variants and to characterise the phenotypes conferred by new mutations.

A. Gamma



B. Kappa



C. Omicron

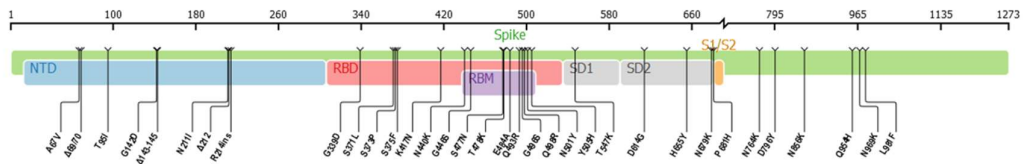


Figure 2: Sequence alignments for SARS-CoV-2 variant spike proteins.

Sequence alignments of three SARS-CoV-2 variant spike proteins, A (Gamma), B (Kappa), and C (Omicron). Labelled mutations represent amino acid substitutions compared to the original SARS-CoV-2 reference genome. Regions including the NTD (N-terminal domain), RBD (receptor binding domain), RBM (receptor binding motif), SD1 (sub-domain/subunit 1), SD2 (sub-domain/subunit 2) and S₁/S₂ boundary are shown. Data obtained from outbreak.info Genomics Reports (Gangavarapu et al. 2022).

1.8 SARS-CoV-2 uses ACE2 for cellular entry.

Despite the known manifestation of COVID-19 as a respiratory illness, the SARS-CoV-2 virus can infect a range of cell and tissue types. The nature of ACE2 as the primary receptor for SARS-CoV-2 entry has defined the presence of this protein as a major indicator for susceptibility to infection. Tissues expressing high levels of ACE2 are therefore targets for SARS-CoV-2. ACE2 receptors are ubiquitously expressed within the heart, kidney, gut, gallbladder, testis and small intestine (Hikmet et al. 2020; M. Y. Li et al. 2020). Epithelial cells of the respiratory system (especially type II pneumocytes) also express ACE2, with the lungs and upper respiratory tract representing the predominant sites for SARS-CoV-2 infection (Zhe Xu et al. 2020; Hamming et al. 2004). This correlates with the pneumonia-associated symptoms exhibited during SARS-CoV-2 infection, including a fever, cough and shortness of breath (Pal et al. 2020). However, a multitude of additional symptoms can accompany COVID-19 infection including protein or blood in the urine, strokes or seizures, cardiac inflammation and injury, and pancreatitis (Temgoua et al. 2020).

Individuals displaying underlying medical conditions including diabetes, heart disease and hypertension are at greater risk of COVID-19. ACE2 expression is significantly increased within patients suffering from hypertension and type I or type II diabetes, suggesting this may be responsible for the heightened risk of disease (Fang, Karakiulakis, and Roth 2020). The involvement of wider organs also contributes towards severe disease and suggests that SARS-CoV-2 may affect a wide range of organs containing cells expressing ACE2. The co-expression of ACE2 and viral spike proteins hints to tissue locations where SARS-CoV-2 infection has or may occur. Presence of both SARS-CoV-2 and ACE2 has been detected in cells of the small intestine, kidney, lung, heart and pancreas (J. Liu et al. 2021). These extrapulmonary organs may function as reservoirs for viral particles, especially within immunocompromised individuals. Viral shedding in these locations following initial recovery can also lead to the false classification of the individual as re-infected (Kalkeri, Goebel, and Sharma 2020).

Immunocompromised patients are high-risk for severe COVID-19 disease and resulting impaired antiviral responses enables greater replication and multi-organ spread of the virus (van Cleemput et al. 2021). SARS-CoV-2 mediated histological lesions have been identified in the kidneys of deceased COVID-19 patients, suggesting direct viral entry can occur (Temgoua et al. 2020). Overall, the pathogenicity of multi-organ damage resulting from SARS-CoV-2 infection is unclear and may arise from a combination of direct viral invasion and indirect systemic inflammation through the overexpression of signalling cytokines.

ACE2 expression levels naturally differ between individuals. The pathophysiology of ACE2 during SARS-CoV-2 infection is extremely complex, although analysis of severely ill patients has identified several correlations with factors affecting ACE2. Sex-related differences within males contributes to

a greater susceptibility towards COVID-19 (Foresta, Rocca, and di Nisio 2021). Immunological investigations suggest that males may mount an attenuated antiviral response compared to females (Viveiros et al. 2021). Although the *ACE2* gene is expressed on the X chromosome, mRNA expression of *ACE2* in oral epithelial cells is not substantially different between genders (Peng et al. 2021). *ACE2* expression within males is, however, more widespread than in females which may contribute to gender disparity in COVID-19 severity (Kaseb et al. 2021). Elderly individuals also express relatively higher levels of *ACE2*, with this group also exhibiting greater susceptibility to severe COVID-19 (Peng et al. 2021).

The presence of *TMPRSS2* alongside *ACE2* is also viewed as a prerequisite for infection as this protease is a major primer and activator of the SARS-CoV-2 spike (Fraser et al. 2022). Overall *TMPRSS2* expression is considerably higher in males than females due to upregulation by the male sex hormone androgen (Strope, PharmD, and Figg 2020). Furthermore, up to three times as many alveolar type II cells co-express *ACE2* and *TMPRSS2* within the lungs of men when compared to women (Okwan-Duodu et al. 2021). This indicates increased cellular penetration can occur during SARS-CoV-2 infection, resulting in poorer disease outcomes for males. Indeed, clinical trials of drugs that directly or indirectly (through the androgen pathway) inhibit *TMPRSS2* expression are promising treatments for managing SARS-CoV-2. The serine protease inhibitors camostat mesylate, bromhexine and nafamostat have all demonstrated potential inhibitory effects against SARS-CoV-2 (Nitulescu et al. 2020). In addition to *ACE2* and *TMPRSS2*, there are a vast number of immunological genes that influence the susceptibility to and outcome of SARS-CoV-2 infections, with *ACE2* polymorphisms also known to affect the outcome of disease (F. Chen et al. 2021).

1.9 SARS-CoV-2-mediated effects on ACE2 and the RAAS.

The high-affinity interaction of the SARS-CoV-2 spike protein with the ACE2 receptor leads to entry of the virus and subsequent viral replication. During this process, spike protein binding results in the internalisation of the protein complex and a reduction in ACE2 surface expression (Silhol et al. 2020; Verdecchia et al. 2020). The loss of ACE2 function during SARS-CoV-2 infection is driven by this endocytosis and subsequent proteolytic processing of the receptor as viral particles infiltrate host cells (Gheblawi et al. 2020). Downregulation of ACE2 disrupts the lung's ability to respond to and heal from acute lung injury (Banu et al. 2020). Depletion of ACE2 thereby removes its protective function and enhances the damaging effects of Ang II (Wong 2016). Whilst ACE2 loss from the cell surface has been extensively reported, internal processing of the spike protein-ACE2 complex is poorly understood. As the SARS-CoV-2-spike induces ACE2 shedding, infection has a direct effect upon the entire RAAS system. ACE2 is required for protection against lung injury and its endocytosis coincides with wide-ranging inflammatory responses.

The RAAS has an important role in the pathogenesis of COVID-19. In a clinical setting, neurohormonal imbalance of the RAAS is associated with a worsened prognosis for COVID-19 patients (Chinonyerem et al. 2021). This is likely due to the importance of the RAAS and ACE2 in regulation of cardiovascular physiology. Individuals with RAAS imbalance also suffer more frequently from pulmonary thromboembolism, poor lung perfusion and kidney failure (Rysz et al. 2021). One biochemical marker of this imbalance is hypokalemia, a deficiency of potassium within the bloodstream (Silhol et al. 2020). Hypokalemia is frequently observed COVID-19 patients, and this is associated with poor clinical outcomes of the disease (D. Chen et al. 2020).

Severe COVID-19 can be considered, in part, a consequence of RAAS dysregulation resulting from excessive activation of the pro-inflammatory classical arm. This process, along with direct viral-induced immune responses can lead to the development of a hyperinflammatory state that presents a major threat to infected individuals. This immune hyperactivation contributes to exacerbated inflammatory responses through proliferation of immune cells releasing pro-inflammatory signalling proteins (di Mauro Gabriella et al. 2020; Darif et al. 2021). The reduction in ACE2, combined with inflammatory cytokine production, results in greater levels of Ang I and Ang II (Gheblawi et al. 2020). Increased Ang II levels contribute towards pulmonary inflammation and the development of ARDS as Ang II acts as both a vasoconstrictor and as a pro-inflammatory cytokine through AT1R (Eguchi et al. 2018).

Isolated spike proteins of the related SARS-CoV promote lung injury through a reduction in protective ACE2 expression (Imai, Kuba, and Penninger 2008; Glowacka et al. 2010). This demonstrates how spike proteins alone may induce Ang II production through ACE2 downregulation, resulting in pulmonary inflammation. Furthermore, cases of acute lung injury can

be rescued through inhibition of AT1R (Y. L. Gao et al. 2020). The Ang II-AT1R signalling mechanism amplifies inflammation through generation of an IL-6 positive feedback loop within the NF- κ B pathway (Hojyo et al. 2020). Excessive inflammatory states can contribute to multiple organ failure, observed in the most severe cases of COVID-19 (Mokhtari et al. 2020). These investigations demonstrate the contribution of human coronaviruses to development of ARDS through pulmonary inflammation, with potentially fatal outcomes.

The COVID-19 pandemic has stimulated greater investigation into the ACE2/Ang 1-7 axis to provide protection against inflammatory lung damage, or conversely, to reduce potential SARS-CoV-2 entry into susceptible cells. Initial observations predicted that elevated ACE2 levels may heighten SARS-CoV-2 infection risk by increasing the number of available entry receptors (Gheware et al. 2022). However, the physiological imbalances caused by viral-induced ACE2 deficiency has since proven to be the more pivotal factor in severe COVID-19 disease. Clinical trials investigating the potential therapeutic administration of ACE2 have demonstrated the in-vivo possibility of RAAS manipulation for reducing systemic inflammation (Hemnes et al. 2018). External delivery of soluble ACE2 (sACE2) may also prevent further viral spread by blocking interaction of the SARS-CoV-2 spike with membrane bound ACE2 (Yi et al. 2020). The effects of RAAS disruption are most potent in patients with comorbidities, such as cardiovascular disease, hypertension or diabetes (Beyerstedt, Casaro, and Rangel 2021). In any case, this delicate RAAS equilibrium must be considered prior to the development of therapeutic interventions as the balance of these neurohormonal molecules and the availability of receptors (e.g ACE2) have major impacts upon COVID-19 patients.

1.10 Inflammatory response and cytokine storm.

During SARS-CoV-2 infection, the body's immune system coordinates responses through a network of interconnected signalling pathways, resulting in the activation of a wide range of immune cells. Signalling is performed by a diverse group of pro- or anti-inflammatory proteins called cytokines (Ramesh, Maclean, and Philipp 2013). The balance of these signalling molecules is crucial for appropriate host responses to disease. However, during SARS-CoV-2 infection, serum levels of critical cytokines are disrupted, leading to exacerbated inflammatory responses and severe COVID-19 disease (R. Chen et al. 2021). Whilst these responses contribute to the neutralising antibody response against SARS-CoV-2, the hyperinflammation caused can severely damage host tissues. This 'cytokine storm' involves immune cell hyperactivation and plays a direct role in the development of ARDS, leading to poor patient outcomes (Tang et al. 2020).

Understanding the roles of key pro-inflammatory cytokines and managing the resulting inflammation is crucial for preventing COVID-19 deterioration. Major increases in serum levels of cytokines IL-6, IL-8 and IL-10 are reported in infected individuals, along with significant generation of anti-SARS-CoV-2 antibodies (Laing et al. 2020). Immunotyping of patients also shows abrupt increases in the levels of inflammatory monocytes, macrophages and neutrophils along with a reduction in lymphocytes (Giamarellos-Bourboulis et al. 2020). T cell responses are manipulated by SARS-CoV-2 infection, with hospitalised patients exhibiting either impaired CD4⁺ function resulting in reduced IFN- γ production, or an over-stimulation of these T cells promoting hyperinflammation (Sattler et al. 2020; Mathew et al. 2020). Viral-induced cell lysis results in production of the major pro-inflammatory cytokines TNF- α and IFN- γ , leading to stimulation of local neutrophils, macrophages and endothelial cells (Shimabukuro-Vornhagen et al. 2018). Activation of these cells results in additional release of pro-inflammatory cytokines under control of positive-feedback loop signalling through the NF- κ B and MAPK pathways (Merad and Martin 2020). Additional studies have also identified high levels of the cytokines IL-1 β , IL-6, IFN- γ and TNF- α within severely ill COVID-19 patients, demonstrating the correlation between pro-inflammatory protein production and worsened disease prognosis (H. Han et al. 2020; Del Valle et al. 2020).

The dysregulation of cytokine production during SARS-CoV-2 infection may also influence the RAAS through manipulation of ACE2 expression. *ACE2* has recently been shown to be an interferon-stimulated gene (ISG) (Ziegler et al. 2020). The production of cytokines, such as type I and type II interferons may upregulate expression of host ACE2 in the presence of SARS-CoV-2 (Busnadiego et al. 2020). The outcome of this enhanced expression may further viral infection through additional entry receptors. However, by protecting against exacerbated inflammatory action, ACE2 production may be beneficial to the host (Yalcin et al. 2021). Regardless, contrasting evidence exists for the effects of SARS-CoV-2 on ACE2 expression. Indeed, isolated spike proteins of SARS-CoV-2 may

suppress production of ACE2 and interferons in lung tissue (Sui et al. 2021). Downregulation of ACE2 through destabilisation of ACE2 mRNA by SARS-CoV-2 spike proteins has also been demonstrated in kidney cells (X. Gao et al. 2022). Therefore, the overall effect of SARS-CoV-2 on ACE2 is likely dependent upon numerous factors including the specific cell types involved and host immune responses. Additional investigations examining SARS-CoV-2-mediated effects upon ACE2 expression are required for all tissues susceptible to viral infection. Furthermore, the effects of cytokine action upon ACE2 expression in these host cells must also be investigated.

1.11 Thesis aims.

Previous investigations have discerned ACE2 expression across a wide range of tissue and cell types, however this data is incomplete and at times contradictory. The objectives of this thesis are to determine whether ACE2 expression can be detected in skin, cervical and placental tissues. Additionally, the effects of cytokine and spike protein treatments upon ACE2 expression within these cells will be investigated. Spike-mediated production of cytokines will be characterised, along with the internal processing of ACE2 in response to these treatments. Presence of variant-dependent effects of spike treatments will also be determined in this study. Finally, a system to allow for the determination of downstream proteomic consequences of ACE2-spike protein engagement will be developed.

Section 2.0 Materials and methods

2.1 Chemicals and reagents.

All chemicals used during these experiments were obtained from Sigma-Aldrich, unless stated otherwise. The constitution of some common buffers, solutions and cell treatments are listed below.

TBST- 10 mM Tris, 150 mM NaCl, 0.1% Tween-20, pH 8.0.

1x MNT buffer- 20 mM MES, 30 mM Tris-HCl, 100 mM NaCl, pH 7.4.

2x Laemmli loading buffer- 65.8 mM Tris-HCl, 26.3% w/v glycerol, 2.1% SDS, 0.01% bromophenol blue, pH 6.8 (BioRad).

Mouse IFN- γ was obtained from Thermofisher Scientific, human IFN- γ was obtained from PeproTech. Human recombinant TNF- α protein was obtained from Sigma Aldrich. Recombinant spike RBD proteins of gamma, kappa and omicron SARS-CoV-2 variants were acquired from ProSci Incorporated.

2.2 Antibodies.

All anti-ACE2 antibodies were purchased from Abcam. This includes the rabbit monoclonal ab108209, the rabbit monoclonal ab108252 and rabbit polyclonal ab15348 antibodies. The anti- β -actin antibody 66009-1-Ig was purchased from Proteintech. The secondary antibodies used in western blot experiments were- goat anti-mouse HRP (GAMPO, P0447) and swine anti-rabbit HRP (SARPO, P0217) conjugates from DAKO Products. Murine HC-10 monoclonal antibody was a gift from Jacques Neefjes, and has also previously been described (Sernee, Ploegh, and Schust 1998).

The dilutions of primary antibodies used in western blotting experiments were as follows- anti-ACE2 ab108209, 1:1500; anti-ACE2 ab108252, 1:1500; anti-ACE2 ab15348, 1:3000 and anti- β -actin 66009-1-Ig (Proteintech), 1:10,000. Secondary antibodies dilutions used in western blotting were the following- goat anti-mouse HRP (GAMPO), 1:3000; swine anti-rabbit HRP (SARPO), 1:3000. The dilutions of primary antibodies used in immunofluorescence microscopy experiments were the following- anti-ACE2 ab15348, 1:100; HC-10, 1:00. The concentrations of secondary antibodies used in immunofluorescence experiments were as follows- donkey anti-rabbit IgG Alexa Fluor 488, 1:500 and donkey anti-mouse Alexa Fluor 594, 1:500.

2.3 Cell culture procedure.

Three different cell lines were used during this investigation, chosen to represent a range of human tissue types. The HaCaT cell line was selected to represent human skin tissue, as these are a form of immortalised epidermal keratinocytes. HaCaT cells utilised in this study were already available within the laboratory and were originally characterised by Boukamp (Boukamp et al. 1988). Foetal placental cells originating from an immortalised human choriocarcinoma (BeWo, ECACC 86082803) were also used. The HeLa cell line (ECACC 93021013) was established originally from immortalised epidermoid carcinoma cells present within a human cervical tumour. HaCaT and HeLa cell lines were obtained from laboratory stocks. Experiments were performed at passage numbers p18-p35 for HaCaT, p5-p12 for BeWo and p10-p35 for HeLa cell lines.

HaCaT cells were subcultured twice-weekly in Dulbecco's Modified Eagle's Medium (DMEM, Thermofisher Scientific) supplemented with 10% foetal bovine serum (FBS), 1% glutaMAX (Invitrogen) and 1% Pen-Strep (100 µg/mL penicillin, 100 µg/mL streptomycin, Invitrogen). The HeLa cell line was subcultured twice-weekly using Minimum Essential Medium (MEM, Thermofisher Scientific) containing 8% FBS along with 2 mM glutaMAX and 1% Pen-Strep. BeWo cells were subcultured weekly, in Ham's F-12 Medium (F-12, Thermofisher Scientific) supplemented with 10% FBS, 1% glutaMAX and 1% Pen-Strep. Passaging of cell lines was performed providing the cells had reached ~80% confluency for HaCaT and HeLa cells, and ~60% confluency for the BeWo cell line due to inability of BeWo cells to reach a high confluency. For cell passaging, cells were initially washed in 5 mL phosphate buffered saline (PBS) twice before 2 mL of Trypsin (Thermosphere Scientific) was added to the flask. Cells were allowed to trypsinise for 5-10 minutes and once detachment was confirmed with light microscopy, cells were re-suspended in fresh medium. The fresh medium containing cells was then diluted into new flasks at a dilution of 1:10 for HaCaT or HeLa cells and 1:2 for BeWo cells. All cell lines were cultured in T25 flasks and grown within a humidified incubator at 37 °C with 5% CO₂.

2.4 Cell treatments.

Cells grown for experimental treatments were trypsinised and transferred from flasks to 10 cm dishes. All cells were allowed to reach log growth phase before treatments were performed, with HaCaT and HeLa cells at 80% confluency, and BeWo cells at 60%. Fresh medium (DMEM for HaCaT, F-12 for BeWo and MEM for HeLa cells) was supplemented with the required chemical treatment and added to experimental dishes before the dishes were returned to the incubator. Once the time-course was completed, cells were removed from the incubator for media removal and cell lysis.

2.5 Cell lysis.

Following incubation of cell treatments for the required time, cells within the 10 cm dishes were lysed in an identical manner. The lysis buffer was prepared with, 10% MNT, 10% protease inhibitor cocktail (10 µg/mL chymotatin, 10 µg/mL leupeptin, 10 µg/mL antipain and 10 µg/mL pepstatin A, Sigma Aldrich) and 1% Triton X-100. The MNT buffer used in the lysis buffer consisted of 20 mM MES, 30 mM Tris-HCl and 100 mM NaCl. The MNT buffer ingredients were dissolved in di-H₂O to a total volume of 100 mL and the pH was adjusted to 7.4 before use. Following treatment, cells were removed from the 37 °C incubator. At this point, cell media was removed by pipette and transferred to Falcon tubes if required for further analysis. During cell lysis, treated cell dishes were kept on ice to halt biological activity. Treated cells were then washed twice with PBS for 5 minutes each. The remaining PBS was removed, and 250 mL lysis buffer was added to each dish. Cell scrapers were used to detach cells from dishes and the resulting cell lysates were collected into 1.5 ml Eppendorf tubes. Cell nuclei and additional cell debris was removed by centrifugation at 14,000 g (Eppendorf microcentrifuge) for 10 minutes at 4 °C. The supernatants present after this centrifugation step were then transferred into fresh Eppendorf tubes. Liquid nitrogen was used to flash-freeze the Eppendorf tubes before storage at -20 °C.

2.6 BCA protein assay.

After cell lysates were collected (section 2.5), protein concentration was determined to ensure equal loading of samples in subsequent experiments. Total protein concentration was quantified using a colorimetric Pierce Bicinchoninic Acid (BCA) Protein Assay Kit (ThermoFisher Scientific), with bovine serum albumin (BSA) used as a standard. The linear relationship between colour change (due to reduction of Cu²⁺ to Cu⁺) and overall protein concentration enabled accurate protein quantification. All BCAs were performed with 9 sets of duplicate BSA protein standards with concentrations ranging from 0-2000 µg/mL. The BSA standard solution was diluted to the required concentration with lysis buffer used during cell lysis (section 2.5). 25 µL measures of each standard and lysate sample were added to microplate wells of a 96-well plate in duplicate fashion. 200 µL of BCA working reagent was then added to each well before the plate was mixed thoroughly using a plate-shaker for 1 minute. The 96-well plate was then incubated at 37 °C for 30 minutes to allow for the colour change to occur. Absorbance values of each well were then measured using a spectrophotometer set at 562 nm. Averages of duplicate readings were calculated and the BSA protein standards were used to plot a standard curve. Absorbance values of lysate samples were then compared to the standard curve to determine overall protein concentration.

2.7 Orangu cytotoxicity assay.

Orangu cytotoxicity assays were performed to determine relative cell viability in response to a range of cell treatments. This assay is based on detection of dehydrogenase activity, which is representative of viable cell metabolism. The Orangu assay was performed according to the manufacturer's instructions. Cells were grown until ~80% confluence in suitable media within a 96-well plate. Cell treatments were then performed as stated above (2.4). After allowing 24 hours for treatment incubation, 10 μ L of Orangu solution was added to each well of the 96-well plate. The plate was then placed in a 37 °C incubator with 5% CO₂ and left for 3 hours to produce a detectable signal. The plate was then removed, and the absorbance of each well was measured at 450 nm using a spectrophotometer. Relative absorbance values of treated wells were used to compare cell viability between treatments.

2.8 SDS-PAGE and sample preparation.

The analysis of proteins within lysate samples was achieved using SDS-PAGE, an electrophoretic system for protein separation based upon molecular weight differences. By running both sample lysates and a molecular weight marker, protein sizes can be attributed to individual bands of protein. This process was performed prior to western blotting.

The acrylamide gels used in SDS-PAGE were cast using a template Hoefer mini dual gel casting system. 10% SDS-PAGE resolving gels were cast along with a stacking gel to improve resolution of proteins during electrophoresis. The recipes for resolving and stacking gels are shown in Table 1. The resolving gel was cast first and allowed to polymerise for 20 minutes, whilst a layer of di-H₂O was used to prevent the gel from shrinking. After the resolving gel had set, the di-H₂O was removed and stacking gel was cast on top of the resolving gel. A 10-well comb was inserted to create equally sized wells as the stacking gel was setting. After the stacking gel had also set, the gels were removed from the Hoefer caster and transferred to a Hoefer Mighty Small Mini Protein Electrophoresis Unit (Thermofisher Scientific). Refrigerated 1x TGS running buffer (5 mM Tris, 192 mM glycine, 0.1% SDS, pH 8.3) was used to fill the central cavity and the base reservoir, with buffer also covering the surface of the gel (BioRad, see Table 2). The comb was then removed to expose wells for loading.

Table 1: Volumes of ingredients required to cast two gels for western blotting experiments.

Ingredient (mL)	10% Resolving Gel	Stacking Gel
di-H ₂ O	7.2	2.2
40% Acrylamide	3.75	0.4
1.5M Tris [pH 8.8]	3.75	0.4
10% w/v SDS	0.15	0.03
10% w/v APS	0.15	0.023
TEMED	0.006	0.002

Sample lysates were stored in a -20 °C freezer until required. Samples were slowly thawed on ice before being spun in a centrifuge at 14,000 g for 5 minutes at 4 °C. The supernatant was used to immediately prepare samples for loading. The known protein concentration of each sample (determined by BCA) was used to prepare aliquots of equivalent total protein to ensure equal loading into wells. 20 µL aliquots of each sample were prepared to a concentration of 20 µg/µL using lysis buffer with the addition of 2 µL 500 mM DTT and 5 µL 2x Laemmli sample loading buffer (BioRad). These samples were then heated to 95 °C for 5 minutes before further centrifugation at 14,000 g for 5 minutes. The resulting supernatant was then loaded into wells of the gel.

6 µL of molecular weight marker (Precision Plus Protein™ Dual Color Standards, BioRad) was added to one or more wells to enable identification of sample band sizes. 15 µL of prepared lysate samples were then loaded into remaining wells. Once loading was completed, the gel was run at 40 mA for ~1 hour. The gels were then removed from the electrophoresis apparatus and used for western blotting and Coomassie staining experiments.

Table 2: Buffer solutions prepared for western blotting experiments.

Ingredient/ Condition	1x TGS Running Buffer (BioRad, 1L)	Transfer Buffer (1L)	5% w/v Milk Solution (100 mL)	Acid Stripping Buffer (200 mL)
Glycine (g)	14.41	14.5	-	3
Tris-Base (g)	3.03	2.9	-	-
SDS (g)	1	-	-	0.2
Non-fat milk powder (g)	-	-	5	-
TBST (mL)	-	-	100	-
di-H ₂ O (mL)	1000	800	-	200
Methanol (mL)	-	200	-	-
Tween-20 (mL)	-	-	-	2
Final pH	8.3	8.3	-	2.2

2.9 Western blotting.

Western blotting was performed following protein separation by molecular weight during SDS-PAGE. Proteins were transferred from gels onto polyvinyl difluoride (PVDF) membranes for further analysis. PVDF membranes were activated by submersion in methanol for 20 seconds. The gel containing proteins was placed into a transfer system (within a cassette) against the activated PVDF membrane, sandwiched between buffer-soaked filter papers and sponges. Electrophoretic transfer was performed at either 150 mA for 2 hours at 25 °C, or at 30 V overnight at 4 °C. In either case, both gel and membrane were fully submerged within transfer buffer during this step (Table 2). After transfer completion, 20 mL of a 5% milk solution was used to block the membrane to prevent non-specific binding from occurring (see Table 2). Membranes were incubated in the milk solution for 1 hour at 25 °C or overnight at 4 °C. After blocking, membranes were washed 5 times in TBST for 5 minutes each.

Primary antibody incubation was subsequently performed with the membranes, for either 1 hour at 25 °C or overnight at 4 °C. Primary antibodies were first diluted to the required concentration in a mixture of 2.7 mL TBST and 0.3 mL 5% milk solution. A further 5 TBST washes of 5 minutes each then followed before secondary antibody incubation for 1 hour at 25 °C. Secondary antibody incubation was performed with either goat anti-mouse HRP (GAMPO) or swine anti-rabbit HRP (SARPO) depending on the primary antibody species used. All antibody concentrations are described in section 2.2. The use of horseradish peroxidase (HRP)- bound secondary antibodies allowed chemiluminescent detection of specific protein-primary antibody complexes. 500 µL of enhanced chemiluminescence (ECL, GE Healthcare) solution was evenly applied to each membrane before visual detection of protein localisation was performed, either by manual development with photographic light-sensitive film, or by use of an iBright Imaging System (Invitrogen).

Membranes were occasionally stripped and re-probed with alternative antibodies. This was performed using an Acid Stripping Buffer described in Table 2. Membranes were first soaked in 25 mL of stripping buffer for 10 minutes. The stripping buffer was then removed and replaced with fresh stripping buffer and allowed to soak for a further 10 minutes. Stripping buffer was then removed and the membrane was washed twice with PBS, for 10 minutes each time. Finally, the membrane was washed twice with TBST for 5 minutes each. The stripped membrane was blocked with 5% milk in TBST as described above, before being washed and incubated with a primary and then secondary antibody.

2.10 Coomassie gel staining.

Following SDS-PAGE protein separation, the gels were gently washed in 100 mL di-H₂O for 10 minutes to remove residual SDS. The di-H₂O was then discarded before 20 mL PageBlue™ Protein Staining Solution (ThermoFisher Scientific) was added to the gel. Gels were gently agitated for 60 minutes before imaging with an iBright Imaging System (Invitrogen).

2.11 Immunofluorescence microscopy.

2 cm glass coverslips were placed into 12-well plates with sterile tweezers to provide a surface for cell growth. Cells used for immunofluorescence microscopy experiments were transferred from flasks into the 12-well plates along with a suitable cell medium and allowed to reach 80% (or 60% for BeWo cells) confluency. Treatments were then performed within the 12-well plates for the required duration. Cell media was removed using an aspirator before coverslips were washed in 2 mL phosphate buffered saline with calcium and magnesium (PBS⁺⁺) for 5 minutes. Cells were fixed to the coverslips with 4% paraformaldehyde (PFA, Agar Scientific) for 15 minutes before being

washed twice with PBS⁺⁺ for 5 minutes each. Cells were then permeabilised by incubation of the coverslips in 0.1% Triton X-100 in PBS⁺⁺ for 10 minutes at 25 °C. For non-permeabilised cells, coverslips were instead incubated in PBS⁺⁺ only. In either case, the coverslips were then washed three times in PBS⁺⁺ for 5 minutes. Sample coverslips were then blocked in a solution of 0.2% bovine serum albumin (BSA) in PBS⁺⁺ for 15 minutes. Primary antibodies were diluted to the required concentration in a 0.2% BSA solution, before incubation with coverslips for 2 hours at 25 °C or overnight at 4 °C. In cases of co-incubation, two primary antibodies were mixed before incubation with coverslips. Cells were then washed 3 times in PBS⁺⁺ for 5 minutes each to remove unbound antibodies. After this, suitable secondary antibodies were diluted to the required concentration of 1:500 in PBS⁺⁺ before incubation with the coverslip for one hour at 25 °C. Coverslips were washed a further 3 times in PBS⁺⁺ for 5 minutes each. After excess PBS⁺⁺ was removed by aspiration, 50 µL of a 5 µg/mL DAPI solution was applied to each coverslip and incubated for 5 minutes. Coverslips were then washed briefly in PBS⁺⁺ before they were mounted onto glass microscope slides with 6 µL soft-set Vectashield mounting medium (Vector Labs). The mounting medium was allowed to dry for 10 minutes before coverslips were sealed with nail varnish. Microscope slides were stored at 4 °C in the dark until inspection using a Carl Zeiss 800 Confocal Microscope. Captured images were analysed using Zen Blue Edition software (Zeiss).

2.12 ELISA assay.

Enzyme linked immunosorbent assays (ELISAs) were utilised for quantification of specific proteins within biological samples. The cell media extracted from treated dishes was used as samples for analysis of potential cytokine secretion. Following incubation of cell treatments, experimental plates were removed from the 37 °C incubator and serological pipettes were used to transfer cell media into 5 mL Falcon tubes. Cell lysates were also obtained from these experimental dishes. Cell media was concentrated using Microcon centrifugal filters to increase protein concentration (Sigma Aldrich). Media was placed into filter tubes with a 3000 Da molecular weight cut-off before centrifugation at 14,000 g for 15 minutes, at 4 °C. The filtered supernatants were retained and used as samples in the ELISA. BCA assays were used to confirm sample concentration had occurred. Two separate ELISA kits were used during the experimental procedure, Human TNF- α ELISA Kit ab181421 (Abcam) and Human TNF- α ELISA Kit (Sigma Aldrich). The Sigma Aldrich kit was used for the initial TNF- α quantifications only, with the Abcam kit being used for all subsequent ELISA experiments. Both sandwich ELISAs were performed according to the manufacturer's instructions.

The Sigma Aldrich ELISA kit was used as follows. All solutions stated here were provided within the kit (Sigma, RAB0476). Reagents and samples were brought to room temperature before powdered TNF- α was dissolved in di-H₂O to create a dilution series of TNF- α . Eight TNF- α

standards were prepared, ranging from 0-6000 pg/mL. 100 μ L of standards and cell media were added into the appropriate wells in duplicate. The ELISA plate was covered for 2.5 hours at 25 $^{\circ}$ C. The wells were then emptied and washed 4 times with 300 μ L 1x Wash Buffer (RABWASH4). 100 μ L of 1x Detection Antibody (RAB0476D) was then added to each well. Wells were covered and allowed to incubate for 1 hour at 25 $^{\circ}$ C. The wash step was then repeated. 100 μ L of HRP-Streptavidin (RABHRP5) was then added to each well before a 45-minute incubation step. This solution was then discarded, and the wells were washed a further 4 times with 1x Wash Buffer. 100 μ L of Colorimetric TMB Reagent (RABTMB3) was added to each well to induce the colour-change reaction. Wells were once again covered and the plate was incubated for 30 minutes in the dark at 25 $^{\circ}$ C, with gentle shaking. 50 μ L of Stop Solution (RABSTOP3) was then added to each well, halting the reaction. A spectrophotometer was used to determine absorbance of wells in the ELISA plate. A standard curve was plotted using the standard absorbance values, enabling quantification of TNF- α concentration in each sample.

The Abcam ELISA Kit ab181421 is a single-wash, 90-minute sandwich ELISA created with SimpleStep ELISA technology (Abcam). All listed buffer solutions and reagents were provided within the ELISA kit. Materials were equilibrated to room temperature prior to use. Lyophilised TNF- α was dissolved in 100 μ L of di-H₂O to produce a stock solution. The stock TNF- α solution was used to create a serial dilution of TNF- α through addition of a sample diluent to generate standards ranging from 0-2000 pg/mL. 50 μ L of concentrated cell culture media samples and 50 μ L of each TNF- α standard were added to individual wells of the 96-well microplate. An antibody cocktail was then prepared with 150 μ L capture antibody, 150 μ L detector antibody and 2.7 mL antibody diluent. 50 μ L of the antibody cocktail was added to each well. The microplate was covered and incubated for 1 hour at 25 $^{\circ}$ C on a plate shaker. Each well was then washed with 350 μ L of wash buffer. Each wash was repeated three times. 100 μ L of TMB substrate was added to each well and incubated on a plate shaker for 10 minutes in the dark. Colour development was stopped by the addition of 100 μ L of stop solution into each well. The microplate was transferred to a plate shaker for 1 minute before the optical density of each well was measured using a spectrophotometer at 450 nm. The signal generated is proportional to the amount of bound analyte. TNF- α standards were then used to produce a standard curve, with sample absorbance readings able to provide quantitative measurements.

Section 3.0 Results

3.1 ACE2 expression in BeWo, HaCaT and HeLa cell lines.

An investigation into ACE2 expression was undertaken based upon previous preliminary findings in the laboratory that detected ACE2 across a range of mammalian tissues and cell types. As ACE2 acts as the functional entry receptor for SARS-CoV-2, the validation of ACE2 detection on a cell line demonstrates the likely susceptibility of the cell to SARS-CoV-2 infection (Jackson et al. 2021). TMPRSS2 expression is also important for priming SARS-CoV-2 spike proteins to facilitate viral invasion.

In order to study the ACE2-spike protein interaction during COVID-19 infection, a range of cell lines were selected to represent a variety of human cell types. Whilst lung epithelial cells have largely been the primary focus of SARS-CoV-2 infection studies, alternative body tissues display susceptibility. HaCaT, BeWo and HeLa cell lines were chosen for this investigation, as these immortalized cell lines are derived from skin keratinocytes, foetal placental cells, and a cervical carcinoma, respectively.

Previous research has suggested that expression of ACE2 and TMPRSS2 varies across these cell lines (Figure 3). mRNA expression data derived from The Human Protein Atlas database was utilized to assist investigation of the cell lines. BeWo and HaCaT cell lines expressed high levels of ACE2 mRNA, with BeWo cells also displaying considerable TMPRSS2 expression. Published transcriptomic data also showed that the HeLa cell line is not expected to express ACE2, with little TMPRSS2 expression. A search of the available literature supported this observation, suggesting HeLa cells are not natural hosts for the SARS-CoV-2 virus (Stelzer-Braid et al. 2020).

However, in contradiction to this, preliminary experiments by members of the laboratory detected possible ACE2 expression in HeLa cells with the anti-ACE2 antibody ab15348. Thus, an aim of this thesis was to clarify whether ACE2 protein could be reproducibly detected within the HeLa cell line. Resolution of this finding may have important implications for the use of cell lines as models for studying the interaction between SARS-CoV-2 and susceptible cells.

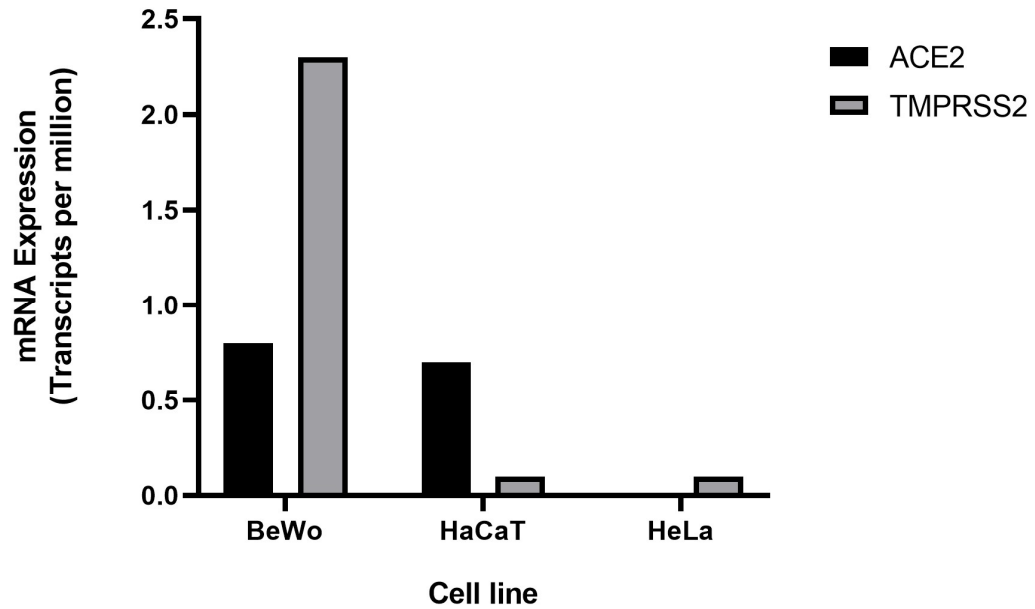


Figure 3: Database-derived ACE2 and TMPRSS2 expression data.

Expression profiles of ACE2 and TMPRSS2 mRNA have been previously determined for several mammalian cell lines, with this data compiled into The Human Protein Atlas database (Uhlén et al. 2015). BeWo cells exhibit substantial expression of both ACE2 and TMPRSS2. HaCaT keratinocytes and HeLa cervical cancer cells exhibit lower TMPRSS2 expression, with HeLa cells determined to not express ACE2.

3.1.1 Effects of mouse derived IFN- γ upon ACE2 expression.

Initial experiments were performed to validate whether ACE2 expression could be detected in lysates obtained from HaCaT, BeWo and HeLa cells. The interaction between the RBD of the viral spike protein and ACE2 of the host cells precedes viral entry and thus efficient virus infectivity requires ACE2 expression. To confirm native ACE2 expression within these three cell lines, western blot experiments were performed. The effects of an IFN- γ cytokine treatment upon expression levels was also investigated. *ACE2* has been characterized as an interferon-stimulated gene (ISG) and as such, the type II interferon IFN- γ was hypothesized to increase levels of ACE2.

To explore this, HaCaT, BeWo and HeLa cell cultures were incubated either with standard media or with media supplemented with 60 ng/mL murine-derived IFN- γ for 24 hours before cell lysates were extracted. Lysates were analysed by SDS-PAGE and immunoblotting with rabbit anti-ACE2 antibody ab15348.

Bands corresponding to ACE2 protein were detected within all three cell lines, suggesting the expression of this membrane receptor (Figure 4). Susceptibility towards SARS-CoV-2 infection can be inferred from this result, suggesting that HaCaT, BeWo and HeLa cell lines could be used to evaluate spike-ACE2 interactions. Two bands corresponding to the known molecular weight of ACE2 (100-130 kDa) were identified for each sample. This likely represents the extensive glycosylation that ACE2 undergoes during post-translational modification.

With previous investigations having identified *ACE2* as an ISG, IFN- γ treatments were performed to determine cytokine-mediated ACE2 upregulation in cell lines derived from skin, placental and cervical tissues. Following 24hr treatment of HaCaT, BeWo and HeLa cells with IFN- γ , ACE2 levels appeared to be slightly upregulated when compared to the untreated controls in each case (Table 3). Expression of β -actin was ascertained with the 66009-1-Ig anti- β -actin antibody. The β -actin band obtained was used as a control to establish equal loading of protein lysates for each sample. Pixel density analyses determined that ACE2 levels were greater following IFN- γ treatment than in untreated cells of the same cell line (Table 3). The relative increase in ACE2 expression was greatest for cells of the HaCaT cell line, whilst BeWo and HeLa cells showed smaller changes in response to IFN- γ treatment (Table 3). Whilst FIJI densitometry suggests some interferon-induced upregulation has occurred, additional repeats are required to perform rigorous statistical analysis of expression.

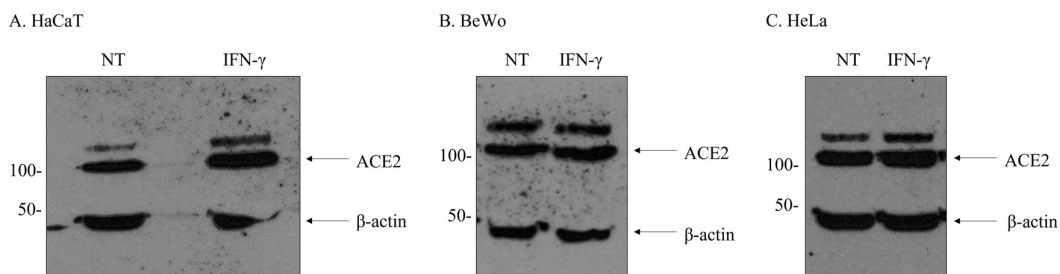


Figure 4: ACE2 expression following murine-derived IFN- γ treatment.

Western blot analysing the expression of ACE2 in cell lysates of HaCaT (A), BeWo (B) and HeLa (C) cells. Cells were either untreated (NT) or treated with 60 ng/mL mouse-derived IFN- γ for 24 hours (IFN- γ). ACE2 doublets at ~110 kDa were observed in all cell lines for both untreated and IFN- γ treated cells, with β -actin control bands present at ~40 kDa. X-ray film was used for imaging chemiluminescent blots.

Table 3: Relative ACE2 expression for untreated (NT) and mouse IFN- γ treated (IFN- γ) cells.

Western blots shown in Figure 4 were analyzed using ImageJ (FIJI) software. Quantitative comparison of band densities was performed, and relative density values were obtained with measurements of protein loading (β -actin). IFN- γ treated cells showed slight ACE2 increases in BeWo and HeLa cells, with HaCaT cells demonstrating the greatest increase in ACE2 expression.

Cell line	Relative density of ACE2 normalized to β -actin (NT:IFN- γ)
HaCaT	1:2.44
BeWo	1:1.12
HeLa	1:1.20

3.1.2 Human-derived IFN- γ mediates ACE2 expression.

The influence of cytokines on the levels of ACE2 expression are especially critical during SARS-CoV-2 infection due to the association of cytokine storms with severe disease phenotypes. Furthermore, maintenance of stable ACE2 levels is required for cardiovascular health and regulation of blood pressure (Burrell et al. 2004). Following analysis of the effects of mouse-derived IFN- γ upon ACE2 levels, additional experiments were performed using human IFN- γ protein. IFN- γ from a non-human species exhibits sequence differences. This may affect how IFN- γ interacts with receptor proteins and their signalling pathways including JAK-STAT, which in turn may alter the regulation of target genes, including ACE2. Therefore, human-derived IFN- γ was used to validate ACE2 upregulation observed with the murine cytokine. TNF- α was tested alongside IFN- γ as an additional example of a proinflammatory cytokine in COVID-19.

Cells of the HaCaT, BeWo and HeLa cell lines were treated with media containing 60 ng/mL IFN- γ or 30 ng/mL TNF- α , alongside untreated controls for 24 hours. Lysates were acquired and subjected to analysis through SDS-PAGE and western blotting using the ab15348 anti-ACE2 antibody. Analysis of western blots was performed using an iBright machine instead of X-ray film for greater sensitivity and ease of analysis. The resulting western blots are depicted in Figure 5. Normalisation of β -actin control band pixel densities were performed to provide semi-quantitative analysis of the western blots (Table 4).

Clear bands corresponding to ACE2 were present in all samples derived from the HaCaT cell line (Figure 5). Clear upregulation of ACE2 was observed in HaCaT cells in response to human-derived IFN- γ and TNF- α (Table 4). Whilst both cytokines induced ACE2, the effect of IFN- γ treatment appeared greater than that of TNF- α . ACE2 doublets were also observed, indicating likely glycosylation of HaCaT ACE2 protein (Figure 5).

For BeWo cells, ACE2 was detected in untreated cells and in the presence of IFN- γ and TNF- α treatments (Figure 5). No doublets were observed for ACE2, although a possible ACE2 fragment was observed at ~80 kDa for untreated BeWo cell lysate. ACE2 expression initially appeared similar between treatments for BeWo cells (Figure 5), however corrections for protein loading showed both IFN- γ and TNF- α mildly upregulated ACE2 levels when compared to the untreated control (Table 4). TNF- α was a more potent inducer of ACE2 than IFN- γ in BeWo cells following 24-hour treatments (Table 4).

HeLa cells showed limited levels of ACE2 expression in this experiment despite sufficient protein loading for both untreated, IFN- γ and TNF- α treated lysates (Figure 5). However, both IFN- γ and TNF- α appeared to mildly induce ACE2 upregulation in HeLa cells (Table 4). Following normalisation of protein loading controls, TNF- α and IFN- γ treatments upregulated ACE2, with

TNF- α acting as a stronger stimulant than IFN- γ in this model (Table 4). Reproducing these results with independent experiments is needed to corroborate the findings displayed here.

Coomassie staining was also performed on the protein lysates used in Figure 5. These lysates were loaded onto additional polyacrylamide gels alongside those used for the western blotting experiments. Coomassie gel staining determined that the overall protein composition of each lysate was not greatly affected by either 60 ng/mL IFN- γ or 30 ng/mL TNF- α treatment after 24 hours (Figure 6). In addition, Coomassie staining also acted as a secondary loading control for western blotting experiments. Furthermore, the presence of well-defined bands also demonstrates the protein quality of the samples, with no apparent protein degradation (Figure 6).

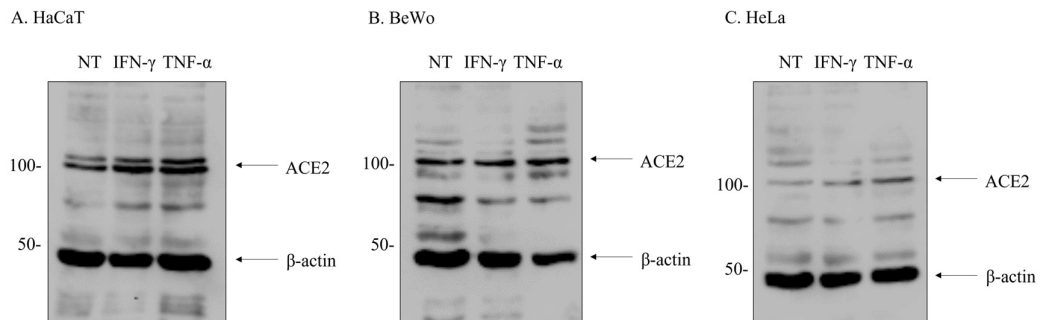


Figure 5: The effects of human IFN- γ and TNF- α upon ACE2 expression.

Western blots demonstrating the effect of cytokine treatments on ACE2 expression in HaCaT (A), BeWo (B) and HeLa (C) cells. Cells were incubated in untreated media (NT), or in media supplemented with either 60 ng/mL IFN- γ (IFN- γ) or 30 ng/mL TNF- α (TNF- α) before samples were loaded on a 10% acrylamide gel. Bands corresponding to ACE2, and β -actin are present at ~100kDa and ~45kDa respectively.

Table 4: Relative ACE2 expression for untreated (NT), human IFN- γ treated (IFN- γ) and TNF- α treated cells.

Western blots depicted in Figure 5 were analyzed using ImageJ (FIJI) software. Quantitative measurements of band densities were taken, and relative density values were calculated and normalized to protein loading with β -actin. All cell lines demonstrated increased ACE2 expression in response to cytokine treatments.

Cell line	Relative density of ACE2 normalized to β -actin (NT:IFN- γ)	Relative density of ACE2 normalized to β -actin (NT:TNF- α)
HaCaT	1:1.93	1:1.74
BeWo	1:1.31	1:1.83
HeLa	1:2.27	1:3.16

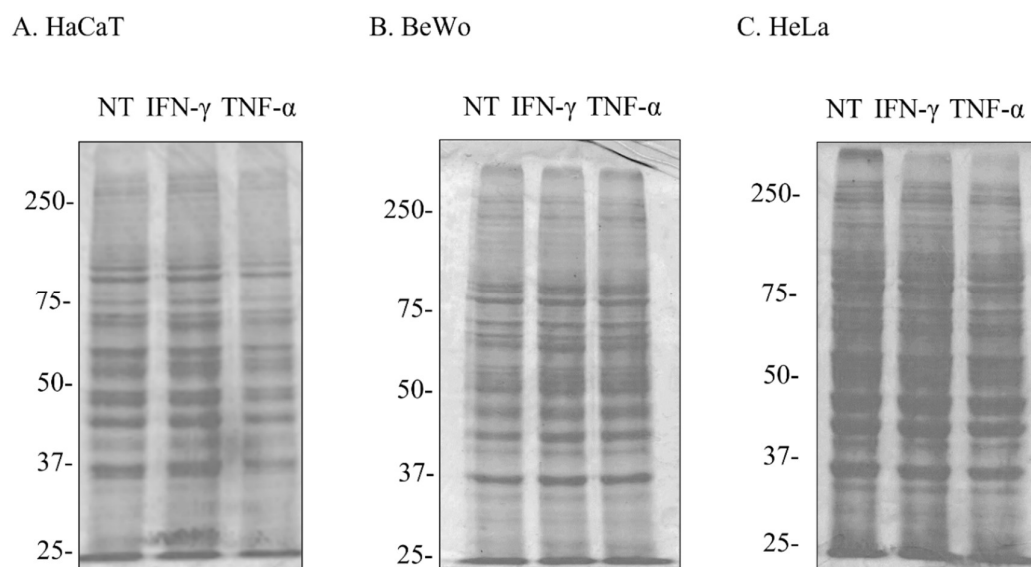


Figure 6: Cell lysate protein composition is unaffected by either IFN- γ or TNF- α treatment. Coomassie stained SDS-PAGE gels showing sample lysates are not greatly altered in HaCaT (A), BeWo (B) and HeLa (C) cells. 10% acrylamide gels were loaded with sample lysate (used in Figure 5) following treatment of cells with either untreated media (NT), 60 ng/mL human IFN- γ (IFN- γ) or 30 ng/mL TNF- α (TNF- α). Molecular weights (kDa) are displayed on the left-hand side of each gel.

3.2 Synergistic effects of IFN- γ and TNF- α on ACE2 expression.

Previous reports of cytokine mediated ACE2 upregulation have been supported by the initial experiments in section 3.1. However, the diversity and interplay of individual cytokine responses is unclear. Combination treatments of multiple cytokines can lead to greater ACE2 expression than the sum of the individual cytokines, indicating that a synergistic effect may exist between immunoregulatory proteins (Coperchini et al. 2020). Regulation of ACE2 through cytokine-induction is likely dependent upon the specific cytokines present and cell type. To test whether regulatory elements of ACE2 production may be influenced by the presence of multiple cytokines, combination treatments were devised. If combined cytokines induce a greater ACE2 response than the additive effects of individual cytokines, a synergistic effect may be observed in western blots.

HaCaT and BeWo cells were treated with media supplemented with either 60 ng/mL IFN- γ or 30 ng/mL TNF- α , or with a combination of both for 24 hours. Lysates were then analysed by SDS-PAGE and western blotting with the anti-ACE2 antibody ab15348 (Figure 7). Untreated cell lysates were used as controls. A β -actin control was unavailable for this experiment.

ACE2 was detected in HaCaT cells following cytokine incubation, with protein doublets identified at ~110 kDa following IFN- γ , TNF- α , combined treatments, as well as in untreated cells (Figure 7). Additional ACE2 bands were also seen at 40 kDa and 140 kDa in each treatment type, possibly reflecting alternative isoforms of ACE2 (Figure 7). Levels of ACE2 were similar in response to IFN- γ and TNF- α treatments. The combination of IFN- γ and TNF- α may have resulted in slightly higher ACE2 expression when compared to individual treatments, suggesting a synergistic response may exist between these cytokines (Figure 7). However, this experiment requires follow-up, since ACE2 expression in the untreated sample was difficult to quantify accurately because of background staining. Nevertheless, glycosylated ACE2 was indicated by bands present at greater than 120 kDa (Figure 7). Potential forms of ACE2 were detected at ~40 kDa, with similar expression apparent for IFN- γ , TNF- α and IFN- γ + TNF- α treatments, with untreated lysates expressing lower levels of these fragments.

BeWo cells that were either untreated, or treated with IFN- γ , TNF- α , or both IFN- γ and TNF- α expressed detectable levels of ACE2 (Figure 7). Levels of ACE2 did not vary considerably between untreated and 60 ng/mL IFN- γ treated BeWo cells, in contrast to previous results (Figure 7). However, TNF- α alone and a combination of IFN- γ and TNF- α appeared to upregulate ACE2 in BeWo cells (Figure 7). Levels of ACE2 expression were not clearly different between TNF- α and IFN- γ + TNF- α treatments, suggesting no synergistic effects between these cytokines. Multiple high molecular weight bands (>110 kDa) were detected for both TNF- α and IFN- γ + TNF- α treated cells, but not in untreated or IFN- γ treated lysates (Figure 7). Low molecular weight bands indicating ACE2 fragment proteins were less apparent in BeWo than HaCaT cell lysates (Figure 7).

A. HaCaT

B. BeWo

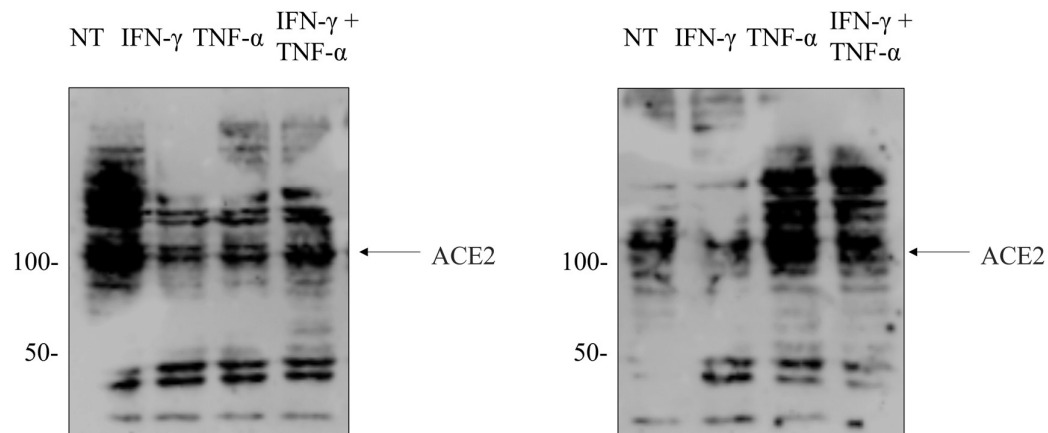


Figure 7: Synergistic effect of IFN- γ and TNF- α on ACE2 expression.

Western blots showing the effects of individual and combined cytokine treatments on levels of ACE2 expression in HaCaT (A) and BeWo (B) cells. Cells were incubated in either untreated media (NT), or in media containing 60 ng/mL IFN- γ (IFN- γ), 30 ng/mL TNF- α (TNF- α) or both 60 ng/mL IFN- γ and 30 ng/mL TNF- α (IFN- γ + TNF- α). Molecular weight markers are indicated on the left (kDa).

A. ab108209

B. ab108252

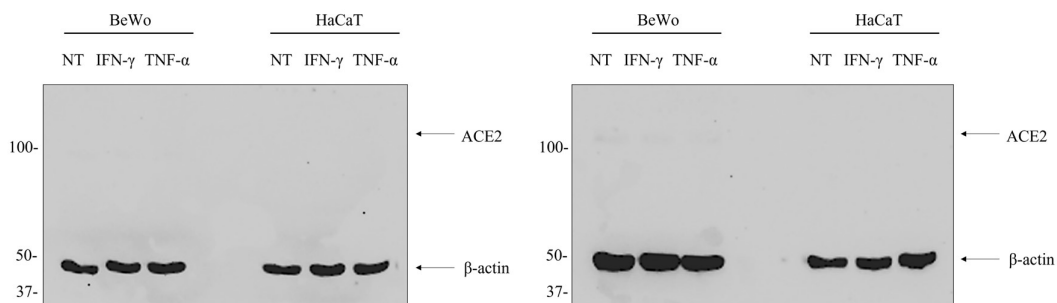


Figure 8: Testing alternative commercially available anti-ACE2 antibodies.

Two monoclonal anti-ACE2 antibodies supplied by Abcam, ab108209 (A) and ab108252 (B), were selected for immunoblotting in cell lines previously determined to express ACE2. Cells were incubated in either untreated media (NT), or in media containing 60 ng/mL IFN- γ (IFN- γ) or 30 ng/mL TNF- α (TNF- α). Molecular weights (kDa) are displayed on the left-hand side and labels corresponding to expected ACE2 and β -actin protein bands are shown.

3.3 ACE2 immunoblotting with alternative anti-ACE2 antibodies.

The western blotting experiments in Figures 4, 5 and 7 demonstrated that the anti-ACE2 antibody ab15348 detected expression of ACE2 in cell lysates derived from a range of cell lines. Having observed clear ACE2 protein in HaCaT and BeWo cell lines, immunoblotting experiments were performed with additional antibodies against the ACE2 protein. This would provide a basis for evaluating the performance of independent anti-ACE2 antibodies and to allow selection of the most appropriate and effective monoclonal antibodies for subsequent experiments. Therefore, western blotting experiments were devised to test two additional commercially available anti-ACE2 antibodies.

HaCaT and BeWo cells were treated for 24 hours with media containing either 60 ng/mL IFN- γ or 30 ng/mL TNF- α before cell lysis was performed. SDS-PAGE and western blotting was then performed using the resulting cell lysates, with two anti-ACE2 monoclonal antibodies selected; ab108209 and ab108252. These antibodies are both rabbit-derived and raised against synthetic peptides. Both primary antibodies were utilised at a dilution recommended by the manufacturer (1:1000). Western blot membranes were subsequently reprobbed with β -actin; the results are displayed in Figure 8.

Both western blots showed that the selected anti-ACE2 antibodies did not detect ACE2 protein under the conditions used. No observable signal was produced at the 110 kDa region following probing with either ab108209 or ab108252 monoclonal antibodies (Figure 8). This was observed for lysates obtained from both HaCaT and BeWo cell lines. Bands corresponding to β -actin at ~45 kDa, showed that loading of samples was equivalent across treatment types for each cell line (Figure 8). The strength of β -actin signal also demonstrated that sufficient protein lysate had been loaded for detection, however positive ACE2 controls are lacking in this experiment.

3.4 Recombinant SARS-CoV-2 spike treatments do not alter ACE2 expression.

Following engagement of the SARS-CoV-2 spike with the ACE2 receptor, internalisation of ACE2 and subsequent degradation can lead to downregulation of surface ACE2 protein within bronchial epithelial cells (Y. Lu et al. 2022). However, treatment with recombinant SARS-CoV-2 spike protein demonstrates conflicting outcomes, with the extent and direction of affected ACE2 expression dependent upon various factors including cell type, spike protein concentration and experimental conditions. Furthermore, the amino acid composition of spike proteins, altered between SARS-CoV-2 variants (Figure 2), may influence the effects of spike treatment through modification of spike-ACE2 binding. To investigate the effects of SARS-CoV-2 spike proteins upon cell lines demonstrated to express ACE2, western blotting experiments were devised for keratinocytes and placental cells using commercially supplied recombinant spike proteins.

HaCaT and BeWo cell lines were subjected to 24-hour treatment +/- 50 ng/mL or 500 ng/mL SARS-CoV-2 spike proteins of variants gamma (γ), kappa (κ) or omicron (\omicron). Protein lysates were then harvested and analysed by western blotting with the ACE2 mAb ab15348 (Figure 9).

Clear bands corresponding to ACE2 protein were detected in both untreated and SARS-CoV-2 spike protein treated cell lysates obtained from both HaCaT and BeWo cell lines (Figure 9). ACE2 expression was observed as a single band in all lysates. No doublets were seen in control or treated cells of the HaCaT and BeWo cell lines (Figure 9), contrasting with results of previous experiments.

For HaCaT cell lysates, there was a strong protein signal. Positive signals in all lanes indicated that ACE2 was detectable in the presence of SARS-CoV-2 spike proteins at concentrations of both 50 ng/mL and 500 ng/mL (Figure 9). ACE2 did not appear to vary considerably between any two HaCaT samples. Furthermore, a ten-fold increase in spike protein concentration (from 50 to 500 ng/mL) had little effect upon ACE2 (Figure 9). The nature of the SARS-CoV-2 variant from which the spike protein was sourced also did not appear to significantly affect ACE2 expression levels following treatment for cells of the HaCaT cell line (Figure 9).

A positive signal at ~105 kDa for BeWo cell lysates demonstrated that ACE2 was detectable following all spike protein treatments (Figure 9). ACE2 expression was greatest in untreated cell lysates, when compared to lysates treated with 500 ng/mL of spike proteins from either gamma, kappa, or omicron variant SARS-CoV-2 (Figure 9). Levels of ACE2 in BeWo cell lysates were also not influenced by the variant type of SARS-CoV-2 from which the spike proteins were derived (Figure 9). However, lack of an available protein loading controls for both HaCaT and BeWo samples limited interpretation of the differences in ACE2 expression between lysates.

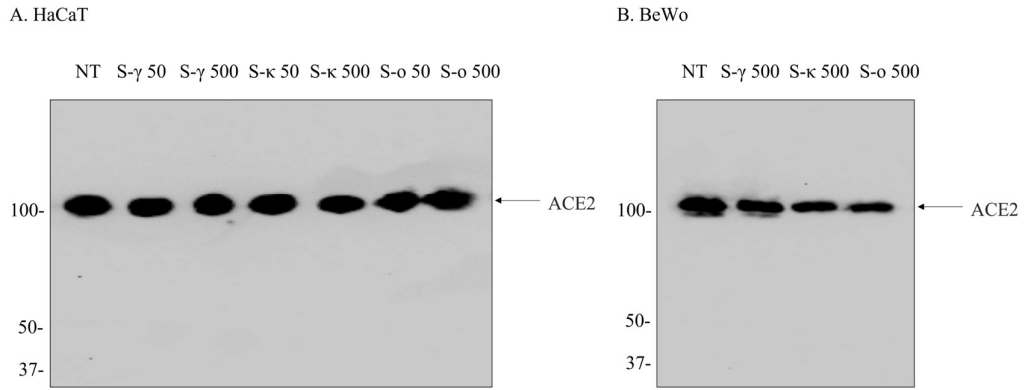


Figure 9: SARS-CoV-2 spike protein treatments do not appear to affect ACE2 expression. Western blots demonstrating the effects of spike protein variants upon expression of the ACE2 receptor in HaCaT (A) and BeWo cells (B). Cells were treated with either 50 ng/mL (50) or 500 ng/mL (500) of spike proteins derived from the SARS-CoV-2 variants gamma (γ), kappa (κ) or omicron (\omicron). Sample lysates were run on 10% acrylamide gels, with ab15348 used for ACE2 detection. A β -actin antibody was unavailable for this experiment. Molecular weights (kDa) are displayed on the left-hand side.

3.5.1 ACE2 detection in HaCaT cells with immunofluorescence microscopy.

Initial experiments indicated that HaCaT cells express ACE2 and that cytokines may induce upregulation of ACE2 expression in this cell line (Figures 4 and 5). Following analysis of these western blots, immunofluorescence microscopy experiments were devised to validate the findings. ACE2 is expressed on the surface of epithelial keratinocytes. Cytokine treatments may induce upregulation of surface ACE2, with detection of this protein hypothesised to increase following incubation of cells with IFN- γ . ACE2 increases were also anticipated in response to greater interferon concentration (Figures 4 and 5).

HaCaT cells were grown to 80% confluence before incubation with media containing +/- 30 ng/mL or 60 ng/mL IFN- γ for 24 hours. Following treatment, cells were fixed before incubation with an antibody against ACE2. DAPI was also applied to stain nuclear DNA. A Zeiss 800 microscope was used to inspect cells.

Immunofluorescence microscopy demonstrated ACE2 expression in HaCaT cells (Figure 10). Staining corresponding to ACE2 was observed following no treatment and for 30 ng/mL and 60 ng/mL IFN- γ treatments. ACE2 expression was detected both at the cell surface and intracellularly for all treatment types (Figure 10). Examination of merged images demonstrated weak distributed ACE2 in HaCaT cells. Overall ACE2 expression appeared unchanged in untreated cells and in both 30 ng/mL IFN- γ and 60 ng/mL IFN- γ treated cells (Figure 10).

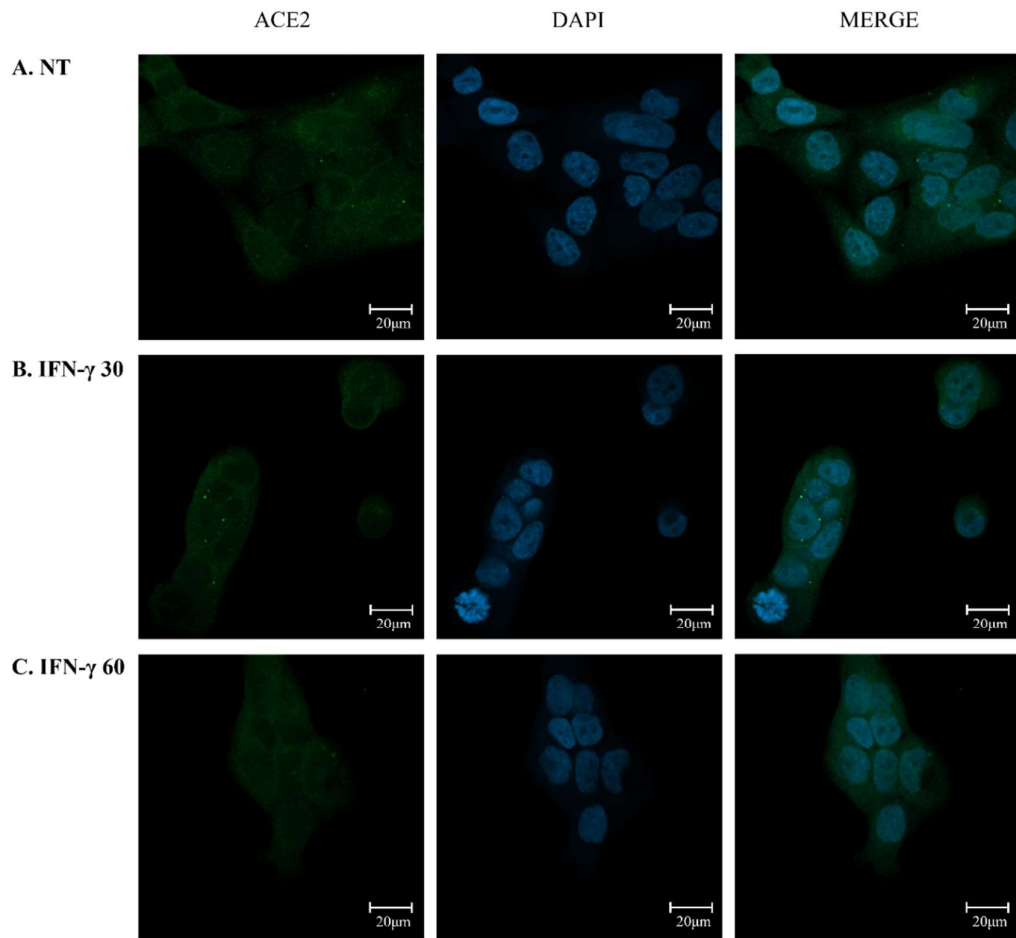


Figure 10: Visualization of ACE2 in HaCaT cells following IFN- γ treatment.

Immunofluorescence microscopy was performed on HaCaT cells that were untreated (A) or treated with either 30 ng/mL IFN- γ (B) or 60 ng/mL IFN- γ (C) for 24 hours. Fixed cells were incubated with the anti-ACE2 antibody ab15348 (green) prior to imaging. DAPI stain was used to visualize nuclear DNA (blue). All images were taken on a Zeiss 800 microscope. Scale bars are displayed.

3.5.2 ACE2 detection in BeWo cells with immunofluorescence microscopy.

Previous experiments have determined ACE2 expression in BeWo cells. Furthermore, possible cytokine stimulated ACE2 upregulation in BeWo cells was observed by western blotting (Figures 4 and 5). To confirm ACE2 expression in the presence and absence of cytokines, immunofluorescence microscopy was performed.

BeWo cells were treated with either 30 ng/mL or 60 ng/mL IFN- γ for 24 hours, alongside untreated controls. Cells were then fixed and incubated with the anti-ACE2 antibody ab15348. DAPI was also applied to indicate nuclear DNA. A Zeiss 800 microscope was used to inspect cells.

ACE2 expression was detected in BeWo cells with immunofluorescence microscopy (Figure 11). ACE2 was expressed in untreated cells and in those treated with 30 ng/mL or 60 ng/mL IFN- γ . Untreated cells appeared to express lower levels of ACE2 than cells treated with either interferon for 24 hours (Figure 11). Indeed, ACE2 signal appeared strongest following 30 ng/mL IFN- γ treatment (Figure 11B). For untreated cells, ACE2 was determined both within the nucleus and at the cell membrane (Figure 11A). For both 30 ng/mL and 60 ng/mL IFN- γ treatments, ACE2 appeared to be predominantly located at the surface of BeWo cells. Irrespective of treatment, dense clusters of BeWo cells expressed greater levels of cell-surface ACE2 and lower levels of internalised ACE2 (Figure 11).

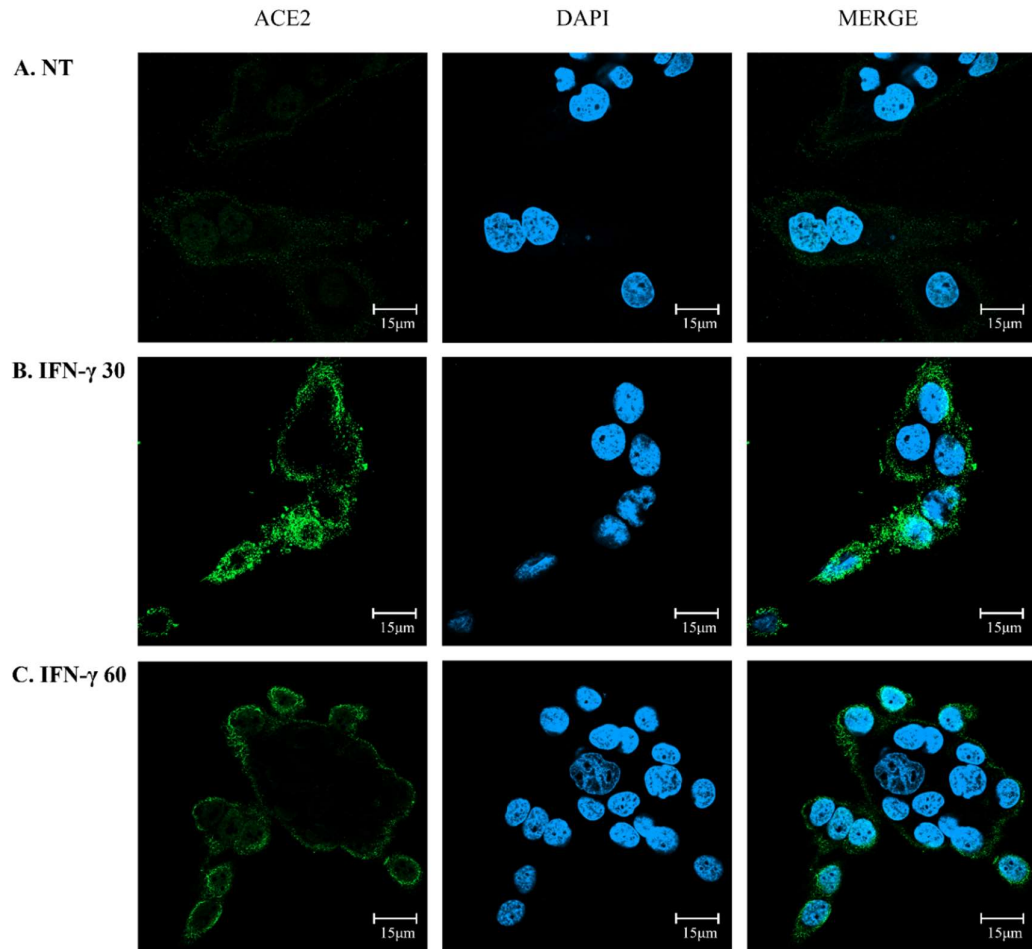


Figure 11: Visualization of ACE2 in BeWo cells after IFN- γ treatment.

BeWo cells were stained with the anti-ACE2 mAb ab15348 (green) and anti-rabbit Alexa Fluor 488 to observe expression of ACE2. DAPI stain (blue) was used to locate nuclear DNA. Prior to fixing, BeWo cells were incubated with untreated media (A), or in media supplemented with either 30 ng/mL IFN- γ (B) or 60 ng/mL IFN- γ (C) for 24 hours. All images were taken on a Zeiss 800 microscope. Scale bars are shown.

3.5.3 ACE2 detection in HeLa cells with immunofluorescence microscopy.

The expression of ACE2 in HeLa cells was uncertain, with contrasting results previously described (Figures 4 and 5). Furthermore, whilst interferon treatments can increase ACE2 expression in certain tissues and cell lines, evidence of this occurring within HeLa cells has not been previously reported.

HeLa cells were grown to 80% confluence before treatment with media containing +/- 30 ng/mL or 60 ng/mL IFN- γ for 24 hours. After treatment, cells were fixed before incubation with antibodies against ACE2. DAPI was also used to stain nuclear DNA. A Zeiss 800 microscope was used to inspect slides.

ACE2 was detected in untreated HeLa cells and those treated with either 30 ng/mL or 60 ng/mL IFN- γ (Figure 12). ACE2 expression was predominantly localised to elongated filopodia-like extensions of the cell membrane in the examined HeLa cells. Overall levels of ACE2 expression were similar for HeLa cells regardless of treatment type (Figure 12). For 60 ng/mL IFN- γ treated HeLa cells, ACE2 expression directly surrounding the nucleus was potentially greater than that observed in untreated and 30 ng/mL IFN- γ treated cells (Figure 12). Whether the ab15348 antibody used is truly detecting ACE2 protein will require future experiments, such as validation with an ACE2 knockout cell line.

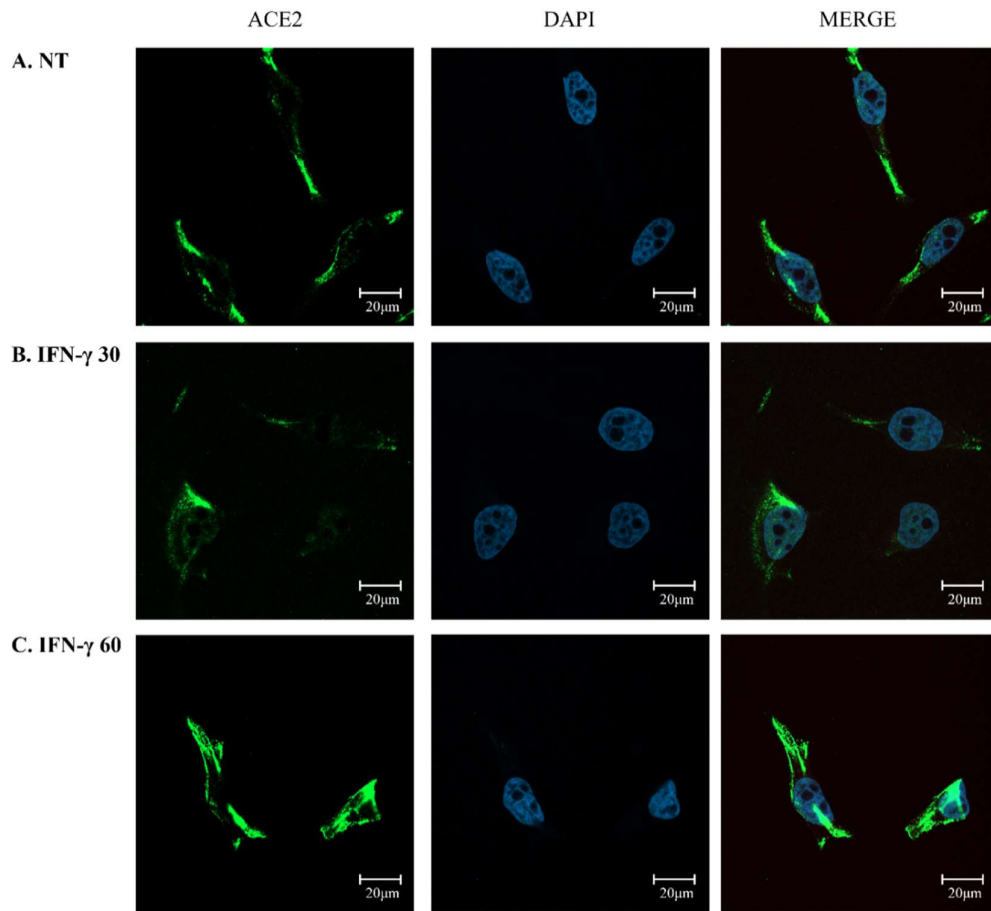


Figure 12: Detection of putative ACE2 in HeLa cells +/- IFN- γ .

Immunofluorescence microscopy was performed on HeLa cells that were either untreated (A), treated with 30 ng/mL IFN- γ (B) or 60 ng/mL IFN- γ (C) for 24 hours. Cells were incubated with the anti-ACE2 antibody ab15348 (green) prior to imaging. DAPI demonstrates nuclear DNA presence (blue). All images were taken on a Zeiss 800 microscope. Scale bars are shown.

3.6.1 HaCaT ACE2 localisation in response to cytokine and spike treatments.

Detection of ACE2 in HaCaT cells has previously been determined, by both immunoblotting and microscopy analysis (Figures 4, 5 and 10). These observations are in accordance with the expected results as prior investigations support ACE2 expression in epidermal keratinocytes (Xue et al. 2021). Whilst preliminary immunofluorescence analysis has detected ACE2, distribution of the SARS-CoV-2 entry protein in HaCaT cells was unclear, with apparent intracellular staining of ACE2 (Figure 10). ACE2 expression was not clearly detected at the cell surface, although ACE2 is thought to be largely localised to the cell surface plasma membrane. To further investigate ACE2 distribution in both the absence and presence of interferon and spike protein treatments, additional immunofluorescence experiments were performed.

HaCaT cells were grown to 80% confluence before incubation with media containing IFN- γ , SARS-CoV-2 spike protein or both, for 24 hours. Following treatment, cells were fixed before co-incubation with antibodies against ACE2 and HC-10. DAPI was also applied to indicate nuclear DNA location.

ACE2 expression in HaCaT cells was largely observed at the cell surface of both untreated and treated cells (Figure 13). Clear punctuate clusters were seen in untreated, interferon treated, and spike treated HaCaT cells, with without colocalization of ACE2 with the HC-10 antibody, which detects MHC class I molecules. No intranuclear ACE2 expression was observed, in contrast to Figure 10. Overall ACE2 expression did not vary considerably between untreated cells and those treated with 60 ng/mL IFN- γ , 5000 ng/mL spike protein or combination treatments (Figure 13). No noticeable ACE2 distribution differences were observed between HaCaT cells treated with either of the three (γ , κ or σ) spike protein variants. The combination of both IFN- γ and spike treatment for 24 hours did not affect overall ACE2 expression levels or intracellular distribution of the protein (Figure 13).

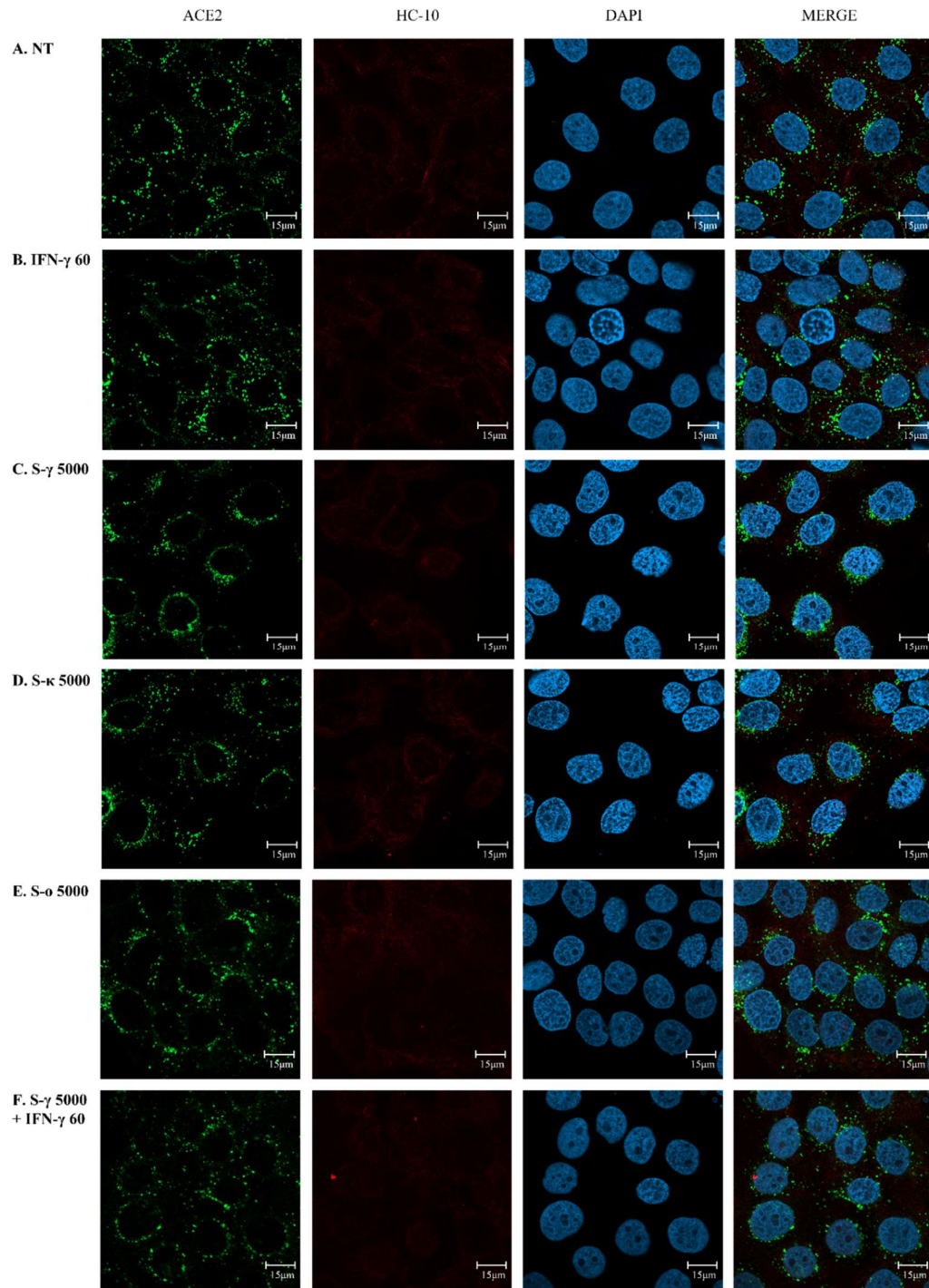


Figure 13: HaCaT ACE2 distribution following cytokine and spike incubation.

HaCaT cells were untreated (A), treated with 60 ng/mL IFN- γ (B), 5000 ng/mL spike protein of γ -variant (C), κ -variant (D) or o-variant (E) or both 60 ng/mL IFN- γ and 5000 ng/mL γ -variant spike (F), for 24 hours before immunofluorescence imaging. Cells were stained with the ACE2 mAb ab15348 (green) and HC-10 antibody (red), with DAPI stain (blue) used to indicate nuclear DNA. Images were taken on a Zeiss 800 microscope; scale bars are shown.

3.6.2 BeWo ACE2 localisation in response to cytokine and spike treatments.

The observation of ACE2 expression in BeWo cells was initially indicated by prior investigations into its mRNA expression (Figure 3), with protein immunoblotting validating this result (Figures 4 and 5). Interferon induced ACE2 upregulation was also observed with both mouse and human IFN- γ . Recombinant SARS-CoV-2 spike protein did not greatly affect overall ACE2 expression (Figure 9). However, the in-vivo interaction between these proteins during SARS-CoV-2 infection may lead to internalisation and proteolytic processing of membranal ACE2 receptors. Therefore, the internal processing of ACE2 following recombinant spike treatment can suggest initial cellular responses to viral infection with SARS-CoV-2. To evaluate whether the localisation of ACE2 in BeWo cells is affected by cytokine and spike protein treatments, a series of immunofluorescence microscopy experiments were performed.

BeWo cells were grown on cover slips before incubation with media supplemented +/- 60 ng/mL IFN- γ , 5000 ng/mL recombinant spike protein of either γ , κ or \omicron variant SARS-CoV-2, or a combination of both IFN- γ and spike protein, for 24 hours. Cells were then fixed before co-staining with anti-ACE2 and HC-10 (anti-MHC class I) antibodies. Microscopy was then performed using a Zeiss 800 to inspect the treated cells.

ACE2 expression and processing in BeWo cells was largely unaffected by recombinant spike protein treatment (Figure 14). Overall ACE2 expression did not vary considerably between untreated cells and those treated with recombinant spike protein alone. However, ACE2 expression did appear to increase slightly in response to 60 ng/mL IFN- γ and 60 ng/mL IFN- γ + 5000 ng/mL spike- γ treatments (Figure 14). The distribution of ACE2 also appeared to be affected by treatment type. For both untreated and IFN- γ treated cells, ACE2 appeared less localised towards the cell membrane, with ACE2 detected across a greater intracellular area than for BeWo cells treated with recombinant spike protein (Figure 14). This observation coincided with decreased clustering of BeWo cells in the untreated and IFN- γ treated experiment, with possible ACE2 staining differences apparent for BeWo clusters of varying cell density. All cells, both untreated and treated appeared healthy and morphologically similar, indicating no toxicity had occurred (Figure 14). ACE2 distribution was similar between variants of spike protein, however overall ACE2 detection appeared slightly weaker for the κ -variant with possible greater non-specific background staining (Figure 14D).

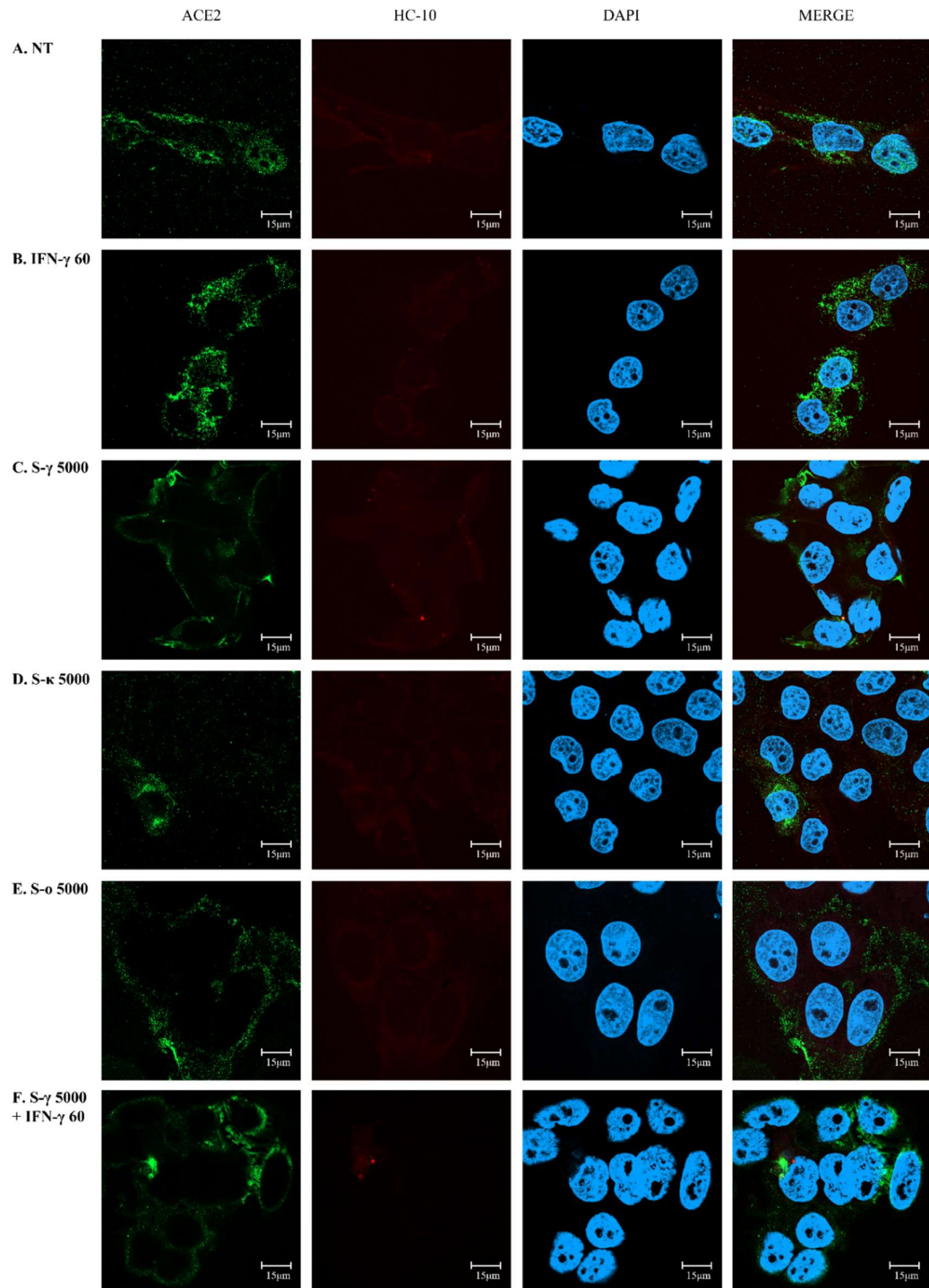


Figure 14: BeWo ACE2 distribution post cytokine and spike protein treatment.

BeWo cells were either untreated (A), treated with 60 ng/mL IFN- γ (B), 5000 ng/mL spike protein of γ -variant (C), κ -variant (D), o-variant (E) or both 60 ng/mL IFN- γ and 5000 ng/mL γ -variant spike (F) for 24 hours. The ACE2 mAb ab15348 (green) and HC-10 antibody (red) were used for staining, with DAPI (blue) used to locate nuclear DNA. Scale bars are shown.

3.6.3 HeLa ACE2 localisation in response to cytokine and spike treatments.

ACE2 was potentially detected in HeLa cells using the anti-ACE2 antibody ab15348 in western blotting (Figure 4) and then followed up by immunofluorescence microscopy (Figure 12). Following investigation of possible cytokine and spike protein mediated ACE2 expression differences within keratinocytes and placental cells, cervical HeLa cells were examined. Treatment of cells with recombinant spike protein may induce ACE2 uptake and degradation within intracellular vesicles.

HeLa cells were grown until 80% confluence before incubation with media treated +/- 60 ng/mL IFN- γ , 5000 ng/mL spike protein from either γ , κ or \omicron variant SARS-CoV-2, or a combination IFN- γ and γ -variant spike protein, for 24 hours. Cells were fixed before staining with the anti-ACE2 mAb ab15348. A Zeiss 800 microscope was then used to inspect treated cells.

ACE2 distribution and expression in HeLa cells is depicted in Figure 15. The staining was relatively weak, and the signal did not appear to be exclusively localized to the cell surface membrane of HeLa cells (Figure 15). ACE2 expression appeared greatest in cells treated with both IFN- γ and recombinant spike protein (Figure 15F). IFN- γ treatment alone appeared to slightly upregulate the putative ACE2 in comparison to untreated cells, although ACE2 staining was weaker when compared to cells treated with both IFN- γ and spike protein (Figure 15). Overlap of ACE2 expression and DAPI nuclear staining may have been due to non-specific staining with the ab15348 antibody in this experiment. Furthermore, the unavailability of a HC-10 control for this experiment hinders clear distinction of the cell surface.

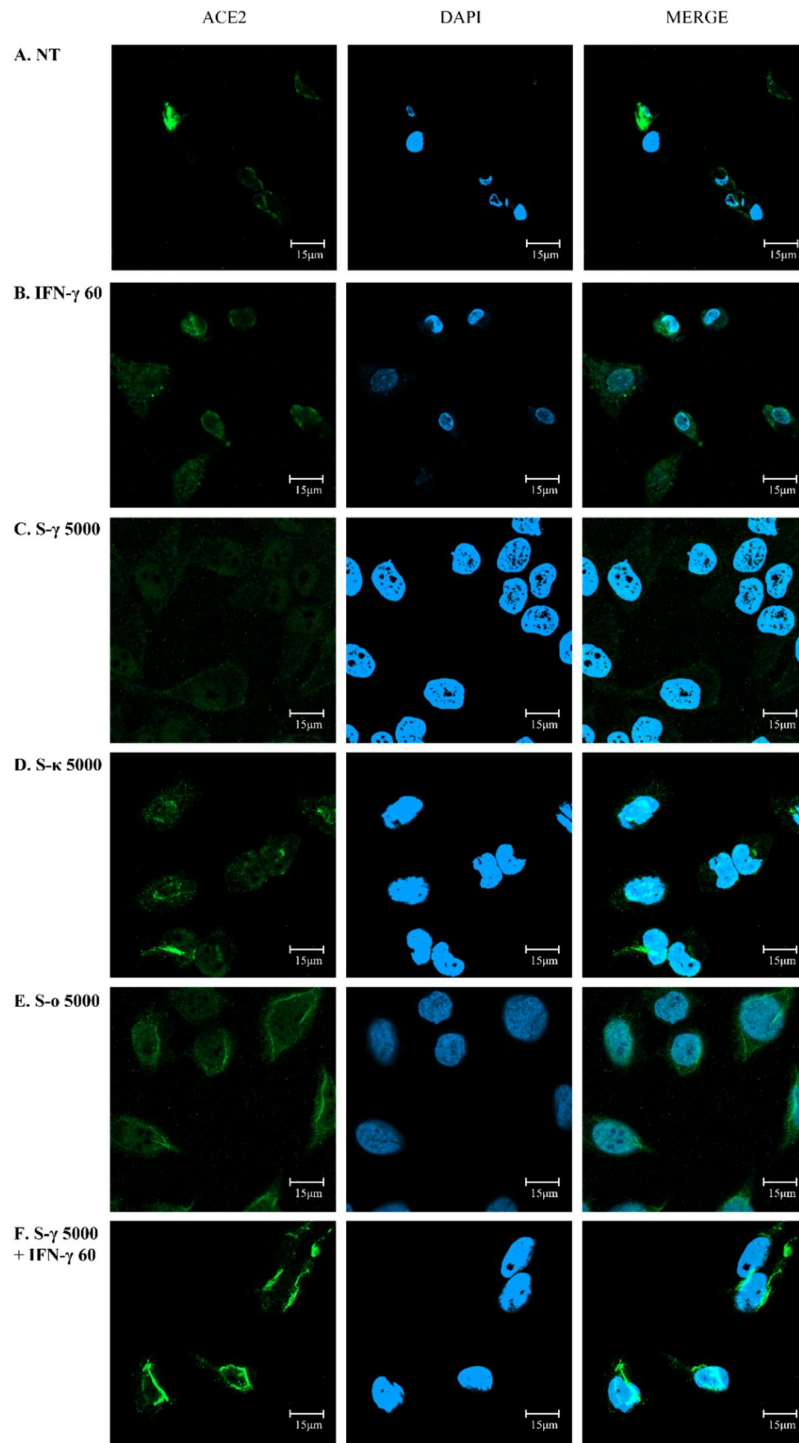


Figure 15: HeLa ACE2 distribution after cytokine and spike protein treatments.

HeLa cells were untreated (A) or treated with either 60 ng/mL IFN- γ (B), 5000 ng/mL spike protein of γ -variant (C), κ -variant (D), o-variant (E) or 60 ng/mL IFN- γ and 5000 ng/mL γ -variant spike protein (F), for 24 hours. Staining was performed with the ACE2 mAb ab15348 (green) with DAPI (blue) indicating the nucleus. Scale bars are shown.

3.7.1 Initial assessment of cytokine and SARS-CoV-2 spike cytotoxicity.

Assaying HaCaT, BeWo or HeLa cells is an important step for investigating the effects of cytokines or SARS-CoV-2 spike protein upon cells expressing ACE2. The previous experiments evaluating treatment-mediated regulation of ACE2 assume that cell viability and behaviour is unaffected by potential cytotoxic effects of the drugs. However, in some cases, poor cell growth was observed following cytokine treatment. Furthermore, the response of individual cell lines to bioreagents varies significantly due to variability in drug uptake and processing. To ensure that experimental outcomes were independent of toxicity, a series of dose-response experiments were designed. These experiments aimed to determine the concentration range at which cytokine and spike protein could be applied to cells. Further, this would enable optimal concentrations to be determined that limit cytotoxicity whilst still producing a measurable biological response.

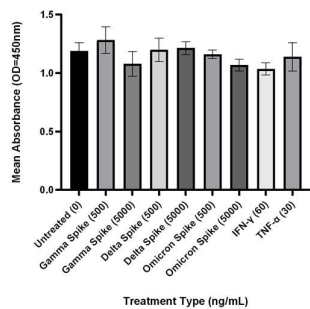
HaCaT, BeWo and HeLa cells grown in 96-well plates were treated for 24 hours with media supplemented +/- 60 ng/mL IFN- γ or 30 ng/mL TNF- α , or with one of three SARS-CoV-2 variant spike proteins- gamma, kappa or omicron, at 500 or 5000 ng/mL. To measure viability, Orangu solution was added to each well before absorbance values were measured following a 3-hour incubation. Comparison of absorbance values between untreated and treated samples can indicate the cytotoxicity of individual drugs, as absorbance is correlated with viable cell metabolism through Orangu-mediated detection of dehydrogenase activity.

For HaCaT cells, SARS-CoV-2 spike protein treatments did not greatly reduce cell viability when used at either 500 or 5000 ng/mL (Figure 16A). The variant of spike protein also did not appear to influence viability of HaCaT cells. Furthermore, IFN- γ and TNF- α did not contribute to a loss in viability (Figure 16A). Indeed, all HaCaT cells examined exhibited similar absorbance values post-Orangu addition, suggesting that none of the treatment regimens inhibited cellular growth.

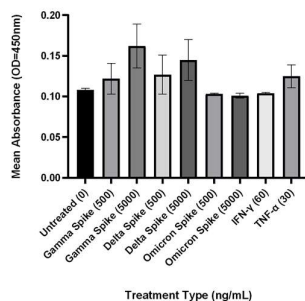
For BeWo cells, no treatment substantially decreased cell viability when compared to untreated cells (Figure 16B). Furthermore, no variant-dependent differences were observed for SARS-CoV-2 spike proteins on the viability of BeWo cells. IFN- γ and TNF- α at 60 ng/mL and 30 ng/mL also did not impede BeWo cell growth when compared to untreated cells (Figure 16B).

For the HeLa cell line, treatment with all three variant SARS-CoV-2 spike proteins resulted in some reduction in cell viability after 24 hours, when compared to the untreated control (Figure 16C). Indeed, absorbance measurements were reduced by >50% for all treatments tested. There were no observed differences in cell viability due to variant type of the spike protein. Furthermore, increasing the dosage of spike protein from 500 ng/mL to 5000 ng/mL did not significantly reduce cell viability in HeLa cells (Figure 16C).

A. HaCaT



B. BeWo



C. HeLa

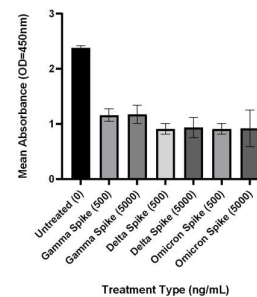


Figure 16: Orangu cytotoxicity assays for cytokine and SARS-CoV-2 spike treatments.

Cytotoxicity of cellular treatments performed for 24 hours was evaluated for HaCaT (A), BeWo (B) and HeLa (C) cell lines. Orangu solution was added to cells before absorbance was measured in triplicate. HaCaT and BeWo cell viability was unaffected by treatments, although HeLa cells viability was reduced following spike protein treatments. Absorbance scales are different for panels A, B and C. Error bars represent standard errors.

3.7.2 Cell viability following SARS-CoV-2 spike and cytokine treatments.

Initial assays examining cell viability when cells were exposed to SARS-CoV-2 spike protein, IFN- γ and TNF- α indicated mild cytotoxicity of spike proteins for HeLa cells. This was unexpected as no growth reduction had previously been noted following spike incubation with any of the cell lines. Whilst the spike protein is known to be the major immunogenic component of the SARS-CoV-2 virus, the protein itself is not considered a toxin (Francesca et al. 2022). Additional investigations were designed to follow up these findings and to determine whether downstream protein expression is a specific result of drug action or a consequence of cellular damage. In order to determine whether the cells were affected by the biological treatments, cells post-treatment were examined under the microscope. The appearance of damaged and dead cells can indicate cytotoxicity, enabling assessment of treatment conditions for individual cell lines.

HaCaT, BeWo and HeLa cells were incubated for 24 hours with media +/- 60 ng/mL IFN- γ , 30 ng/mL TNF- α or 5000 ng/mL of either gamma, kappa or omicron variant SARS-CoV-2 spike proteins. Following treatment, light microscopy was used to examine cells.

Inspection of HaCaT cells post-treatment did not show evidence of drug cytotoxicity affecting cell viability following treatment with either cytokines or SARS-CoV-2 spike proteins (Figure 17A). There were no apparent changes in cell morphology in response to the treatments, with high levels of cell growth displayed in each case. Cellular detachment was also not observed following all treatment types, with a similar number of floating cells identified for untreated and both spike protein and cytokine treated cells (Figure 17A).

BeWo cells appeared unaffected by IFN- γ , TNF- α and spike protein treatments (Figure 17B). All cells inspected post-treatment were morphologically similar and displayed similar growth patterns compared to untreated controls, irrespective of the treatment performed. Growth also appeared uniform, with comparable cell densities across untreated and treated dishes (Figure 17B). No signs of notable cell death were observed in BeWo cells.

HeLa cells were also unaffected by all cell treatments. Examination of microscopy images demonstrated uniform growth patterns in response to all treatments (Figure 17C). Overall cell density of HeLa colonies was standard, and the majority of cells appeared morphologically similar. SARS-CoV-2 spike protein and TNF- α treatments did not affect the growth of HeLa cells (Figure 17C). The variant type of SARS-CoV-2 spike protein was not determined to be a factor for influencing growth of cells at the tested concentrations in HaCaT, BeWo or HeLa cell lines (Figure 17).

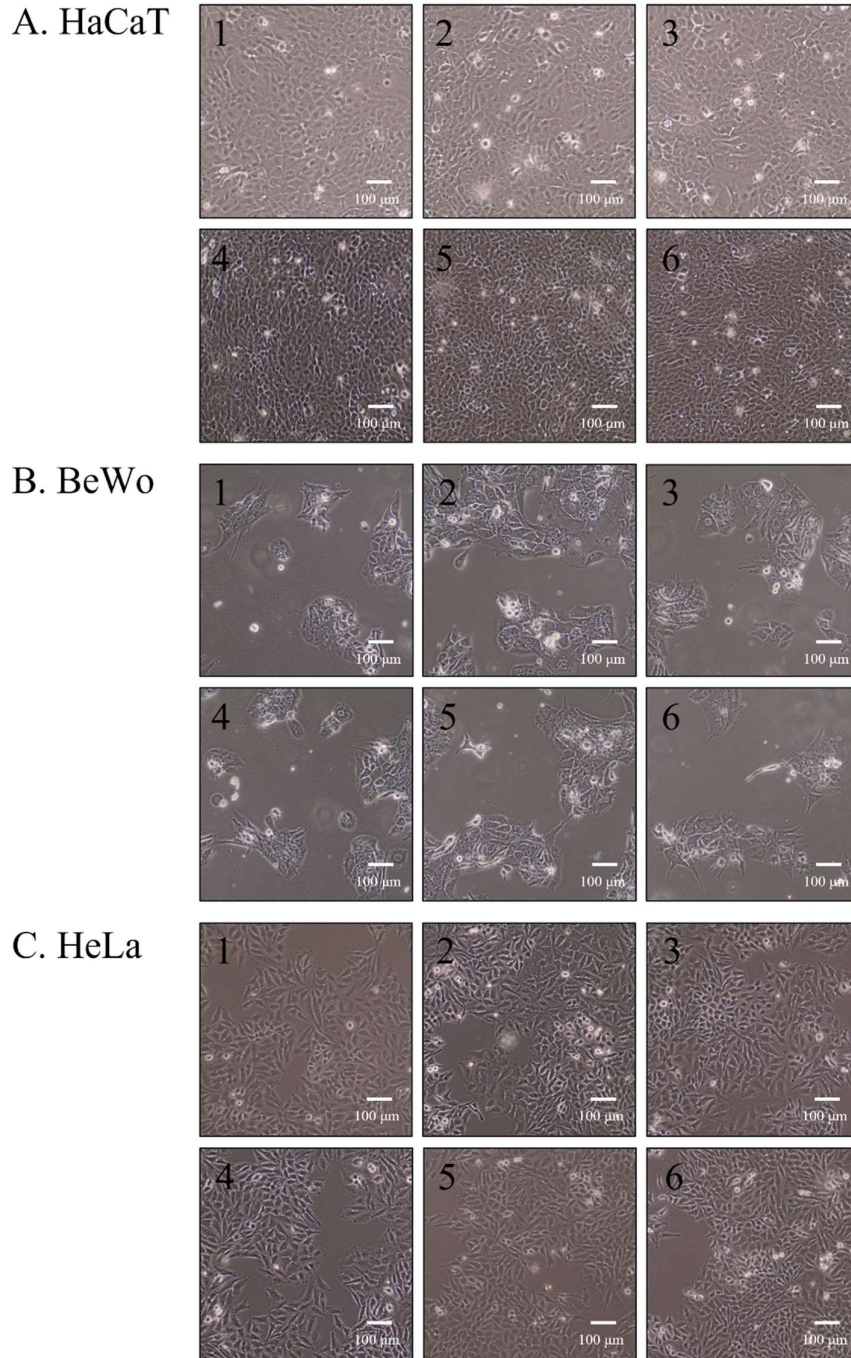


Figure 17: Cell morphology is unaffected by cytokines and the SARS-CoV-2 spike protein.

HaCaT (A), BeWo (B) and HeLa (C) cells were either untreated (1), incubated with 60 ng/mL IFN- γ (2), 30 ng/mL TNF- α (3), or 5000 ng/mL of recombinant SARS-CoV-2 spike proteins of variants gamma (4), kappa (5) and omicron (6). Treatments were applied for 24 hours before imaging. No growth inhibition was observed following cytokine or spike protein treatment. Magnification:100x.

3.8.1 SARS-CoV-2 spike treatment does not induce TNF- α production.

Infection of susceptible cells by SARS-CoV-2 results in the production of inflammatory cytokines including TNF- α , IFN- γ , IL-6 and IL-8, contributing towards a cytokine storm (Darif et al. 2021). As the SARS-CoV-2 spike protein is the critical component for attaching to cells and triggering viral invasion, the association of spike proteins to the ACE2 alone may be sufficient to induce cytokine responses. Indeed, the SARS-CoV spike protein, which has an equivalent function to that of SARS-CoV-2, was reported to stimulate production of inflammatory cytokines including IL-8 and TNF- α in human peripheral blood mononuclear cells (PBMCs) (Olajide et al. 2021). To observe possible stimulation of inflammatory responses against SARS-CoV-2 S protein in a range of cell types, HaCaT, BeWo and HeLa cell lines were exposed to recombinant SARS-CoV-2 spike proteins before ELISAs were used to measure the cytokine responses.

Cells of the HaCaT, BeWo and HeLa cell lines were administered 50 ng/mL of SARS-CoV-2 spike protein from either the gamma, kappa or omicron SARS-CoV-2 variants. Untreated cells were grown as controls. Following 24-hour incubation, culture medium was removed and sampled for secreted TNF- α by ELISA (RAB0476 kit).

Measurements of TNF- α produced by cells of the HaCaT, BeWo and HeLa cell lines in response to SARS-CoV-2 spike protein treatment are displayed in Figure 18. In HaCaT cells, treatment with 50 ng/mL of S protein from the SARS-CoV-2 gamma variant appeared to significantly decrease ($P < 0.05$) the production of TNF- α compared to the untreated control (Figure 18A). However, this measurement, along with a further four across the HaCaT, BeWo and HeLa cell lines, determined TNF- α readings < 0 pg/mL and may thus be within background levels. No additional significant changes in TNF- α were observed between control and spike-treated samples in any of the cell lines tested (Figure 18). Considerable variability in TNF- α was observed between the triplicate measurements performed for each individual sample. Furthermore, no variant dependent differences in TNF- α production were identified, either within or between the three cell lines (Figure 18).

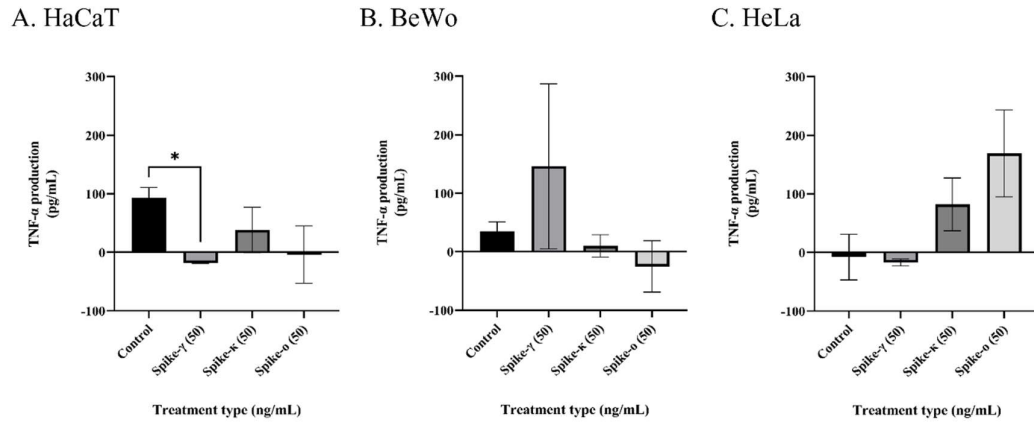


Figure 18: Initial ELISA for SARS-CoV-2 spike induced TNF- α production.

HaCaT (A), BeWo (B) and HeLa (C) cells were treated in triplicate with 50 ng/mL recombinant spike protein from SARS-CoV-2 variants gamma (γ), kappa (κ) and omicron (o) for 24 hours. TNF- α presence was determined with an ELISA kit (RAB0476). 50 ng/mL spike- γ treatment decreased TNF- α production within the HaCaT cell line, however TNF- α was unaffected by spike protein treatments in BeWo, HeLa and remaining HaCaT samples. Error bars represent standard errors. * = $P \leq 0.05$.

3.8.2 SARS-CoV-2 spike alone does not induce TNF- α

immunostimulation.

Challenging HaCaT, BeWo and HeLa cells with S protein (Figure 18) was insufficient to stimulate production of TNF- α under the conditions investigated. Indeed, a decrease in HaCaT TNF- α was observed following treatment with SARS-CoV-2 γ -spike protein. This was an unexpected result in contrast to the current literature reporting upregulation or unchanged cytokine levels post-treatment, and most likely due to the technical limitations of the assay at low cytokine concentrations. In order to re-examine the immune response towards recombinant SARS-CoV-2 spike proteins within the HaCaT cell line, additional ELISAs were performed.

HaCaT cells were grown to 80% confluence before treatments of 60 ng/mL IFN- γ or either 50 or 500 ng/mL spike proteins of SARS-CoV-2 variants gamma (γ), kappa (κ) or omicron (\omicron). 3 ng/mL TNF- α and untreated media were also administered as positive and negative controls. Treatments were performed in triplicate. Following 24-hour treatments, cell media was removed and concentrated with centrifugal filter tubes prior to TNF- α determination with an ELISA (ab181421 kit).

Immune responses towards spike proteins of the SARS-CoV-2 virus were limited in HaCaT cells (Figure 19). No significant increase in TNF- α production was observed in cells treated with either 50 or 500 ng/mL spike protein, when compared to untreated controls. Furthermore, TNF- α was not affected by the variant type of spike protein used (Figure 19). Treatment with 60 ng/mL IFN- γ also did not significantly stimulate increased production of TNF- α (Figure 19). Observed TNF- α presence in the positive 3 ng/mL TNF- α control demonstrated that the immune signalling protein was able to be detected in cell culture supernatants within this model.

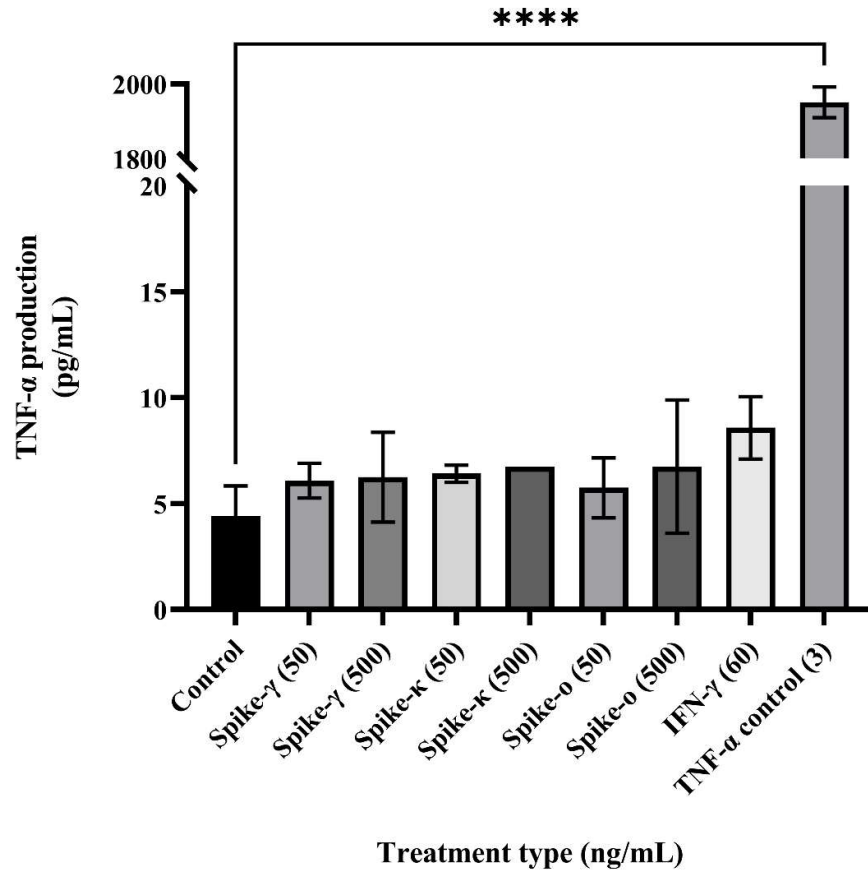


Figure 19: Improved ELISA for SARS-CoV-2 spike protein induced TNF- α secretion.

HaCaT cells were treated +/- 50 ng/mL or 500 ng/mL of recombinant spike protein from the SARS-CoV-2 variants gamma (γ), kappa (κ) and omicron (o). 60 ng/mL IFN- γ and 3 ng/mL treatments were also performed. Cell media was removed and tested for TNF- α post-treatment with an ELISA kit (ab181421). No differences in TNF- α production were observed following spike protein or IFN- γ treatment. Error bars represent standard errors. **** = $P \leq 0.0001$.

3.9 Experimental summary.

The experiments performed within this thesis contribute towards expanding the understanding of ACE2 expression, its regulation by cytokine factors and the effects of ACE2-spike interactions. Preliminary experiments detected ACE2 expression within keratinocyte, placental and cervical cell lines, with additional investigation validating this expression for HaCaT and BeWo cells. Whilst there is some evidence for ACE2 expression within the HeLa cell line, this observation warrants more rigorous investigation. Future experimentation with ACE2 knockout cell lines would assist in confirmation of HeLa ACE2. Immunofluorescence investigations determined cell-surface expression of ACE2 in line with the available literature, however intracellular expression was also detected. Further experiments examining co-expression of ACE2 alongside TMPRSS2 would provide stronger evidence for susceptibility of the investigated cell lines to SARS-CoV-2.

Evidence of cytokine mediated ACE2 expression was detected for both HaCaT and BeWo cell lines, with putative ACE2 upregulation also observed in HeLa cells. Immunoblotting and immunofluorescence experiments were both implemented to investigate this hypothesis, with western blots demonstrating the strongest evidence for both IFN- γ and TNF- α induced upregulation of ACE2.

Recombinant spike protein and cytokine treatments did not adversely affect cell growth in HaCaT and BeWo cell lines, enabling characterisation of suitable treatment concentrations for the cell lines tested. For HeLa cells, spike protein treatments initially appeared to reduce cell viability when compared to untreated cells, however visual examination determined no reduction in growth or altered morphology.

The effect of isolated spike protein upon ACE2 expression was also investigated, with possible downregulation of ACE2 observed in BeWo cells. However, additional controls for these experiments are required to draw clear conclusions about ACE2 expression.

The SARS-CoV-2 spike protein alone was insufficient to stimulate TNF- α production in keratinocyte, placental or cervical cells with the experimental conditions tested. Significant improvements in the ELISA protocol (e.g the use of a centrifugal spin column) and an alternative ELISA kit assisted in validation of these findings, showing that the Abcam supplied recombinant S protein was not able to stimulate cytokine secretion in HaCaT cells.

Section 4.0 Discussion

4.1 HaCaT and BeWo cell lines express ACE2.

The presence of ACE2 receptors at the plasma membrane indicates likely susceptibility of cells to the SARS-CoV-2 virus, along with host priming factors including TMPRSS2 (Devaux, Rolain, and Raoult 2020). Whilst the focus of ACE2 expression investigations has involved cell lines derived from upper and lower respiratory tract tissue, concerns surrounding the possibility of extrapulmonary infections have been raised. ACE2 was reproducibly demonstrated in HaCaT (keratinocyte) and BeWo (placental) cell lines using western blotting (Figures 4, 5, 7 and 9) and immunofluorescence microscopy (Figures 10, 11, 13 and 14). Colocalization of ACE2 with MHC class I (HC-10) staining also indicates likely ACE2 localization in these cell lines (Figures 13 and 14), in accordance with known ACE2 function and distribution as a membrane bound receptor (Samavati and Uhal 2020). These findings corroborate initial predictions of ACE2 expression in keratinocyte and placental cells following a database search of ACE2 transcription data in HaCaT and BeWo cell lines (Figure 3). This is supported by independent observations of ACE2 expression in HaCaT and BeWo cell lines, suggesting possible susceptibility to SARS-CoV-2 infection (D. Ma et al. 2020; Y. Wang et al. 2012).

Demonstration of expression of the receptor required for SARS-CoV-2 cellular entry was less certain for HeLa cells. Western blots provided conflicting evidence for ACE2 expression (Figures 4 and 5) and whilst immunofluorescence experiments indicated ACE2, background staining may have contributed to a non-specific signal (Figures 12 and 15). HeLa cells have previously been determined to have no exogenous ACE2 expression, with database derived transcriptomic data (Figure 3) supporting this observation (Nie et al. 2004; P. Zhou et al. 2020). Alongside ACE2, expression of host priming factors for activation of the SARS-CoV-2 spike protein is also a prerequisite for infection (Piva et al. 2021). Therefore, future TMPRSS2 coexpression could be determined in these cell types to fully evaluate the predisposition of HaCaT, BeWo and HeLa cells to SARS-CoV-2 infection. Deriving an organ-specific map of ACE2 expression, particularly for extrapulmonary organ types, would further the understanding of the interactions between these cell types and SARS-CoV-2 during viral infection.

Expression of ACE2 also indicates potential HaCaT and BeWo (and putative HeLa) cell involvement in the RAAS pathway. The RAAS pathway has systemic effects through mediation of blood pressure and fluid balance (Mascolo et al. 2021). Through expressing ACE2, HaCaT and BeWo cells could assist in the modulation of Ang II levels by catalyzing conversion of this hormone into Ang 1-7. Ang II is a vasoconstrictive hormone within the RAAS which causes muscular walls of arterioles to narrow, increasing blood pressure (Fountain and Lappin 2022). Vasoconstrictive effects of Ang II

are inhibited by ACE2 through Ang II degradation and thus, HaCaT and BeWo cells could assist in regulation of the anti-inflammatory arm of the RAAS. The use of these immortalized cancer cell lines is suggestive, though not fully representative of human tissue. RAAS balance is particularly important in placental tissue as the RAAS is involved in angiogenesis, which is crucial for placental development (Pan et al. 2013). Furthermore, maintenance of a balanced RAAS is important for escaping damaging inflammatory responses during infections (Sparks et al. 2014).

Potentially variable glycoforms of ACE2 were identified in western blotting experiments (Figures 4, 5 and 7). Evidence for ACE2 isoforms in mammalian cells has previously been reported as mRNA transcripts and expressed protein (Onabajo et al. 2020). N-linked glycosylation of ACE2 is reported at N53, N90, N103, N322, N432, N546 and N690 residues (Gong et al. 2021). ACE2 glycosylation has been suggested to affect SARS-CoV-2 infectivity through modulation of the binding interaction between ACE2 and the S protein RBD (Allen et al. 2021). Although ACE2 glycosylation was not a major aim of this study, the mechanisms by which glycosylation can affect spike binding may be of future interest in evaluating individual spike-ACE2 interactions of SARS-CoV-2 variants.

4.2 IFN- γ and TNF- α mediate upregulation of ACE2 expression.

Precise roles of individual cytokines in immune action and protein regulation are complex as they act upon multiple targets in diverse pathways alongside additional factors. Investigation of possible cytokine-mediated ACE2 expression is important for consideration of RAAS regulation and SARS-CoV-2 infection. Whether ACE2 expression is mediated by cytokines acting on specific target cell subsets is not fully described, however cytokine induced ACE2 upregulation has been reported in lung pneumocytes, thyroid cells and macrophages (Coperchini et al. 2020; Albini et al. 2021; Pantazi et al. 2021). Conversely, ACE2 expression in kidney Vero cells is downregulated by IFN- γ and IL-4, suggesting cell type specific responses to cytokines may exist (de Lang, Osterhaus, and Haagmans 2006). Immunoblotting experiments performed in this study determined that IFN- γ and TNF- α may induce ACE2 production in both keratinocytes and placental cells (Figures 4 and 5). Whilst ACE2 expression in cervical tissue is still uncertain, both IFN- γ and TNF- α appeared to upregulate expression of this receptor in HeLa cells. Due to the uncertain nature of HeLa ACE2, this observation requires further independent validation, possibly with ACE2 knockout and gain-of-function experiments.

Both murine and human IFN- γ was determined to upregulate ACE2 in the three cell lines examined (Tables 3 and 4). Human IFN- γ was a stronger stimulant of ACE2 than mouse derived IFN- γ in HeLa cells (2.27 versus 1.2-fold increase), although a weaker inducer of ACE2 in HaCaT cells (1.93 versus

2.44-fold change). BeWo cells responded in a similar manner (~1.2-fold increase in ACE2) to either cytokine. Initial predictions that mouse derived IFN- γ would be less effective than human IFN- γ for stimulating these mammalian cell lines were not substantiated here. Indeed, IFN- γ proteins from humans and mice display only 40% sequence homology and species specificity has previously been reported (Alspach, Lussier, and Schreiber 2019).

Overall, the two interferon cytokines appear to activate signalling responses in mammalian cells, resulting in observed ACE2 upregulation in either case. This suggests that the differences between human and murine IFN- γ are insufficient to greatly affect stimulation of mammalian cells, however clarification of the functional roles of mouse IFN- γ upon human cell lines is required. TNF- α was seen to increase ACE2 upregulation in HaCaT, BeWo and HeLa cell lines (Figure 5). TNF- α is known to induce expression of many genes under IFN- γ control (Schroder et al. 2004). ACE2 upregulation has also been reported in cardiac tissue following TNF- α treatment, exacerbating SARS-CoV-2 entry potential (C. Y. Lee et al. 2021). Therefore, this observation was predicted for the mammalian cells tested, although confirmation of cytokine-controlled regulation is important due to possible cell line specific effects. Cellular expression of members of the TNF receptor superfamily is important for specific signalling responses against TNF- α (Ward-Kavanagh et al. 2016). If no surface receptors are present, weaker non-specific bystander effects towards this cytokine may be observed. However, previous studies report TNF receptor expression in HaCaT, BeWo and HeLa cell lines (Udommethaporn et al. 2016; Knöfler, Stenzel, and Husslein 1998; Tsujimoto and Vilcek 1986). This indicates specific responses to TNF- α treatments are occurring in these cells, leading to increased ACE2 expression.

These observations support the cytokine mediated ACE2 hypothesis that follows previous designation of the *ACE2* gene as an ISG, with experiments demonstrating interferon mediated ACE2 increases within airway epithelial cells (Ziegler et al. 2020). Previous identification of ACE2 isoforms disrupts reporting of interferon regulation, as truncated ACE2 isoforms (including δ -ACE2) which cannot act as SARS-CoV-2 entry receptors are also under positive IFN- γ control (Onabajo et al. 2020). Although ACE2 expression is largely cell line specific, the signalling pathways underpinning its regulation may be shared, and as such, multi-organ expression of ACE2 may be dependent upon similar factors. Regulation of ACE2 is required for maintaining the homeostasis of the RAAS, as this receptor negatively regulates the RAAS through counterbalancing the effects of ACE (Burrell et al. 2004). ACE2 thus plays a pivotal role in reducing inflammation in both placental and skin epithelial tissues.

The mechanism responsible for interferon stimulation of *ACE2* is incompletely understood, though JAK-STAT signalling may be involved, with IFN- γ induced STAT1 and STAT2 phosphorylation observed during ACE2 upregulation (Y. Zhou et al. 2021). The importance of IFN- γ in resolution of

viral infections is well characterised. Heightened production of IFN- γ and TNF- α is associated with antiviral immunity through regulatory effects upon the innate immune system (A. J. Lee and Ashkar 2018; Alejo et al. 2018). Indeed, SARS-CoV-2 infection stimulates interferon production, which may lead to exacerbated cytokine responses observed in severe COVID-19. Development of this cytokine storm causes life-threatening inflammation, leading to development of ARDS and poor patient outcomes (Del Valle et al. 2020).

IFN- γ and TNF- α induced ACE2 upregulation during COVID-19 may theoretically enhance viral pathogenicity through increasing the number of available entry receptors in skin and placental tissues. This observation suggests that the immune response to SARS-CoV-2 may inadvertently assist in furthering viral invasion, despite the potent overarching outcomes of cytokines as antiviral agents. Mild to moderate ACE2 deficiencies have been proposed as protective factors against SARS-CoV-2 infection by lessening viral invasion, however this seems improbable given the strong binding affinity for SARS-CoV-2 to ACE2 (Salamanna et al. 2020). Furthermore, low ACE2 expression is associated with known risk factors for severe COVID-19, including diabetes and cardiovascular disease (South, Diz, and Chappell 2020). ACE2 deficiency is also linked with hyperinflammatory responses during COVID-19, and soluble ACE2 (sACE2) treatments are being considered as possible therapeutic interventions (Ragab et al. 2020; Michaud et al. 2020). This is likely due to stabilisation of the RAAS system, which is crucial for preventing exacerbated inflammatory responses leading to fatal cases. It is important to note that whilst placental and skin epithelial cells are potentially susceptible to SARS-CoV-2, severe COVID-19 correlates predominantly with lung pathology. As such, resulting cytokine induced ACE2 dysregulation in keratinocyte or placental cells may be less severe than in susceptible pulmonary or cardiovascular tissue, although these cell types do represent possible reservoirs of infection.

4.3 Synergistic effects of IFN- γ and TNF- α on ACE2.

As cytokines, TNF- α and IFN- γ control immune functions, which can contribute towards a synergistic antiviral state when concurrently present (Bartee, Mohamed, and McFadden 2008). This combined action of cytokine-mediated ACE2 increases in keratinocyte and placental tissues, led to the development of a hypothesis for synergistic upregulation of ACE2 by IFN- γ and TNF- α . Synergy of these cytokines has been observed during SARS-CoV-2 infection, with co-treatment activating the JAK/STAT1/IRF1 axis, which may cause inflammatory damage during severe COVID-19 (Karki et al. 2021). Furthermore, synergism of IFN- γ and TNF- α is reported for increasing ACE2 mRNA in thyroid cells, demonstrating how these inflammatory cytokines can have important regulatory functions (Coperchini et al. 2020). However, in this study, synergistic effects of IFN- γ and TNF- α

for ACE2 upregulation were not clearly identified in either HaCaT or BeWo cell lines (Figure 7). This suggests no direct interplay between these signalling molecules under the experimental conditions in this thesis, although both cytokines did independently upregulate ACE2. Strong background signal in this experiment complicated identification of possible synergistic effects upon ACE2. The previous characterization of IFN- γ and TNF- α induced ACE2 mRNA production in thyroid cells does indicate that these cytokines may function in collaboration to affect ACE2 expression, suggesting further quantitative approaches are required to investigate this expression in specific target cell subsets.

4.4 Characterisation of alternative anti-ACE2 antibodies.

ACE2 detection was initially confirmed in western blotting and immunofluorescence experiments using the anti-ACE2 mAb ab15348. ACE2 staining was clear and well described for many of these experiments. Following this, it was decided to investigate whether alternative commercially available antibodies stain ACE2 in a similar, or improved manner. Comparison of antibody efficacy allows selection of high-performance antibodies for subsequent experiments. ACE2 staining using the monoclonal antibodies ab108209 and ab108252 was investigated, with no signal detected for either HaCaT or BeWo sample lysates known to express ACE2 (Figure 8). Both ab108209 and ab108252 were used at the manufacturers recommended dilution (1:1000), suggesting absence of ACE2 staining was due to another factor. The presence of β -actin bands also demonstrates successful protein loading of each sample. Therefore, ACE2 detection with ab108209 and ab108252 may require experimental conditions not present during this analysis.

Both ab108209 and ab108252 antibodies are rabbit derived and have been raised against a synthetic peptide. ACE2 detection with ab108252 has previously been described in western blotting experiments with liver and pancreatic cell lysates, demonstrating this antibody is feasible for ACE2 staining (An et al. 2021). Ab108209 is also shown to detect ACE2 in lung epithelial cells with immunofluorescence microscopy experiments (Liang et al. 2020). Furthermore, ACE2 bands at 130 kDa have also been reported by western blotting with ab108209 (F. Ren et al. 2023). These studies display efficacy of ACE2 detection with these anti-ACE2 antibodies and suggest the lack of detectable ACE2 in this thesis may be due to the experimental conditions. Furthermore, positive ACE2 controls were not present within the western blot described here (Figure 8), therefore this experiment requires follow up to investigate ACE2 detection with ab108209 and ab108252. Future use of ab15348 for ACE2 detection is suggested in this thesis, with experiments demonstrating the efficacy of this antibody for ACE2 staining. However, additional investigation of ab108209 and ab108252 is needed to determine the conditions required for ACE2 staining.

4.5 Recombinant SARS-CoV-2 spike protein does not dysregulate ACE2.

Interactions between SARS-CoV-2 spike protein and membrane bound ACE2 occur during initial association between the virus and susceptible cells. In-vivo investigations have determined that a consequence of spike-RBD complex formation during SARS-CoV-2 infection is internalization and subsequent degradation of ACE2 during viral penetration of the cell. Indeed, it has been well documented that binding of the SARS-CoV-2 virus to ACE2 leads to downregulation of this receptor (Silhol et al. 2020; Verdecchia et al. 2020). Although this process is reported for SARS-CoV-2, the effects of recombinant spike protein upon susceptible cells are less clear. Whether the SARS-CoV-2 spike protein alone is sufficient to induce comparable effects upon ACE2 expression in-vitro was an aim of this investigation.

In this study, HaCaT and BeWo cells incubated with recombinant spike protein did not show clear evidence of ACE2 protein dysregulation (Figure 9). Immunoblotting determined similar ACE2 expression following 24-hour spike RBD treatment for HaCaT cells and whilst slight ACE2 decreases were potentially observed for BeWo cells, protein loading was not controlled for here. These findings suggest that purified spike protein alone is unable to induce internalization of ACE2 from the cell surface membrane. The recombinant spike proteins utilized in this study encode the RBD of the spike alone and as such can be used to model binding to ACE2 receptors. As ACE2 expression appears unaffected, RBD-ACE2 binding appears insufficient to alter stabilization of the RAAS in these systems. Furthermore, the effect of spike binding upon further susceptibility to SARS-CoV-2 infection appears negligible as no change in entry receptor expression is observed.

SARS-CoV-2 spike RBD protein constructs have previously been implicated in Ang II elevation through downregulation of ACE2 expression in animal models (L. Zhang et al. 2022). Spike RBD proteins of the related SARS-CoV virus are also known to bind to ACE2 on susceptible cells, resulting in endocytosis of the RBD-ACE2 complex (S. Wang et al. 2008). These studies suggest ACE2 internalization does occur following spike-ACE2 binding, in contrast to results displayed here. The SARS-CoV-2 spike protein has also been found to enhance expression of some ISG's in bronchial epithelial cells, including ACE2 (Y. Zhou et al. 2021). This may be due to activation of host immune responses against the spike protein, which trigger expression of ISGs through type I interferons. Conversely, SARS-CoV-2 spike proteins have been shown to downregulate ACE2 mRNA in transfected kidney epithelial cells (X. Gao et al. 2022). This demonstrates possible tissue specific responses to recombinant spike proteins.

The initial hypotheses that SARS-CoV-2 spike RBD protein can downregulate ACE2 in cell lines expressing ACE2 are not supported by preliminary experiments reported here. This may be the result of the ACE2 expression system used, with the spike RBD alone employed, rather than the complete spike glycoprotein or viral particle. Viral-induced ACE2 internalization observed during in-vivo

infection may be dependent upon the presence of additional factors, including an activated S₂ subunit and associated priming enzymes. The active S₂ subunit is known to play an important role in inducing membrane fusion and facilitating SARS-CoV-2 entry (Y. Huang et al. 2020). Host proteases including TMPRSS2 are also required for viral entry (Hoffmann, Hofmann-Winkler, and Pöhlmann 2018). The SARS-CoV-2 RBD protein is suitable for modelling binding of spike protein to host ACE2. Although, the effect of additional viral factors, including the S₂ domain may potentially result in affected ACE2 expression. This reasoning, however, is not supported by independent observations of SARS-CoV and SARS-CoV-2 spike RBD proteins inducing ACE2 endocytosis (Inoue et al. 2007; Bayati et al. 2021). Therefore, it is more likely that expression of surface ACE2 was unaltered in the cell lines tested, regardless of spike-ACE2 binding. However, future characterisation of spike RBD-ACE2 binding is proposed, as complex formation is assumed here.

Both direct SARS-CoV-2 spike-mediated downregulation of ACE2 protein and intracellular degradation of ACE2 mRNA has previously been reported, suggesting the spike protein may cause both endogenous and exogenous ACE2 to decrease (X. Gao et al. 2022). For the keratinocyte and placental cells evaluated here, no ACE2 expression changes were observed. However, RNA levels were not quantified in this study and as such, transcriptional control of ACE2 was not investigated. Repeat western blot experiments are required to determine whether the slight ACE2 reductions observed in BeWo cells following spike protein treatment are reproducible and are the result of spike-ACE2 binding, rather than protein loading concerns.

Immunofluorescence microscopy experiments suggested that SARS-CoV-2 spike treatments did not affect localisation of ACE2 in HaCaT, BeWo or HeLa cell lines (Figures 13, 14 and 15). Although ACE2 internalisation and degradation has been reported following SARS-CoV-2 spike protein treatment, no evidence of protein internalisation was determined here (X. Gao et al. 2022). Following spike-ACE2 binding, endocytosis of the ACE2 protein along with associated S protein is thought to be utilised by the SARS-CoV-2 virus for entry. Clathrin-mediated or AP2-dependent endocytosis of the virus-ACE2 complex into endolysosomes is an important step in SARS-CoV-2 infectivity, where additional proteolytic processing of S₂'cleavage sites can occur (Jackson et al. 2021). Lysosomal degradation of ACE2 occurs following internalisation, suggesting SARS-CoV-2 S protein may induce ACE2 downregulation (Y. Lu et al. 2022). Direct evidence of receptor proteolysis was not investigated in this study, whilst localisation of ACE2 in HaCaT, BeWo or HeLa cells did not appear affected by the spike protein. Since SARS-CoV-2 induced ACE2 downregulation is linked with severe COVID-19 through an imbalance of the RAAS, future investigation of ACE2 protein fate following uptake may partially explain the associated inflammatory actions known to contribute to poor prognosis following SARS-CoV-2 infection (Babajani et al. 2021). Furthermore, performance of co-immunoprecipitation experiments to verify spike-ACE2 interactions in this model would also strengthen these findings.

4.6 Spike protein and cytokine treatments do not inhibit cell growth.

Experiments performed upon HaCaT, BeWo and cell lines utilised IFN- γ , TNF- α and SARS-CoV-2 spike RBD protein treatments. Slight growth inhibition was reported in initial experiments following cytokine treatments, leading to the investigation of potential cytotoxic effects of the drugs for the three cell lines. An Orangu cytotoxicity assay was performed to determine toxic effects of IFN- γ , TNF- α and the viral spike protein (Figure 16). The Orangu assay utilises WST-8, a tetrazolium salt which produces a formazan orange dye when reduced. The formazan dye is produced by the activity of dehydrogenase enzymes within live cells and as such, colour intensity is directly proportional to the number of viable cells present (Chamchoy et al. 2019). This technique requires equal seeding of cells prior to treatment as cell death is assumed by observed reductions in colour intensity compared to other samples, rather than direct observation.

The Orangu assays demonstrated that HaCaT and BeWo cells were unaffected by treatment with either cytokine or spike for 24 hours. This was expected due to previous reporting of HaCaT cell stimulation to induce the expression of surface receptors using TNF- α and IFN- γ in a 10-100 ng/mL range (Konur et al. 2005; El Darzi et al. 2017). Modulation of BeWo signalling pathways has also been demonstrated following incubation of cells with 1-100 ng/mL IFN- γ and TNF- α cytokines (Barbosa et al. 2015; Konur et al. 2005). This indicates that these cell lines respond to cytokines used in this concentration range, without adverse cell growth being reported in the 24 hours post treatment.

Excessive TNF- α presence in the environment is toxic to cells as signalling through the TNF-R1 and TNF-R2 receptors causes activation of NF- κ B and MAPKs, leading to generation of apoptotic signals (Z. G. Liu 2005). IFN- γ also triggers apoptotic cell death through activation of NF- κ B (Schroder et al. 2004). Indeed, many cytokine induced responses result in cellular apoptosis or necrosis, demonstrating the consequences of excessive IFN- γ or TNF- α cellular treatment. Furthermore, reported expression of TNF receptor superfamily members on the cell surface of HaCaT, BeWo and HeLa cell lines indicates that specific TNF- α mediated responses following stimulation occurs in these cells (Udommethaporn et al. 2016; Knöfler, Stenzel, and Husslein 1998; Tsujimoto and Vilcek 1986). Therefore, an overstimulation with the TNF- α cytokine may result in direct cell signalling responses leading to apoptosis in these cell lines. However, no cytokine mediated inhibition was seen in the HaCaT or BeWo cell lines.

Cell growth for the HeLa cell line appeared to be adversely affected by all SARS-CoV-2 spike proteins, independent of variant type (Figure 16). This was unexpected, because whilst the SARS-CoV-2 spike protein is known to be a key immunogenic region for antibody neutralisation, the spike RBD protein itself is not considered a toxin (M. Y. Wang et al. 2020). Furthermore, no loss in cell viability was reported following spike treatment with either the HaCaT or BeWo cell lines used. Subsequent cell treatment experiments were performed, using a bright-field microscope to inspect

cells for signs of growth inhibition and death. Visual inspection of treated cells showed that no treatment performed upon either cell line resulted in adverse growth (Figure 17). Neither cell density nor morphology appeared to be altered by either cytokine or spike treatment, suggesting that no signalling resulting in apoptosis was occurring within the HaCaT, BeWo or HeLa cell lines. Whilst the initial Orangu suggested a loss in viability for HeLa cells in the presence of spike proteins, this was not supported by the microscope inspection. Furthermore, incubation with IFN- γ or TNF- α also did not affect HeLa cell growth. This demonstrates that the treatments were performed at a suitable concentration for the HaCaT, BeWo and HeLa cell lines tested.

4.7 SARS-CoV-2 spike variants do not affect ACE2 expression or localisation.

The emergence of SARS-CoV-2 variants has fueled recent surges in COVID-19 infections, with evolutionary selection of spike proteins able to facilitate pathogenicity and immune escape (Lauring and Hodcroft 2021). Indeed, novel SARS-CoV-2 variants express mutated spike proteins to either enhance ACE2 binding or to lessen the neutralizing antibody response, improving viral success (Harvey et al. 2021). Sequence alignments for the three SARS-CoV-2 variant spike proteins utilized in this study are shown in Figure 2. Whilst γ -S and κ -S proteins demonstrate relatively high amino acid similarity, the o-S protein exhibits 34 mutations in this region (Zepeng Xu, Liu, and Gao 2022). Knowledge of altered spike variant binding to the ACE2 receptor, alongside reported ACE2 dysregulation during SARS-CoV-2 infection led to development of a hypothesis that the SARS-CoV-2 spike may display variant dependent effects upon ACE2 expression. Additionally, whether immune stimulation following spike incubation differs depending on variant type was examined.

In this study, variant dependent effects of recombinant SARS-CoV-2 spike proteins were not identified. ACE2 expression and/or localization was not greatly affected by the variant type of spike protein used for treating HaCaT, BeWo and HeLa cells (Figures 9, 13, 14 and 15). Although spike induced downregulation of ACE2 expression in BeWo cells was not confirmed here, treatment with o-S did appear to reduce ACE2 more so than spike proteins of either γ or κ variants (Figure 9). However, lack of sufficient protein loading controls prevents variant dependent effects being adequately identified in this experiment. Sufficient TNF- α stimulation was also not determined for any spike protein variant, therefore variant differences in spike induced immune activation were also not observed (Figures 18 and 19). These findings do not support the initial hypothesis that differential binding of spike variants to the ACE2 receptor leads to individual responses. Furthermore, immune

stimulation with any SARS-CoV-2 spike protein alone was not significant, thereby preventing variant-dependent differences in spike proteins from being observed.

Differences in binding affinities between RBDs from SARS-CoV-2 variants and cellular ACE2 have previously been characterized with free energy profiles. Omicron S has the greatest binding affinity for ACE2 ($-1.35\beta w_{\min}$), followed by kappa-S ($-1.15\beta w_{\min}$), and then gamma-S ($-1.11\beta w_{\min}$) (Giron, Laaksonen, and Barroso da Silva 2022). Although strength of the spike-ACE2 interaction is similar for kappa and gamma spike proteins, the omicron spike protein binds considerably tighter. If ACE2 dysregulation is a product of spike-ACE2 binding, then the omicron spike protein would be expected to have the greatest effect upon ACE2. This reasoning may support the spike treated BeWo cell findings demonstrated in Figure 9, as despite lacking the full controls, o-S treatment appeared to downregulate ACE2 more strongly than either κ -S or γ -S. No ACE2 changes were observed for the HaCaT cell line, irrespective of the variant type, suggesting the spike protein alone does not alter ACE2 levels in this system (Figure 9). As before, follow up experiments are needed to confirm this observation is biologically robust.

Aside from ACE2 dysregulation, additional SARS-CoV-2 variant dependent responses upon susceptible cells exist. Disturbances to S protein structure can facilitate accessibility of viral and host membranes or prevent recognition by neutralising antibodies to reduce humoral immune activation (Hirabara et al. 2022). Immune signalling by the host cell in response to SARS-CoV-2 viral attachment may also be affected. Although direct spike-induced stimulation of immunity was not determined in this study (Figures 18 and 19), host responses to the SARS-CoV-2 spike protein provides the basis for COVID-19 vaccines. Furthermore, recombinant spike treatments have previously been shown to be sufficient for promoting cell signalling in various cell types, in the absence of additional viral components (Suzuki and Gychka 2021; L. Zhang et al. 2022).

To investigate whether S variant type affects protein regulation downstream of spike-ACE2 interactions, quantitative analysis of protein fold-changes may be performed. A suggested workflow for quantitative SWATH mass spectrometry is described (Figure 20). This experimental design could involve immune stimulation alongside spike protein treatment, however as noted above, spike induction has been deemed sufficient to elicit cell signalling responses in certain cell types. Whether recombinant SARS-CoV-2 spike proteins induce signalling responses, and potential variant dependent effects could be determined through analysis of downstream proteomic changes.

SWATH Mass Spectrometry Workflow

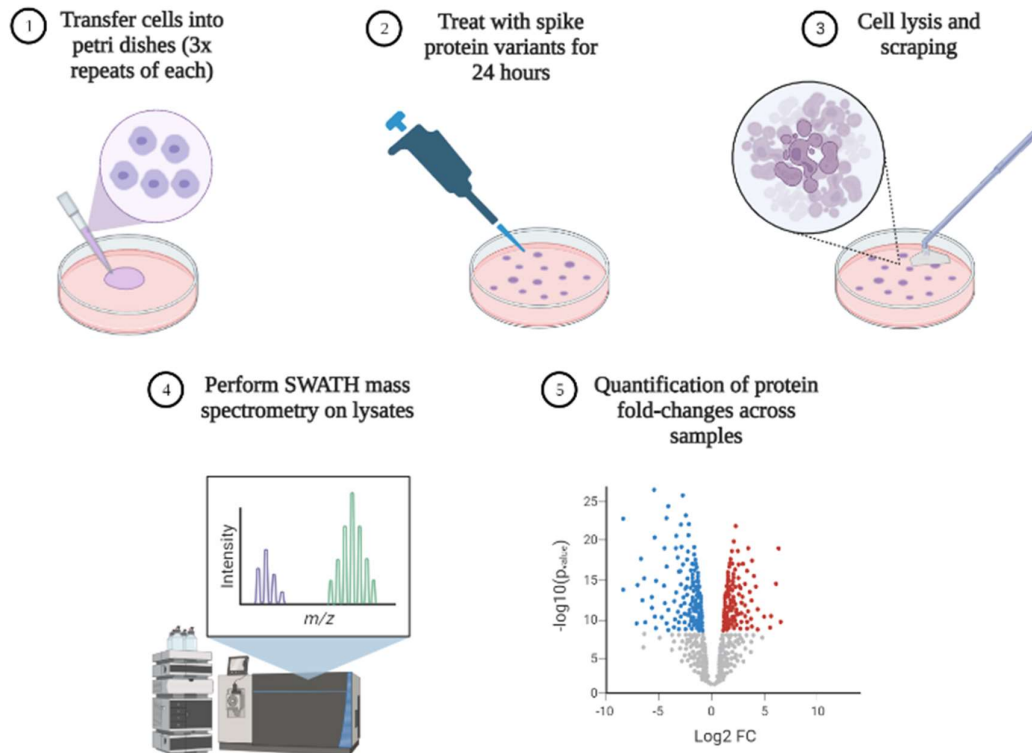


Figure 20: SWATH mass spectrometry workflow.

Experimental steps required to perform sequential window acquisition of all theoretical fragment ion spectra mass spectrometry (SWATH MS) (Krasny et al. 2018). Quantitative analysis of downstream translational targets can determine fold-changes in proteins induced by SARS-CoV-2 spike proteins.

4.8 SARS-CoV-2 spike protein alone is unable to stimulate TNF- α production.

SARS-CoV-2 infection of susceptible cells results in activation of immune responses and production of antiviral cytokines and chemokines. These responses are crucial for positive resolution of COVID-19 disease and demonstrate stimulation of protective immune responses towards pathogen activity. Previous studies investigating SARS-CoV-2 antigenicity have led to designation of the spike glycoprotein as a major immunogenic region of this coronavirus. Indeed, ~90% of neutralising antibody activity in infected individuals is targeted against the RBD of the viral spike (Piccoli et al. 2020). Furthermore, the majority of current SARS-CoV-2 vaccines are targeted towards the spike glycoprotein, indicating that generation of neutralising antibodies against this region is important for protecting against severe disease (Martínez-Flores et al. 2021).

It was hypothesised that incubation of recombinant spike protein with cell lines expressing cell surface ACE2 would lead to a biological response. Indeed, spike proteins of the closely related SARS-CoV virus have been determined to induce production of inflammatory cytokines such as TNF- α and IL-8 in human PBMC cells (Olajide et al. 2021). Furthermore, whilst no direct inflammatory actions were determined for the SARS-CoV-2 structural proteins M, E and N, S proteins have been shown to induce IL-6, IL-1 β , TNF- α and CCL2 production in both human and mouse macrophage cells (Khan et al. 2021). This inflammation was found to be TLR2-dependent, with activation of the NF- κ B pathway leading to cytokine secretion.

In this study, ELISA assays were performed to characterise whether the spike protein alone is sufficient to induce production of an inflammatory cytokine. Although HaCaT, BeWo and HeLa cells are not professional TNF- α secreting cells (such as macrophages), a biological response to viral spike protein was expected (Parameswaran and Patial 2010). The recombinant spike was determined to be unable to induce TNF- α immunostimulation in either HaCaT, BeWo or HeLa cells (Figure 18). Failure of perceived TNF- α immunostimulation post spike treatment was unexpected, especially in the HaCaT cell line as TLR2 expression is confirmed, with these keratinocytes previously shown to be suitable for investigation of innate immune mechanisms in the skin (Olaru and Jensen 2010). For BeWo and HeLa cells however, TLR2 expression is either minimal or undetectable (Pridmore et al. 2003; Tangerås et al. 2014). Regardless, a response to the SARS-CoV-2 spike protein may still occur through additional downstream pathways.

The initial ELISA findings (Figure 18) led to repetition of TNF- α secretion experiments with protocol improvements including use of a centrifugal spin column to increase supernatant protein concentration and triplicate rather than duplicate measurements being taken. The HaCaT cell line was selected for re-investigation due to known expression of TLR2 receptors and previous determination of spike-induced inflammation via TLR2-dependent activation of the NF- κ B (Khan et

al. 2021; Pivarcsi et al. 2003). Improved ELISA experiments did not identify TNF- α secretion, although a positive TNF- α control established that TNF- α detection in the ELISA system was feasible (Figure 19). Furthermore, although use of a centrifugal spin column did not appear to increase TNF- α measurements, BCA assays did demonstrate that total protein in supernatant samples was increased.

Further experiments to demonstrate spike-ACE2 complex formation post spike treatment would prove that this association alone is insufficient for signalling to occur. Whether the presence of SARS-CoV-2 spike RBD protein can augment the stimulation of immune responses by secondary factors is also unknown, however the activation of MAPK and NF- κ B signalling molecules has been determined previously (Barreda et al. 2021). Promotion of host inflammatory responses to SARS-CoV-2 infection by the spike protein may be advantageous to the virus, as disrupted immune responses benefits viral replication.

4.9 Conclusions.

The experiments reported in this thesis have demonstrated ACE2 expression in HaCaT and BeWo cell lines. Both mouse and human IFN- γ appeared to increase levels of detectable ACE2. Subsequent cytokine challenge experiments did not detect clear synergistic effects between IFN- γ and TNF- α , however this requires follow up. Putative expression of ACE2 was also observed in HeLa cells with western blotting. Comparison of anti-ACE2 antibodies demonstrated that the monoclonal antibody ab15348 was the most effective for characterising ACE2 in both western blotting and immunofluorescence experiments. Whilst SARS-CoV-2 infection induces ACE2 internalisation and degradation, recombinant spike protein alone was not seen to affect ACE2 expression in epithelial keratinocytes, however slight downregulation was indicated for placental cells. Identification of variant-dependent effects of SARS-CoV-2 spike RBD proteins upon ACE2 regulation and distribution were not observed, indicating that dysregulation of this protein and subsequent RAAS imbalance is similar, regardless of variant type. Following this, spike-induced stimulation of HaCaT, BeWo and HeLa cells was evaluated by ELISA and determined to be insufficient to produce detectable TNF- α . Protocol improvement was described and a workflow for future quantitative analysis of downstream translational targets was generated. Identification of variant dependent differences in proteomic regulation of infected cells may be characterised by this method.

Section 5.0 References

- Albini, Adriana, Luana Calabrone, Valentina Carlini, Nadia Benedetto, Michele Lombardo, Antonino Bruno, and Douglas M. Noonan. 2021. 'Preliminary Evidence for IL-10-Induced ACE2 mRNA Expression in Lung-Derived and Endothelial Cells: Implications for SARS-Cov-2 ARDS Pathogenesis'. *Frontiers in Immunology* 12 (September): 3921. <https://doi.org/10.3389/FIMMU.2021.718136/BIBTEX>.
- Alejo, Alí, M. Begoña Ruiz-Argüello, Sergio M. Pontejo, María Del Mar Fernández De Marco, Margarida Saraiva, Bruno Hernáez, and Antonio Alcamí. 2018. 'Chemokines Cooperate with TNF to Provide Protective Anti-Viral Immunity and to Enhance Inflammation'. *Nature Communications* 2018 9:1 9 (1): 1–16. <https://doi.org/10.1038/s41467-018-04098-8>.
- Allen, Joel D., Yasunori Watanabe, Himanshi Chawla, Maddy L. Newby, and Max Crispin. 2021. 'Subtle Influence of ACE2 Glycan Processing on SARS-CoV-2 Recognition'. *Journal of Molecular Biology* 433 (4). <https://doi.org/10.1016/J.JMB.2020.166762>.
- Alspach, Elise, Danielle M. Lussier, and Robert D. Schreiber. 2019. 'Interferon γ and Its Important Roles in Promoting and Inhibiting Spontaneous and Therapeutic Cancer Immunity'. *Cold Spring Harbor Perspectives in Biology* 11 (3). <https://doi.org/10.1101/CSHPERSPECT.A028480>.
- An, Xiang, Wenlong Lin, Huan Liu, Weixiang Zhong, Xiuming Zhang, Yimin Zhu, Xiaojian Wang, Jun Li, and Qinsong Sheng. 2021. 'SARS-CoV-2 Host Receptor ACE2 Protein Expression Atlas in Human Gastrointestinal Tract'. *Frontiers in Cell and Developmental Biology* 9 (June). <https://doi.org/10.3389/FCELL.2021.659809>.
- Andersen, Kristian G, Andrew Rambaut, W Ian Lipkin, Edward C Holmes, and Robert F Garry. n.d. 'The Proximal Origin of SARS-CoV-2'. *Nature Medicine*. Accessed 21 December 2022. <https://doi.org/10.1038/s41591-020-0820-9>.
- Babajani, Fatemeh, Atefeh Kakavand, Hossien Mohammadi, Armin Sharifi, Saba Zakeri, Soheila Asadi, Zeinab Mohseni Afshar, Zohreh Rahimi, and Babak Sayad. 2021. 'COVID-19 and Renin Angiotensin Aldosterone System: Pathogenesis and Therapy'. *Health Science Reports* 4 (4). <https://doi.org/10.1002/HSR2.440>.
- Bagdonaite, Ieva, and Hans H. Wandall. 2018. 'Global Aspects of Viral Glycosylation'. *Glycobiology* 28 (7): 443–67. <https://doi.org/10.1093/GLYCOB/CWY021>.
- Bai, Chongzhi, Qiming Zhong, and George Fu Gao. 2022. 'Overview of SARS-CoV-2 Genome-Encoded Proteins' 65 (2): 280–94. <https://doi.org/10.1007/s11427-021-1964-4>.
- Banu, Nehla, Sandeep Surendra Panikar, Lizbeth Riera Leal, and Annie Riera Leal. 2020. 'Protective Role of ACE2 and Its Downregulation in SARS-CoV-2 Infection Leading to Macrophage Activation Syndrome: Therapeutic Implications'. *Life Sciences* 256 (September): 117905. <https://doi.org/10.1016/J.LFS.2020.117905>.
- Barbosa, Bellisa Freitas, Janice Buiate Lopes-Maria, Angelica Oliveira Gomes, Mariana Bodini Angeloni, Andressa Silva Castro, Priscila Silva Franco, Marise Lopes Fermino, et al. 2015. 'IL10, TGF Beta1, and IFN Gamma Modulate Intracellular Signaling Pathways and Cytokine

- Production to Control Toxoplasma Gondii Infection in BeWo Trophoblast Cells'. *Biology of Reproduction* 92 (3): 82–83. <https://doi.org/10.1095/BIOLREPROD.114.124115/2434124>.
- Barreda, Dante, César Santiago, Juan R. Rodríguez, José F. Rodríguez, José M. Casasnovas, Isabel Mérida, and Antonia Ávila-Flores. 2021. 'SARS-CoV-2 Spike Protein and Its Receptor Binding Domain Promote a Proinflammatory Activation Profile on Human Dendritic Cells'. *Cells* 10 (12). <https://doi.org/10.3390/CELLS10123279/S1>.
- Bartee, Eric, Mohamed R. Mohamed, and Grant McFadden. 2008. 'Tumor Necrosis Factor and Interferon: Cytokines in Harmony'. *Current Opinion in Microbiology* 11 (4): 378–83. <https://doi.org/10.1016/J.MIB.2008.05.015>.
- Bayati, Armin, Rahul Kumar, Vincent Francis, and Peter S. McPherson. 2021. 'SARS-CoV-2 Infects Cells after Viral Entry via Clathrin-Mediated Endocytosis'. *Journal of Biological Chemistry* 296 (January). <https://doi.org/10.1016/j.jbc.2021.100306>.
- Benigni, Ariela, Paola Cassis, and Giuseppe Remuzzi. 2010. 'Angiotensin II Revisited: New Roles in Inflammation, Immunology and Aging'. *EMBO Molecular Medicine* 2 (7): 247. <https://doi.org/10.1002/EMMM.201000080>.
- Beyerstedt, Stephany, Expedito Barbosa Casaro, and Érika Bevilaqua Rangel. 2021. 'COVID-19: Angiotensin-Converting Enzyme 2 (ACE2) Expression and Tissue Susceptibility to SARS-CoV-2 Infection'. *European Journal of Clinical Microbiology & Infectious Diseases* 40 (5): 905. <https://doi.org/10.1007/S10096-020-04138-6>.
- Bollavaram, Keval, Tiffanie H. Leeman, Maggie W. Lee, Akhil Kulkarni, Sophia G. Upshaw, Jiabei Yang, Hannah Song, and Manu O. Platt. 2021. 'Multiple Sites on SARS-CoV-2 Spike Protein Are Susceptible to Proteolysis by Cathepsins B, K, L, S, and V'. *Protein Science* 30 (6): 1131–43. <https://doi.org/10.1002/PRO.4073>.
- Boukamp, P., R. T. Petrussevska, D. Breitkreutz, J. Hornung, A. Markham, and N. E. Fusenig. 1988. 'Normal Keratinization in a Spontaneously Immortalized Aneuploid Human Keratinocyte Cell Line.' *Journal of Cell Biology* 106 (3): 761–71. <https://doi.org/10.1083/JCB.106.3.761>.
- Burrell, Louise M., Colin I. Johnston, Christos Tikellis, and Mark E. Cooper. 2004. 'ACE2, a New Regulator of the Renin–Angiotensin System'. *Trends in Endocrinology and Metabolism* 15 (4): 166. <https://doi.org/10.1016/J.TEM.2004.03.001>.
- Busnadiego, Idoia, Sonja Fernbach, Marie O Pohl, Umut Karakus, Michael Huber, Alexandra Trkola, Silke Stertz, and Benjamin G Hale. 2020. 'Antiviral Activity of Type I, II, and III Interferons Counterbalances ACE2 Inducibility and Restricts SARS-CoV-2'. <https://doi.org/10.1128/mBio.01928-20>.
- Casalino, Lorenzo, Zied Gaieb, Jory A. Goldsmith, Christy K. Hjorth, Abigail C. Dommer, Aoife M. Harbison, Carl A. Fogarty, et al. 2020. 'Beyond Shielding: The Roles of Glycans in the SARS-CoV-2 Spike Protein'. *ACS Central Science* 6 (10): 1722–34. https://doi.org/10.1021/ACSCENTSCI.0C01056/SUPPL_FILE/OC0C01056_SI_006.ZIP.
- Cevik, Muge, Krutika Kuppalli, Jason Kindrachuk, and Malik Peiris. 2020. 'Virology, Transmission, and Pathogenesis of SARS-CoV-2'. *British Medical Journal*, October. <https://doi.org/10.1136/bmj.m3862>.

- Chamchoy, Kamonwan, Danaya Pakotiprapha, Pornpan Pumirat, Ubolsree Leartsakulpanich, and Usa Boonyuen. 2019. 'Application of WST-8 Based Colorimetric NAD(P)H Detection for Quantitative Dehydrogenase Assays'. *BMC Biochemistry* 20 (1).
<https://doi.org/10.1186/S12858-019-0108-1>.
- Chan, Yujia Alina, and Shing Hei Zhan. 2022. 'The Emergence of the Spike Furin Cleavage Site in SARS-CoV-2'. *Molecular Biology and Evolution* 39 (1).
<https://doi.org/10.1093/MOLBEV/MSAB327>.
- Chen, Dong, Dong Chen, Xiaokun Li, Qifa Song, Chenchan Hu, Chenchan Hu, Feifei Su, et al. 2020. 'Assessment of Hypokalemia and Clinical Characteristics in Patients With Coronavirus Disease 2019 in Wenzhou, China'. *JAMA Network Open* 3 (6).
<https://doi.org/10.1001/JAMANETWORKOPEN.2020.11122>.
- Chen, Fei, Yankun Zhang, Xiaoyun Li, Wen Li, Xuan Liu, and Xinyu Xue. 2021. 'The Impact of ACE2 Polymorphisms on COVID-19 Disease: Susceptibility, Severity, and Therapy'. *Frontiers in Cellular and Infection Microbiology* 11 (October).
<https://doi.org/10.3389/FCIMB.2021.753721>.
- Chen, Ruirong, Zhien Lan, Jujian Ye, Limin Pang, Yi Liu, Wei Wu, Xiaohuan Qin, Yang Guo, and Peidong Zhang. 2021. 'Cytokine Storm: The Primary Determinant for the Pathophysiological Evolution of COVID-19 Deterioration'. *Frontiers in Immunology* 12 (April): 1409.
<https://doi.org/10.3389/FIMMU.2021.589095/BIBTEX>.
- Cheng, Xiao Wen, Jie Li, Lu Zhang, Wen Jun Hu, Lu Zong, Xiang Xu, Jin Ping Qiao, et al. 2022. 'Identification of SARS-CoV-2 Variants and Their Clinical Significance in Hefei, China'. *Frontiers in Medicine* 8 (January). <https://doi.org/10.3389/FMED.2021.784632>.
- Chupp, Geoffrey, Anne Spichler-Moffarah, Ole S. Sjøgaard, Denise Esserman, James Dziura, Lisa Danzig, Reetika Chaurasia, et al. 2022. 'A Phase 2 Randomized, Double-Blind, Placebo-Controlled Trial of Oral Camostat Mesylate for Early Treatment of COVID-19 Outpatients Showed Shorter Illness Course and Attenuation of Loss of Smell and Taste'. *MedRxiv*, January. <https://doi.org/10.1101/2022.01.28.22270035>.
- Cleemput, Jolien van, Willem van Snippenberg, Laurens Lambrechts, Amélie Dendooven, Valentino D'Onofrio, Liesbeth Couck, Wim Trypsteen, et al. 2021. 'Organ-Specific Genome Diversity of Replication-Competent SARS-CoV-2'. *Nature Communications* 2021 12:1 12 (1): 1–11. <https://doi.org/10.1038/s41467-021-26884-7>.
- Coperchini, Francesca, Gianluca Ricci, Laura Croce, Marco Denegri, Rubina Ruggiero, Laura Villani, Flavia Magri, Luca Chiovato, and Mario Rotondi. 2020. 'Modulation of ACE-2 mRNA by Inflammatory Cytokines in Human Thyroid Cells: A Pilot Study'.
<https://doi.org/10.1007/s12020-021-02807-w>.
- Darif, Dounia, Ikram Hammi, Ayyoub Kihel, Imane el Idrissi Saik, Fadila Guessous, and Khadija Akarid. 2021. 'The Pro-Inflammatory Cytokines in COVID-19 Pathogenesis: What Goes Wrong?' *Microbial Pathogenesis* 153 (April): 104799.
<https://doi.org/10.1016/J.MICPATH.2021.104799>.
- Darzi, Emale El, Samer Bazzi, Sarah Daoud, Karim S. Echtay, and Georges M. Bahr. 2017. 'Differential Regulation of Surface Receptor Expression, Proliferation, and Apoptosis in HaCaT Cells Stimulated with Interferon- γ , Interleukin-4, Tumor Necrosis Factor- α , or

- Muramyl Dipeptide'. *International Journal of Immunopathology and Pharmacology* 30 (2): 130. <https://doi.org/10.1177/0394632017707611>.
- Dejnirattisai, Wanwisa, Daming Zhou, Helen M. Ginn, Helen M.E. Duyvesteyn, Piyada Supasa, James Brett Case, Yuguang Zhao, et al. 2021. 'The Antigenic Anatomy of SARS-CoV-2 Receptor Binding Domain'. *Cell* 184 (8): 2183-2200.e22. <https://doi.org/10.1016/J.CELL.2021.02.032>.
- Devaux, Christian A, Jean-Marc Rolain, and Didier Raoult. 2020. 'ACE2 Receptor Polymorphism: Susceptibility to SARS-CoV-2, Hypertension, Multi-Organ Failure, and COVID-19 Disease Outcome'. *Immunology and Infection* 53: 425–35. <https://doi.org/10.1016/j.jmii.2020.04.015>.
- Dhawan, Manish, Abhilasha Sharma, Priyanka, Nanamika Thakur, Tridib Kumar Rajkhowa, and Om Prakash Choudhary. 2022. 'Delta Variant (B.1.617.2) of SARS-CoV-2: Mutations, Impact, Challenges and Possible Solutions'. *Human Vaccines & Immunotherapeutics* 18 (5). <https://doi.org/10.1080/21645515.2022.2068883>.
- Donoghue, M., F. Hsieh, E. Baronas, K. Godbout, M. Gosselin, N. Stagliano, M. Donovan, et al. 2000. 'A Novel Angiotensin-Converting Enzyme-Related Carboxypeptidase (ACE2) Converts Angiotensin I to Angiotensin 1-9'. *Circulation Research* 87 (5). <https://doi.org/10.1161/01.RES.87.5.E1>.
- Du, Yaoqiang, Hao Wang, Linjie Chen, Quan Fang, Biqin Zhang, Luxi Jiang, Zhaoyu Wu, et al. 2021. 'Non-RBM Mutations Impaired SARS-CoV-2 Spike Protein Regulated to the ACE2 Receptor Based on Molecular Dynamic Simulation'. *Frontiers in Molecular Biosciences* 8 (July): 736. <https://doi.org/10.3389/FMOLB.2021.614443/BIBTEX>.
- Eguchi, Satoru, Tatsuo Kawai, Rosario Scalia, and Victor Rizzo. 2018. 'Understanding Angiotensin II Type 1 Receptor Signaling in Vascular Pathophysiology'. *Hypertension (Dallas, Tex. : 1979)* 71 (5): 804–10. <https://doi.org/10.1161/HYPERTENSIONAHA.118.10266>.
- Essalmani, Rachid, Jaspreet Jain, Delia Susan-Resiga, Ursula Andréo, Alexandra Evagelidis, Rabeb Mouna Derbali, David N. Huynh, et al. 2022. 'Distinctive Roles of Furin and TMPRSS2 in SARS-CoV-2 Infectivity'. *Journal of Virology* 96 (8). <https://doi.org/10.1128/JVI.00128-22>.
- Fang, Lei, George Karakiulakis, and Michael Roth. 2020. 'Are Patients with Hypertension and Diabetes Mellitus at Increased Risk for COVID-19 Infection?' *The Lancet. Respiratory Medicine* 8 (4): e21. [https://doi.org/10.1016/S2213-2600\(20\)30116-8](https://doi.org/10.1016/S2213-2600(20)30116-8).
- Ferreira, Isabella A.T.M., Steven A. Kemp, Rawlings Datir, Akatsuki Saito, Bo Meng, Partha Rakshit, Akifumi Takaori-Kondo, et al. 2021. 'SARS-CoV-2 B.1.617 Mutations L452R and E484Q Are Not Synergistic for Antibody Evasion'. *The Journal of Infectious Diseases* 224 (6): 989–94. <https://doi.org/10.1093/INFDIS/JIAB368>.
- Fleur Sernee, M., Hidde L. Ploegh, and Danny J. Schust. 1998. 'Why Certain Antibodies Cross-React with HLA-A and HLA-G: Epitope Mapping of Two Common MHC Class I Reagents'. *Molecular Immunology* 35 (3): 177–88. [https://doi.org/10.1016/S0161-5890\(98\)00026-1](https://doi.org/10.1016/S0161-5890(98)00026-1).
- Foresta, C., M. S. Rocca, and A. di Nisio. 2021. 'Gender Susceptibility to COVID-19: A Review of the Putative Role of Sex Hormones and X Chromosome'. *Journal of Endocrinological Investigation* 44 (5): 951–56. <https://doi.org/10.1007/S40618-020-01383-6/FIGURES/1>.

- Fountain, John H., and Sarah L. Lappin. 2022. 'Physiology, Renin Angiotensin System'. *StatPearls*, June. <https://www.ncbi.nlm.nih.gov/books/NBK470410/>.
- Francesca, Pistollato, Petrillo Mauro, Laure Alix Clerbaux, Gabriele Leoni, Jessica Ponti, Alessia Bogni, Carlo Brogna, et al. 2022. 'Effects of Spike Protein and Toxin-like Peptides Found in COVID-19 Patients on Human 3D Neuronal/Glial Model Undergoing Differentiation: Possible Implications for SARS-CoV-2 Impact on Brain Development'. *Reproductive Toxicology (Elmsford, N.y.)* 111 (August): 34. <https://doi.org/10.1016/J.REPROTOX.2022.04.011>.
- Fraser, Bryan J., Serap Beldar, Almagul Seitova, Ashley Hutchinson, Dhiraj Mannar, Yanjun Li, Daniel Kwon, et al. 2022. 'Structure and Activity of Human TMPRSS2 Protease Implicated in SARS-CoV-2 Activation'. *Nature Chemical Biology* 2022 18:9 18 (9): 963–71. <https://doi.org/10.1038/s41589-022-01059-7>.
- Gangavarapu, Karthik, Alaa Abdel Latif, Julia L. Mullen, Manar Alkuzweny, Emory Hufbauer, Ginger Tsueng, Emily Haag, et al. 2022. 'Outbreak.Info Genomic Reports: Scalable and Dynamic Surveillance of SARS-CoV-2 Variants and Mutations'. *MedRxiv*, June, 2022.01.27.22269965. <https://doi.org/10.1101/2022.01.27.22269965>.
- Gao, Xiang, Shengyuan Zhang, Jizhou Gou, Yanling Wen, Lujie Fan, Jian Zhou, Guangde Zhou, Gang Xu, and Zheng Zhang. 2022. 'Spike-Mediated ACE2 down-Regulation Was Involved in the Pathogenesis of SARS-CoV-2 Infection'. *Journal of Infection* 85 (4): 418–27. <https://doi.org/10.1016/j.jinf.2022.06.030>.
- Gao, Yan Lei, Yue Du, Chao Zhang, Cheng Cheng, Hai Yan Yang, Yue Fei Jin, Guang Cai Duan, and Shuai Yin Chen. 2020. 'Role of Renin-Angiotensin System in Acute Lung Injury Caused by Viral Infection'. *Infection and Drug Resistance* 13: 3715–25. <https://doi.org/10.2147/IDR.S265718>.
- Gheblawi, Mahmoud, Kaiming Wang, Anissa Viveiros, Quynh Nguyen, Jiu Chang Zhong, Anthony J. Turner, Mohan K. Raizada, Maria B. Grant, and Gavin Y. Oudit. 2020. 'Angiotensin-Converting Enzyme 2: SARS-CoV-2 Receptor and Regulator of the Renin-Angiotensin System: Celebrating the 20th Anniversary of the Discovery of ACE2'. *Circulation Research* 126 (10): 1456–74. <https://doi.org/10.1161/CIRCRESAHA.120.317015>.
- Gheware, Atish, Animesh Ray, Deeksha Rana, Prashant Bajpai, Aruna Nambirajan, S. Arulselvi, Purva Mathur, et al. 2022. 'ACE2 Protein Expression in Lung Tissues of Severe COVID-19 Infection'. *Scientific Reports* 2022 12:1 12 (1): 1–10. <https://doi.org/10.1038/s41598-022-07918-6>.
- Giamarellos-Bourboulis, Evangelos J., Mihai G. Netea, Nikoletta Rovina, Karolina Akinosoglou, Anastasia Antoniadou, Nikolaos Antonakos, Georgia Damoraki, et al. 2020. 'Complex Immune Dysregulation in COVID-19 Patients with Severe Respiratory Failure'. *Cell Host & Microbe* 27 (6): 992-1000.e3. <https://doi.org/10.1016/J.CHOM.2020.04.009>.
- Giron, Carolina Corrêa, Aatto Laaksonen, and Fernando Luís Barroso da Silva. 2022. 'Differences between Omicron SARS-CoV-2 RBD and Other Variants in Their Ability to Interact with Cell Receptors and Monoclonal Antibodies'. *Journal of Biomolecular Structure & Dynamics*. <https://doi.org/10.1080/07391102.2022.2095305>.
- Glowacka, Ilona, Stephanie Bertram, Petra Herzog, Susanne Pfefferle, Imke Steffen, Marcus O. Muench, Graham Simmons, et al. 2010. 'Differential Downregulation of ACE2 by the Spike

- Proteins of Severe Acute Respiratory Syndrome Coronavirus and Human Coronavirus NL63'. *Journal of Virology* 84 (2): 1198–1205. <https://doi.org/10.1128/JVI.01248-09>.
- Gomes, Caio P., Danilo E. Fernandes, Fernanda Casimiro, Gustavo F. da Mata, Michelle T. Passos, Patricia Varela, Gianna Mastroianni-Kirsztajn, and João Bosco Pesquero. 2020. 'Cathepsin L in COVID-19: From Pharmacological Evidences to Genetics'. *Frontiers in Cellular and Infection Microbiology* 10 (December): 777. <https://doi.org/10.3389/FCIMB.2020.589505/BIBTEX>.
- Gong, Yanqiu, Suideng Qin, Lunzhi Dai, and Zhixin Tian. 2021. 'The Glycosylation in SARS-CoV-2 and Its Receptor ACE2'. *Signal Transduction and Targeted Therapy* 6 (1). <https://doi.org/10.1038/S41392-021-00809-8>.
- Guang, Cuie, Robert D. Phillips, Bo Jiang, and Franco Milani. 2012. 'Three Key Proteases – Angiotensin-I-Converting Enzyme (ACE), ACE2 and Renin – within and beyond the Renin-Angiotensin System'. *Archives of Cardiovascular Diseases* 105 (6): 373. <https://doi.org/10.1016/J.ACVD.2012.02.010>.
- Gusev, Evgenii, Alexey Sarapultsev, Liliya Solomatina, and Valeriy Chereshevnev. 2022. 'SARS-CoV-2-Specific Immune Response and the Pathogenesis of COVID-19'. *International Journal of Molecular Sciences* 23 (3). <https://doi.org/10.3390/IJMS23031716>.
- Hamming, I, W Timens, Mlc Bulthuis, A T Lely, G J Navis, and H van Goor. 2004. 'Rapid Communication Tissue Distribution of ACE2 Protein, the Functional Receptor for SARS Coronavirus. A First Step in Understanding SARS Pathogenesis'. *Journal of Pathology J Pathol* 203: 631–37. <https://doi.org/10.1002/path.1570>.
- Han, Huan, Qingfeng Ma, Cong Li, Rui Liu, Li Zhao, Wei Wang, Pingan Zhang, et al. 2020. 'Profiling Serum Cytokines in COVID-19 Patients Reveals IL-6 and IL-10 Are Disease Severity Predictors'. *Emerging Microbes & Infections* 9 (1): 1123–30. <https://doi.org/10.1080/22221751.2020.1770129>.
- Han, Seunghye, and Rama K Mallampalli. n.d. 'The Acute Respiratory Distress Syndrome: From Mechanism to Translation'. Accessed 18 January 2023. <https://doi.org/10.4049/jimmunol.1402513>.
- Harvey, William T., Alessandro M. Carabelli, Ben Jackson, Ravindra K. Gupta, Emma C. Thomson, Ewan M. Harrison, Catherine Ludden, et al. 2021. 'SARS-CoV-2 Variants, Spike Mutations and Immune Escape'. *Nature Reviews Microbiology* 2021 19:7 19 (7): 409–24. <https://doi.org/10.1038/s41579-021-00573-0>.
- Hassan, Sk Sarif, Pabitra Pal Choudhury, Guy W. Dayhoff, Alaa A.A. Aljabali, Bruce D. Uhal, Kenneth Lundstrom, Nima Rezaei, et al. 2022. 'The Importance of Accessory Protein Variants in the Pathogenicity of SARS-CoV-2'. *Archives of Biochemistry and Biophysics* 717 (March). <https://doi.org/10.1016/J.ABB.2022.109124>.
- Hemnes, Anna R., Anandharajan Rathinasabapathy, Eric A. Austin, Evan L. Brittain, Erica J. Carrier, Xiping Chen, Joshua P. Fessel, et al. 2018. 'A Potential Therapeutic Role for Angiotensin-Converting Enzyme 2 in Human Pulmonary Arterial Hypertension'. *The European Respiratory Journal* 51 (6). <https://doi.org/10.1183/13993003.02638-2017>.
- Hikmet, FERIA, Loren Méar, Åsa Edvinsson, Patrick Micke, Mathias Uhlén, and Cecilia Lindskog. 2020. 'The Protein Expression Profile of ACE2 in Human Tissues'. *Molecular Systems Biology* 16 (7). <https://doi.org/10.15252/MSB.20209610>.

- Hirabara, Sandro M., Tamires D.A. Serdan, Renata Gorjao, Laureane N. Masi, Tania C. Pithon-Curi, Dimas T. Covas, Rui Curi, and Edison L. Durigon. 2022. 'SARS-COV-2 Variants: Differences and Potential of Immune Evasion'. *Frontiers in Cellular and Infection Microbiology* 11 (January): 1401. <https://doi.org/10.3389/FCIMB.2021.781429/BIBTEX>.
- Hoffmann, Markus, Heike Hofmann-Winkler, and Stefan Pöhlmann. 2018. 'Priming Time: How Cellular Proteases Arm Coronavirus Spike Proteins'. *Activation of Viruses by Host Proteases*, May, 71. https://doi.org/10.1007/978-3-319-75474-1_4.
- Hoffmann, Markus, Heike Hofmann-Winkler, Joan C. Smith, Nadine Krüger, Perna Arora, Lambert K. Sørensen, Ole S. Sjøgaard, et al. 2021. 'Camostat Mesylate Inhibits SARS-CoV-2 Activation by TMPRSS2-Related Proteases and Its Metabolite GBPA Exerts Antiviral Activity'. *EBioMedicine* 65 (March): 103255. <https://doi.org/10.1016/j.ebiom.2021.103255>.
- Hojyo, Shintaro, Mona Uchida, Kumiko Tanaka, Rie Hasebe, Yuki Tanaka, Masaaki Murakami, and Toshio Hirano. 2020. 'How COVID-19 Induces Cytokine Storm with High Mortality'. *Inflammation and Regeneration* 40 (1). <https://doi.org/10.1186/S41232-020-00146-3>.
- Hu, Ben, Hua Guo, Peng Zhou, and Zheng-Li Shi. 2021. 'Characteristics of SARS-CoV-2 and COVID-19'. *Nature*. <https://doi.org/10.1038/s41579-020-00459-7>.
- Huang, Chaolin, Yeming Wang, Xingwang Li, Lili Ren, Jianping Zhao, Yi Hu, Li Zhang, et al. 2020. 'Clinical Features of Patients Infected with 2019 Novel Coronavirus in Wuhan, China'. *The Lancet* 395 (10223): 497–506. [https://doi.org/10.1016/S0140-6736\(20\)30183-5](https://doi.org/10.1016/S0140-6736(20)30183-5).
- Huang, Yuan, Chan Yang, Xin-Feng Xu, Wei Xu, and Shu-Wen Liu. 2020. 'Structural and Functional Properties of SARS-CoV-2 Spike Protein: Potential Antivirus Drug Development for COVID-19'. <https://doi.org/10.1038/s41401-020-0485-4>.
- Iheanacho, Chinonyerem O, Valentine U Odili, and Uchenna I H Eze. n.d. 'Risk of SARS-CoV-2 Infection and COVID-19 Prognosis with the Use of Renin-Angiotensin-Aldosterone System (RAAS) Inhibitors: A Systematic Review'. Accessed 27 December 2022. <https://doi.org/10.1186/s43094-021-00224-4>.
- Imai, Yumiko, Keiji Kuba, and Josef M. Penninger. 2008. 'The Discovery of Angiotensin-Converting Enzyme 2 and Its Role in Acute Lung Injury in Mice'. *Experimental Physiology* 93 (5): 543–48. <https://doi.org/10.1113/EXPPHYSIOL.2007.040048>.
- Inoue, Yuuki, Nobuyuki Tanaka, Yoshinori Tanaka, Shingo Inoue, Kouichi Morita, Min Zhuang, Toshio Hattori, and Kazuo Sugamura. 2007. 'Clathrin-Dependent Entry of Severe Acute Respiratory Syndrome Coronavirus into Target Cells Expressing ACE2 with the Cytoplasmic Tail Deleted'. *Journal of Virology* 81 (16): 8722–29. <https://doi.org/10.1128/JVI.00253-07>.
- Iwata-Yoshikawa, Naoko, Tadashi Okamura, Yukiko Shimizu, Hideki Hasegawa, Makoto Takeda, and Noriyo Nagata. 2019. 'TMPRSS2 Contributes to Virus Spread and Immunopathology in the Airways of Murine Models after Coronavirus Infection'. *Journal of Virology* 93 (6): 1815–33. <https://doi.org/10.1128/JVI.01815-18>.
- Jackson, Cody B., Michael Farzan, Bing Chen, and Hyeryun Choe. 2021. 'Mechanisms of SARS-CoV-2 Entry into Cells'. *Nature Reviews Molecular Cell Biology* 23:1 23 (1): 3–20. <https://doi.org/10.1038/s41580-021-00418-x>.

- Jaimes, Javier A., Nicole M. André, Joshua S. Chappie, Jean K. Millet, and Gary R. Whittaker. 2020. 'Phylogenetic Analysis and Structural Modeling of SARS-CoV-2 Spike Protein Reveals an Evolutionary Distinct and Proteolytically Sensitive Activation Loop'. *Journal of Molecular Biology* 432 (10): 3309–25. <https://doi.org/10.1016/J.JMB.2020.04.009>.
- Jangra, Sonia, Chengjin Ye, Raveen Rathnasinghe, Daniel Stadlbauer, PVI study group, Florian Krammer, Viviana Simon, Luis Martinez-Sobrido, Adolfo García-Sastre, and Michael Schotsaert. 2021. 'The E484K Mutation in the SARS-CoV-2 Spike Protein Reduces but Does Not Abolish Neutralizing Activity of Human Convalescent and Post-Vaccination.' *MedRxiv*, January. <https://doi.org/10.1101/2021.01.26.21250543>.
- Kalkeri, Raj, Scott Goebel, and Guru Dutt Sharma. 2020. 'SARS-CoV-2 Shedding from Asymptomatic Patients: Contribution of Potential Extrapulmonary Tissue Reservoirs'. *The American Journal of Tropical Medicine and Hygiene* 103 (1): 18. <https://doi.org/10.4269/AJTMH.20-0279>.
- Karki, Rajendra, Bhesh Raj Sharma, Shraddha Tuladhar, Evan Peter Williams, Lillian Zalduondo, Parimal Samir, Min Zheng, et al. 2021. 'Synergism of TNF- α and IFN- γ Triggers Inflammatory Cell Death, Tissue Damage, and Mortality in SARS-CoV-2 Infection and Cytokine Shock Syndromes'. *Cell* 184 (1): 149-168.e17. <https://doi.org/10.1016/J.CELL.2020.11.025>.
- Kaseb, Ahmed O, Yehia I Mohamed, Alexandre E Malek, Issam I Raad, Lina Altameemi, Dan Li, Omar A Kaseb, Safa A Kaseb, Abdelhafez Selim, and Qing Ma. 2021. 'The Impact of Angiotensin-Converting Enzyme 2 (ACE2) Expression on the Incidence and Severity of COVID-19 Infection'. <https://doi.org/10.3390/pathogens10030379>.
- Khan, Shahanshah, Mahnoush S. Shafiei, Christopher Longoria, John W. Schoggins, Rashmin C. Savani, and Hasan Zaki. 2021. 'SARS-CoV-2 Spike Protein Induces Inflammation via TLR2-Dependent Activation of the NF-KB Pathway'. *ELife* 10 (December): 68563. <https://doi.org/10.7554/ELIFE.68563>.
- Khateeb, Jasmin, Yuchong Li, and Haibo Zhang. 2021. 'Emerging SARS-CoV-2 Variants of Concern and Potential Intervention Approaches'. *Critical Care (London, England)* 25 (1). <https://doi.org/10.1186/S13054-021-03662-X>.
- Kinoshita, Taku, Masahiro Shinoda, Yasuhiro Nishizaki, Katsuya Shiraki, Yuji Hirai, Yoshiko Kichikawa, Kenji Tsushima, et al. 2022. 'A Multicenter, Double-Blind, Randomized, Parallel-Group, Placebo-Controlled Study to Evaluate the Efficacy and Safety of Camostat Mesilate in Patients with COVID-19 (CANDLE Study)'. *BMC Medicine* 20 (1): 1–14. <https://doi.org/10.1186/S12916-022-02518-7/TABLES/3>.
- Kirchdoerfer, Robert N, Nianshuang Wang, Jesper Pallesen, Daniel Wrapp, Hannah L Turner, Christopher A Cottrell, Kizzmekia S Corbett, Barney S Graham, Jason S McLellan, and Andrew B Ward. 2018. 'Stabilized Coronavirus Spikes Are Resistant to Conformational Changes Induced by Receptor Recognition or Proteolysis OPEN'. <https://doi.org/10.1038/s41598-018-34171-7>.
- Knöfler, Martin, Martin Stenzel, and Peter Husslein. 1998. 'Shedding of Tumour Necrosis Factor Receptors from Purified Villous Term Trophoblasts and Cytotrophoblastic BeWo Cells'. *Human Reproduction (Oxford, England)* 13 (8): 2308–16. <https://doi.org/10.1093/HUMREP/13.8.2308>.

- Konur, Abdo, U. Schulz, G. Eissner, R. Andreesen, and E. Holler. 2005. 'Interferon (IFN)- γ Is a Main Mediator of Keratinocyte (HaCaT) Apoptosis and Contributes to Autocrine IFN- γ and Tumour Necrosis Factor- α Production'. *British Journal of Dermatology* 152 (6): 1134–42. <https://doi.org/10.1111/J.1365-2133.2005.06508.X>.
- Krasny, Lukas, Philip Bland, Naoko Kogata, Patty Wai, Beatrice A. Howard, Rachael C. Natrajan, and Paul H. Huang. 2018. 'SWATH Mass Spectrometry as a Tool for Quantitative Profiling of the Matrisome'. *Journal of Proteomics* 189 (October): 11–22. <https://doi.org/10.1016/J.JPROT.2018.02.026>.
- Kumar, Swatantra, Rajni Nyodu, Vimal K. Maurya, and Shailendra K. Saxena. 2020. 'Morphology, Genome Organization, Replication, and Pathogenesis of Severe Acute Respiratory Syndrome Coronavirus 2 (SARS-CoV-2)', 23–31. https://doi.org/10.1007/978-981-15-4814-7_3.
- Laing, Adam G., Anna Lorenc, Irene del Molino del Barrio, Abhishek Das, Matthew Fish, Leticia Monin, Miguel Muñoz-Ruiz, et al. 2020. 'A Dynamic COVID-19 Immune Signature Includes Associations with Poor Prognosis'. *Nature Medicine* 26 (10): 1623–35. <https://doi.org/10.1038/S41591-020-1038-6>.
- Lan, Jun, Jiwan Ge, Jinfang Yu, Sisi Shan, Huan Zhou, Shilong Fan, Qi Zhang, et al. 2020. 'Structure of the SARS-CoV-2 Spike Receptor-Binding Domain Bound to the ACE2 Receptor'. <https://doi.org/10.1038/s41586-020-2180-5>.
- Lang, Anna de, Albert D.M.E. Osterhaus, and Bart L. Haagmans. 2006. 'Interferon- γ and Interleukin-4 Downregulate Expression of the SARS Coronavirus Receptor ACE2 in Vero E6 Cells'. *Virology* 353 (2): 474–81. <https://doi.org/10.1016/J.VIROL.2006.06.011>.
- Lanza, Katharina, Lucas G Perez, Larissa B Costa, Thiago M Cordeiro, Vitria A Palmeira, Victor T Ribeiro, Ana Cristina SimõesSim, and Simões Silva. 2020. 'Covid-19: The Renin-Angiotensin System Imbalance Hypothesis'. *Clinical Science* 134: 1259–64. <https://doi.org/10.1042/CS20200492>.
- Lauring, Adam S., and Emma B. Hodcroft. 2021. 'Genetic Variants of SARS-CoV-2—What Do They Mean?' *JAMA* 325 (6): 529–31. <https://doi.org/10.1001/JAMA.2020.27124>.
- Lee, Amanda J., and Ali A. Ashkar. 2018. 'The Dual Nature of Type I and Type II Interferons'. *Frontiers in Immunology* 9 (SEP): 2061. <https://doi.org/10.3389/FIMMU.2018.02061/BIBTEX>.
- Lee, Chiu Yang, Chih Heng Huang, Elham Rastegari, Vimalan Rengganaten, Ping Cheng Liu, Ping Hsing Tsai, Yuan Fan Chin, et al. 2021. 'Tumor Necrosis Factor-Alpha Exacerbates Viral Entry in SARS-CoV2-Infected iPSC-Derived Cardiomyocytes'. *International Journal of Molecular Sciences* 22 (18): 9869. <https://doi.org/10.3390/IJMS22189869>.
- Li, Meng Yuan, Lin Li, Yue Zhang, and Xiao Sheng Wang. 2020. 'Expression of the SARS-CoV-2 Cell Receptor Gene ACE2 in a Wide Variety of Human Tissues'. *Infectious Diseases of Poverty* 9 (1): 1–7. <https://doi.org/10.1186/S40249-020-00662-X/FIGURES/2>.
- Li, Wenhui, Michael J. Moore, Natalya Vasllieva, Jianhua Sui, Swee Kee Wong, Michael A. Berne, Mohan Somasundaran, et al. 2003. 'Angiotensin-Converting Enzyme 2 Is a Functional Receptor for the SARS Coronavirus'. *Nature* 426 (6965): 450–54. <https://doi.org/10.1038/NATURE02145>.

- Liang, Yan, Heng Li, Jing Li, Ze Ning Yang, Jia Li Li, Hui Wen Zheng, Yan Li Chen, Hai Jing Shi, Lei Guo, and Long Ding Liu. 2020. 'Role of Neutrophil Chemoattractant CXCL5 in SARS-CoV-2 Infection-Induced Lung Inflammatory Innate Immune Response in an in Vivo HACE2 Transfection Mouse Model'. *Zoological Research* 41 (6): 621–31. <https://doi.org/10.24272/J.ISSN.2095-8137.2020.118>.
- Liu, Jia, Yufeng Li, Qian Liu, Qun Yao, Xi Wang, Huanyu Zhang, Rong Chen, et al. 2021. 'SARS-CoV-2 Cell Tropism and Multiorgan Infection'. *Cell Discovery* 2021 7:1 7 (1): 1–4. <https://doi.org/10.1038/s41421-021-00249-2>.
- Liu, Yang, Jianying Liu, Kenneth S Plante, Jessica A Plante, Xuping Xie, Xianwen Zhang, Zhiqiang Ku, et al. 2022. 'The N501Y Spike Substitution Enhances SARS-CoV-2 Infection and Transmission'. *Nature* | 294. <https://doi.org/10.1038/s41586-021-04245-0>.
- Liu, Zheng Gang. 2005. 'Molecular Mechanism of TNF Signaling and Beyond'. *Cell Research* 2005 15:1 15 (1): 24–27. <https://doi.org/10.1038/sj.cr.7290259>.
- Lok, John, Man Law, Michael Logan, Michael A Joyce, Abdolamir Landi, Darren Hockman, Kevin Crawford, et al. 2021. 'SARS-COV-2 Recombinant Receptor-Binding-Domain (RBD) Induces Neutralizing Antibodies against Variant Strains of SARS-CoV-2 and SARS-CoV-1'. <https://doi.org/10.1016/j.vaccine.2021.08.081>.
- Lu, Roujian, Xiang Zhao, Juan Li, Peihua Niu, Bo Yang, Honglong Wu, Wenling Wang, et al. 2020. 'Genomic Characterisation and Epidemiology of 2019 Novel Coronavirus: Implications for Virus Origins and Receptor Binding'. *Lancet (London, England)* 395 (10224): 565–74. [https://doi.org/10.1016/S0140-6736\(20\)30251-8](https://doi.org/10.1016/S0140-6736(20)30251-8).
- Lu, Yi, Qingwei Zhu, Douglas M. Fox, Carol Gao, Sarah A. Stanley, and Kunxin Luo. 2022. 'SARS-CoV-2 down-Regulates ACE2 through Lysosomal Degradation'. *Molecular Biology of the Cell* 33 (14): ar147. <https://doi.org/10.1091/MBC.E22-02-0045>.
- Lubbe, Lizelle, Gyles E Cozier, Delia Oosthuizen, K Ravi Acharya, and Edward D Sturrock. 2020. 'ACE2 and ACE: Structure-Based Insights into Mechanism, Regulation and Receptor Recognition by SARS-CoV'. *Clinical Science* 134: 2851–71. <https://doi.org/10.1042/CS20200899>.
- Lubinski, Bailey, Javier A Jaimes, and Gary R Whittaker. 2022. 'Intrinsic Furin-Mediated Cleavability of the Spike S1/S2 Site from SARS-CoV-2 Variant B.1.1.529 (Omicron)'. *BioRxiv*, July. <https://doi.org/10.1101/2022.04.20.488969>.
- Lupala, Cecylia S., Xuanxuan Li, Jian Lei, Hong Chen, Jianxun Qi, Haiguang Liu, and Xiao-dong Su. 2020. 'Computational Simulations Reveal the Binding Dynamics between Human ACE2 and the Receptor Binding Domain of SARS-CoV-2 Spike Protein'. *BioRxiv*, March, 2020.03.24.005561. <https://doi.org/10.1101/2020.03.24.005561>.
- Lv, Huibin, Nicholas C. Wu, Owen Tak Yin Tsang, Meng Yuan, Ranawaka A.P.M. Perera, Wai Shing Leung, Ray T.Y. So, et al. 2020. 'Cross-Reactive Antibody Response between SARS-CoV-2 and SARS-CoV Infections'. *Cell Reports* 31 (9). <https://doi.org/10.1016/J.CELREP.2020.107725>.
- Ma, Di, Chong Bo Chen, Vishal Jhanji, Ciyan Xu, Xiang Ling Yuan, Jia Jian Liang, Yuqiang Huang, Ling Ping Cen, and Tsz Kin Ng. 2020. 'Expression of SARS-CoV-2 Receptor ACE2 and TMPRSS2 in Human Primary Conjunctival and Pterygium Cell Lines and in Mouse Cornea'. *Eye (London, England)* 34 (7): 1212–19. <https://doi.org/10.1038/S41433-020-0939-4>.

- Ma, Terry K.W., Kevin K.H. Kam, Bryan P. Yan, and Yat Yin Lam. 2010. 'Renin–Angiotensin–Aldosterone System Blockade for Cardiovascular Diseases: Current Status'. *British Journal of Pharmacology* 160 (6): 1273. <https://doi.org/10.1111/J.1476-5381.2010.00750.X>.
- Mannar, Dhiraj, James W. Saville, Xing Zhu, Shanti S. Srivastava, Alison M. Berezuk, Katharine S. Tuttle, Ana Citlali Marquez, Inna Sekirov, and Sriram Subramaniam. 2022. 'SARS-CoV-2 Omicron Variant: Antibody Evasion and Cryo-EM Structure of Spike Protein–ACE2 Complex'. *Science* 375 (6582): 760–64. https://doi.org/10.1126/SCIENCE.ABN7760/SUPPL_FILE/SCIENCE.ABN7760_MДАР_REPRODUCIBILITY_CHECKLIST.PDF.
- Martínez-Flores, Daniel, Jesús Zepeda-Cervantes, Adolfo Cruz-Reséndiz, Sergio Aguirre-Sampieri, Alicia Sampieri, and Luis Vaca. 2021. 'SARS-CoV-2 Vaccines Based on the Spike Glycoprotein and Implications of New Viral Variants'. *Frontiers in Immunology* 12 (July): 701501. <https://doi.org/10.3389/FIMMU.2021.701501>.
- Mascolo, Annamaria, Cristina Scavone, Concetta Rafaniello, Antonella De Angelis, Konrad Urbanek, Gabriella di Mauro, Donato Cappetta, Liberato Berrino, Francesco Rossi, and Annalisa Capuano. 2021. 'The Role of Renin-Angiotensin-Aldosterone System in the Heart and Lung: Focus on COVID-19'. *Frontiers in Pharmacology* 12 (April). <https://doi.org/10.3389/FPHAR.2021.667254>.
- Mathew, Divij, Josephine R Giles, Amy E Baxter, Allison R Greenplate, Jennifer E Wu, Cécile Alanio, Derek A Oldridge, et al. 2020. 'Deep Immune Profiling of COVID-19 Patients Reveals Patient Heterogeneity and Distinct Immunotypes with Implications for Therapeutic Interventions'. *BioRxiv : The Preprint Server for Biology*, May. <https://doi.org/10.1101/2020.05.20.106401>.
- Mauro Gabriella, di, Scavone Cristina, Rafaniello Concetta, Rossi Francesco, and Capuano Annalisa. 2020. 'SARS-Cov-2 Infection: Response of Human Immune System and Possible Implications for the Rapid Test and Treatment'. *International Immunopharmacology* 84 (July). <https://doi.org/10.1016/J.INTIMP.2020.106519>.
- Mcaloon, Conor, Áine Collins, Kevin Hunt, Ann Barber, Andrew W Byrne, Francis Butler, Miriam Casey, et al. n.d. 'Incubation Period of COVID-19: A Rapid Systematic Review and Meta-Analysis of Observational Research'. Accessed 21 December 2022. <https://doi.org/10.1136/bmjopen-2020-039652>.
- McCallum, Matthew, Anna de Marco, Florian A. Lempp, M. Alejandra Tortorici, Dora Pinto, Alexandra C. Walls, Martina Beltramello, et al. 2021. 'N-Terminal Domain Antigenic Mapping Reveals a Site of Vulnerability for SARS-CoV-2'. *Cell* 184 (9): 2332-2347.e16. <https://doi.org/10.1016/J.CELL.2021.03.028>.
- Merad, Miriam, and Jerome C. Martin. 2020. 'Pathological Inflammation in Patients with COVID-19: A Key Role for Monocytes and Macrophages (Nature Reviews Immunology, (2020), 20, 6, (355-362), 10.1038/S41577-020-0331-4)'. *Nature Reviews Immunology* 20 (7): 448. <https://doi.org/10.1038/S41577-020-0353-Y>.
- Michaud, Veronique, Malavika Deodhar, Meghan Arwood, Sweilem B. Al Rihani, Pamela Dow, and Jacques Turgeon. 2020. 'ACE2 as a Therapeutic Target for COVID-19; Its Role in Infectious Processes and Regulation by Modulators of the RAAS System'. *Journal of Clinical Medicine* 9 (7): 1–27. <https://doi.org/10.3390/JCM9072096>.

- Mokhtari, Tahmineh, Fatemeh Hassani, Neda Ghaffari, Babak Ebrahimi, Atousa Yarahmadi, and Ghomareza Hassanzadeh. 2020. 'COVID-19 and Multiorgan Failure: A Narrative Review on Potential Mechanisms'. *Journal of Molecular Histology* 51 (6): 613. <https://doi.org/10.1007/S10735-020-09915-3>.
- Motozono, Chihiro, Mako Toyoda, Jiri Zahradnik, Akatsuki Saito, Hesham Nasser, Toong Seng Tan, Isaac Ngare, et al. 2021. 'SARS-CoV-2 Spike L452R Variant Evades Cellular Immunity and Increases Infectivity'. *Cell Host & Microbe* 29 (7): 1124-1136.e11. <https://doi.org/10.1016/J.CHOM.2021.06.006>.
- Müller, Sabrina, Julia Dennemärker, and Thomas Reinheckel. 2012. 'Specific Functions of Lysosomal Proteases in Endocytic and Autophagic Pathways'. *Biochimica et Biophysica Acta. Proteins and Proteomics* 1824 (1): 34. <https://doi.org/10.1016/J.BBAPAP.2011.07.003>.
- Naqvi, Ahmad Abu Turab, Kisa Fatima, Taj Mohammad, Urooj Fatima, Indrakant K. Singh, Archana Singh, Shaikh Muhammad Atif, Gururao Hariprasad, Gulam Mustafa Hasan, and Md Imtaiyaz Hassan. 2020. 'Insights into SARS-CoV-2 Genome, Structure, Evolution, Pathogenesis and Therapies: Structural Genomics Approach'. *Biochimica et Biophysica Acta - Molecular Basis of Disease* 1866 (10). <https://doi.org/10.1016/J.BBADIS.2020.165878>.
- Naveca, Felipe Gomes, Valdinete Nascimento, Victor Souza, André de Lima Corado, Fernanda Nascimento, George Silva, Matilde Contreras Mejía, et al. 2022. 'Spread of Gamma (P.1) Sub-Lineages Carrying Spike Mutations Close to the Furin Cleavage Site and Deletions in the N-Terminal Domain Drives Ongoing Transmission of SARS-CoV-2 in Amazonas, Brazil'. *Microbiology Spectrum* 10 (1). <https://doi.org/10.1128/SPECTRUM.02366-21>.
- Newby, Maddy L., Carl A. Fogarty, Joel D. Allen, John Butler, Elisa Fadda, and Max Crispin. 2023. 'Variations within the Glycan Shield of SARS-CoV-2 Impact Viral Spike Dynamics'. *Journal of Molecular Biology* 435 (4): 167928. <https://doi.org/10.1016/J.JMB.2022.167928>.
- Nie, Yuchun, Peigang Wang, Xuanling Shi, Guangwen Wang, Jian Chen, Aihua Zheng, Wei Wang, et al. 2004. 'Highly Infectious SARS-CoV Pseudotyped Virus Reveals the Cell Tropism and Its Correlation with Receptor Expression'. *Biochemical and Biophysical Research Communications* 321 (4): 994. <https://doi.org/10.1016/J.BBRC.2004.07.060>.
- Nitulescu, George Mihai, Horia Paunescu, Sterghios A. Moschos, Dimitrios Petrakis, Georgiana Nitulescu, George Nicolae Daniel Ion, Demetrios A. Spandidos, Taxiarchis Konstantinos Nikolouzakis, Nikolaos Drakoulis, and Aristidis Tsatsakis. 2020. 'Comprehensive Analysis of Drugs to Treat SARS-CoV-2 Infection: Mechanistic Insights into Current COVID-19 Therapies (Review)'. *International Journal of Molecular Medicine* 46 (2): 467. <https://doi.org/10.3892/IJMM.2020.4608>.
- Okwan-Duodu, Derick, Eun Cheon Lim, Sungyong You, and David M. Engman. 2021. 'TMPRSS2 Activity May Mediate Sex Differences in COVID-19 Severity'. *Signal Transduction and Targeted Therapy* 2021 6:1 6 (1): 1–3. <https://doi.org/10.1038/s41392-021-00513-7>.
- Olajide, Olumayokun A, Victoria U Iwuanyanwu, Izabela Lepiarz-Raba, and Alaa A Al-Hindawi. 2021. 'Induction of Exaggerated Cytokine Production in Human Peripheral Blood Mononuclear Cells by a Recombinant SARS-CoV-2 Spike Glycoprotein S1 and Its Inhibition by Dexamethasone'. *Inflammation* 44 (5). <https://doi.org/10.1007/s10753-021-01464-5>.

- Olaru, Florina, and Liselotte E. Jensen. 2010. 'Chemokine Expression by Human Keratinocyte Cell Lines after Activation of Toll-like Receptors (TLRs)'. *Experimental Dermatology* 19 (8): e314. <https://doi.org/10.1111/J.1600-0625.2009.01026.X>.
- Onabajo, Olusegun O., A. Rouf Banday, Megan L. Stanifer, Wusheng Yan, Adeola Obajemu, Deanna M. Santer, Oscar Florez-Vargas, et al. 2020. 'Interferons and Viruses Induce a Novel Truncated ACE2 Isoform and Not the Full-Length SARS-CoV-2 Receptor'. *Nature Genetics* 52 (12): 1283–93. <https://doi.org/10.1038/S41588-020-00731-9>.
- Pal, Mahendra, Gemechu Berhanu, Chaltu Desalegn, and Venkataramana Kandi. 2020. 'Severe Acute Respiratory Syndrome Coronavirus-2 (SARS-CoV-2): An Update'. *Cureus* 12 (3). <https://doi.org/10.7759/CUREUS.7423>.
- Pan, Nan, Wayne L. Frome, Richard A. Dart, Duane Tewksbury, and Jiangming Luo. 2013. 'Expression of the Renin-Angiotensin System in a Human Placental Cell Line'. *Clinical Medicine & Research* 11 (1): 1. <https://doi.org/10.3121/CMR.2012.1094>.
- Pantazi, Ioanna, Ahmed A. Al-Qahtani, Fatimah S. Alhamlan, Hani Alotheid, Sabine Matou-Nasri, George Sourvinos, Eleni Vergadi, and Christos Tsatsanis. 2021. 'SARS-CoV-2/ACE2 Interaction Suppresses IRAK-M Expression and Promotes Pro-Inflammatory Cytokine Production in Macrophages'. *Frontiers in Immunology* 12 (June): 2347. <https://doi.org/10.3389/FIMMU.2021.683800/BIBTEX>.
- Parameswaran, Narayanan, and Sonika Patial. 2010. 'Tumor Necrosis Factor- α Signaling in Macrophages'.
- Peacock, Thomas P, Daniel H Goldhill, Jie Zhou, Laury Baillon, and Rebecca Frise. n.d. 'The Furin Cleavage Site in the SARS-CoV-2 Spike Protein Is Required for Transmission in Ferrets'. Accessed 18 January 2023. <https://doi.org/10.1038/s41564-021-00908-w>.
- Peng, Jinfeng, Jiwei Sun, Jiajia Zhao, Xuliang Deng, Fengyuan Guo, and Lili Chen. 2021. 'Age and Gender Differences in ACE2 and TMPRSS2 Expressions in Oral Epithelial Cells'. *Journal of Translational Medicine* 19 (1): 1–11. <https://doi.org/10.1186/S12967-021-03037-4/FIGURES/5>.
- Petrović, Tea, Gordan Lauc, and Irena Trbojević-Akmačić. 2021. 'The Importance of Glycosylation in COVID-19 Infection'. *Advances in Experimental Medicine and Biology* 1325: 239–64. https://doi.org/10.1007/978-3-030-70115-4_12.
- Piccoli, Luca, Young Jun Park, M. Alejandra Tortorici, Nadine Czudnochowski, Alexandra C. Walls, Martina Beltramello, Chiara Silacci-Fregni, et al. 2020. 'Mapping Neutralizing and Immunodominant Sites on the SARS-CoV-2 Spike Receptor-Binding Domain by Structure-Guided High-Resolution Serology'. *Cell* 183 (4): 1024-1042.e21. <https://doi.org/10.1016/J.CELL.2020.09.037>.
- Pilz, Stefan, Verena Theiler-Schwetz, Christian Trummer, Robert Krause, and John P.A. Ioannidis. 2022. 'SARS-CoV-2 Reinfections: Overview of Efficacy and Duration of Natural and Hybrid Immunity'. *Environmental Research* 209 (June): 112911. <https://doi.org/10.1016/J.ENVRES.2022.112911>.
- Piva, Francesco, Berina Sabanovic, Monia Cecati, and Matteo Giulietti. 2021. 'Expression and Co-Expression Analyses of TMPRSS2, a Key Element in COVID-19'. *European Journal of Clinical*

Microbiology and Infectious Diseases 40 (2): 451–55. <https://doi.org/10.1007/S10096-020-04089-Y/TABLES/2>.

Pivarcsi, Andor, Laszlo Bodai, Bence Réthi, Anna Kenderessy-Szabó, Andrea Koreck, Márta Széll, Zsuzsanna Beer, et al. 2003. 'Expression and Function of Toll-like Receptors 2 and 4 in Human Keratinocytes'. *International Immunology* 15 (6): 721–30. <https://doi.org/10.1093/INTIMM/DXG068>.

Plante, Jessica A., Yang Liu, Jianying Liu, Hongjie Xia, Bryan A. Johnson, Kumari G. Lokugamage, Xianwen Zhang, et al. 2021. 'Spike Mutation D614G Alters SARS-CoV-2 Fitness'. *Nature* 592 (7852): 116–21. <https://doi.org/10.1038/S41586-020-2895-3>.

Polak, Yasmin, Robert C Speth, and Faaas Faha. 2021. 'Metabolism of Angiotensin Peptides by Angiotensin Converting Enzyme 2 (ACE2) and Analysis of the Effect of Excess Zinc on ACE2 Enzymatic Activity HHS Public Access Graphical Abstract'. *Peptides* 137: 170477. <https://doi.org/10.1016/j.peptides.2020.170477>.

Pridmore, Alison C., Gary A. Jarvis, Constance M. John, Dominic L. Jack, Steven K. Dower, and Robert C. Read. 2003. 'Activation of Toll-Like Receptor 2 (TLR2) and TLR4/MD2 by Neisseria Is Independent of Capsule and Lipooligosaccharide (LOS) Sialylation but Varies Widely among LOS from Different Strains'. *Infection and Immunity* 71 (7): 3901. <https://doi.org/10.1128/IAI.71.7.3901-3908.2003>.

Ragab, Dina, Haitham Salah Eldin, Mohamed Taeimah, Rasha Khattab, and Ramy Salem. 2020. 'The COVID-19 Cytokine Storm; What We Know So Far'. *Frontiers in Immunology* 11 (June): 1446. <https://doi.org/10.3389/FIMMU.2020.01446/BIBTEX>.

Rahbar Saadat, Yalda, Seyed Mahdi Hosseiniyan Khatibi, Sepideh Zununi Vahed, and Mohammadreza Ardalan. 2021. 'Host Serine Proteases: A Potential Targeted Therapy for COVID-19 and Influenza'. *Frontiers in Molecular Biosciences* 8 (August). <https://doi.org/10.3389/FMOLB.2021.725528>.

Ramesh, Geeta, Andrew G. Maclean, and Mario T. Philipp. 2013. 'Cytokines and Chemokines at the Crossroads of Neuroinflammation, Neurodegeneration, and Neuropathic Pain'. *Mediators of Inflammation* 2013: 20. <https://doi.org/10.1155/2013/480739>.

Ravichandran, Supriya, Elizabeth M. Coyle, Laura Klenow, Juanjie Tang, Gabrielle Grubbs, Shufeng Liu, Tony Wang, Hana Golding, and Surender Khurana. 2020. 'Antibody Signature Induced by SARS-CoV-2 Spike Protein Immunogens in Rabbits'. *Science Translational Medicine* 12 (550). <https://doi.org/10.1126/SCITRANSLMED.ABC3539>.

Redondo, Natalia, Sara Zaldívar-López, Juan J. Garrido, and Maria Montoya. 2021. 'SARS-CoV-2 Accessory Proteins in Viral Pathogenesis: Knowns and Unknowns'. *Frontiers in Immunology* 12 (July): 2698. <https://doi.org/10.3389/FIMMU.2021.708264/BIBTEX>.

Ren, Fangyuan, Hongyang Jiang, Lin Shi, Lan Zhang, Xiao Li, Qinkang Lu, and Qiang Li. 2023. '68Ga-Cyc-DX600 PET/CT in ACE2-Targeted Tumor Imaging'. *European Journal of Nuclear Medicine and Molecular Imaging*, 1. <https://doi.org/10.1007/S00259-023-06159-7>.

Ren, Wenlin, Xiaohui Ju, Mingli Gong, Jun Lan, Yanying Yu, Quanxin Long, Devin J. Kenney, et al. 2022. 'Characterization of SARS-CoV-2 Variants B.1.617.1 (Kappa), B.1.617.2 (Delta), and B.1.618 by Cell Entry and Immune Evasion'. *MBio* 13 (2). <https://doi.org/10.1128/MBIO.00099-22>.

- Rysz, Susanne, Jonathan Al-Saadi, Anna Sjöström, Maria Farm, Francesca Campoccia Jalde, Michael Plattén, Helen Eriksson, et al. 2021. 'COVID-19 Pathophysiology May Be Driven by an Imbalance in the Renin-Angiotensin-Aldosterone System'. *Nature Communications* 2021 12:1 12 (1): 1–12. <https://doi.org/10.1038/s41467-021-22713-z>.
- Saito, Akatsuki, Takashi Irie, Rigel Suzuki, Tadashi Maemura, Hesham Nasser, Keiya Uriu, Yusuke Kosugi, et al. 2021. 'SARS-CoV-2 Spike P681R Mutation, a Hallmark of the Delta Variant, Enhances Viral Fusogenicity and Pathogenicity'. *BioRxiv*, July, 2021.06.17.448820. <https://doi.org/10.1101/2021.06.17.448820>.
- Salamanna, Francesca, Melania Maglio, Maria Paola Landini, and Milena Fini. 2020. 'Body Localization of ACE-2: On the Trail of the Keyhole of SARS-CoV-2'. *Frontiers in Medicine* 7 (December): 935. <https://doi.org/10.3389/FMED.2020.594495/BIBTEX>.
- Samavati, Lobelia, and Bruce D. Uhal. 2020. 'ACE2, Much More Than Just a Receptor for SARS-CoV-2'. *Frontiers in Cellular and Infection Microbiology* 10 (June): 317. <https://doi.org/10.3389/FCIMB.2020.00317/BIBTEX>.
- Sattler, Arne, Stefan Angermair, Helena Stockmann, Katrin Moira Heim, Dmytro Khadzhynov, Sascha Treskatsch, Fabian Halleck, Martin E. Kreis, and Katja Kotsch. 2020. 'SARS-CoV-2-Specific T Cell Responses and Correlations with COVID-19 Patient Predisposition'. *The Journal of Clinical Investigation* 130 (12): 6477–89. <https://doi.org/10.1172/JCI140965>.
- Saville, James W, Dhiraj Mannar, Xing Zhu, Shanti S Srivastava, Alison M Berezuk, Jean-Philippe Demers, Steven Zhou, et al. 2022. 'Structural and Biochemical Rationale for Enhanced Spike Protein Fitness in Delta and Kappa SARS-CoV-2 Variants'. *Nature* 742. <https://doi.org/10.1038/s41467-022-28324-6>.
- Schroder, Kate, Paul J. Hertzog, Timothy Ravasi, and David A. Hume. 2004. 'Interferon- γ : An Overview of Signals, Mechanisms and Functions'. *Journal of Leukocyte Biology* 75 (2): 163–89. <https://doi.org/10.1189/JLB.0603252>.
- Shang, Jian, Gang Ye, Ke Shi, Yushun Wan, Chuming Luo, Hideki Aihara, Qibin Geng, Ashley Auerbach, and Fang Li. 2020. 'Structural Basis of Receptor Recognition by SARS-CoV-2'. *Nature* 2020 581:7807 581 (7807): 221–24. <https://doi.org/10.1038/s41586-020-2179-y>.
- Shimabukuro-Vornhagen, Alexander, Philipp Gödel, Marion Subklewe, Hans Joachim Stemmler, Hans Anton Schläßer, Max Schlaak, Matthias Kochanek, Boris Böll, and Michael S von Bergwelt-Baildon. 2018. 'Cytokine Release Syndrome'. *Journal for Immunotherapy of Cancer* 6 (56). <https://doi.org/10.1186/s40425-018-0343-9>.
- Shrestha, Lok Bahadur, Charles Foster, William Rawlinson, Nicodemus Tedla, and Rowena A. Bull. 2022. 'Evolution of the SARS-CoV-2 Omicron Variants BA.1 to BA.5: Implications for Immune Escape and Transmission'. *Reviews in Medical Virology* 32 (5): 32. <https://doi.org/10.1002/RMV.2381>.
- Silhol, François, Gabrielle Sarlon, Jean Claude Deharo, and Bernard Vaisse. 2020. 'Downregulation of ACE2 Induces Overstimulation of the Renin-Angiotensin System in COVID-19: Should We Block the Renin-Angiotensin System?' *Hypertension Research : Official Journal of the Japanese Society of Hypertension* 43 (8): 854–56. <https://doi.org/10.1038/S41440-020-0476-3>.

- South, Andrew M., Debra I. Diz, and Mark C. Chappell. 2020. 'COVID-19, ACE2, and the Cardiovascular Consequences'. *American Journal of Physiology - Heart and Circulatory Physiology* 318 (5): H1084–90.
<https://doi.org/10.1152/AJPHEART.00217.2020/ASSET/IMAGES/LARGE/ZH40052030810002.JPEG>.
- Sparks, Matthew A, Steven D Crowley, Susan B Gurley, Maria Mirotsoy, and Thomas M Coffman. 2014. 'Classical Renin-Angiotensin System in Kidney Physiology'.
<https://doi.org/10.1002/cphy.c130040>.
- Starr, Tyler N., Allison J. Greaney, Sarah K. Hilton, Daniel Ellis, Katharine H.D. Crawford, Adam S. Dingens, Mary Jane Navarro, et al. 2020. 'Deep Mutational Scanning of SARS-CoV-2 Receptor Binding Domain Reveals Constraints on Folding and ACE2 Binding'. *Cell* 182 (5): 1295-1310.e20. <https://doi.org/10.1016/J.CELL.2020.08.012>.
- Stelzer-Braid, Sacha, Gregory J. Walker, Anupriya Aggarwal, Sonia R. Isaacs, Malinna Yeang, Zin Naing, Alberto Ospina Stella, Stuart G. Turville, and William D. Rawlinson. 2020. 'Virus Isolation of Severe Acute Respiratory Syndrome Coronavirus 2 (SARS-CoV-2) for Diagnostic and Research Purposes'. *Pathology* 52 (7): 760.
<https://doi.org/10.1016/J.PATHOL.2020.09.012>.
- Sternberg, Ariane, and Cord Naujokat. 2020. 'Structural Features of Coronavirus SARS-CoV-2 Spike Protein: Targets for Vaccination'. *Life Sciences* 257 (September).
<https://doi.org/10.1016/J.LFS.2020.118056>.
- Strope, Jonathan D., Cindy H. Chau, PharmD, and William D. Figg. 2020. 'TMPRSS2: Potential Biomarker for COVID-19 Outcomes'. *The Journal of Clinical Pharmacology* 60 (7): 801–7.
<https://doi.org/10.1002/JCPH.1641>.
- Sturrock, Edward D., and K. Ravi Acharya. 2021. 'ACE Inhibitors'. *Encyclopedia of Molecular Pharmacology*, 8–17. https://doi.org/10.1007/978-3-030-57401-7_1.
- Sui, Yongjun, Jianping Li, David J. Venzon, and Jay A. Berzofsky. 2021. 'SARS-CoV-2 Spike Protein Suppresses ACE2 and Type I Interferon Expression in Primary Cells From Macaque Lung Bronchoalveolar Lavage'. *Frontiers in Immunology* 12 (June): 2061.
<https://doi.org/10.3389/FIMMU.2021.658428/BIBTEX>.
- Suzuki, Yuichiro J., and Sergiy G. Gychka. 2021. 'SARS-CoV-2 Spike Protein Elicits Cell Signaling in Human Host Cells: Implications for Possible Consequences of COVID-19 Vaccines'. *Vaccines* 9 (1): 1–8. <https://doi.org/10.3390/VACCINES9010036>.
- Tang, Yujun, Jiajia Liu, Dingyi Zhang, Zhenghao Xu, Jinjun Ji, and Chengping Wen. 2020. 'Cytokine Storm in COVID-19: The Current Evidence and Treatment Strategies'. *Frontiers in Immunology* 11 (July): 1708. <https://doi.org/10.3389/FIMMU.2020.01708/FULL>.
- Tangerås, Line H., Guro S. Stødle, Guro D. Olsen, Ann Helen Leknes, Astrid S. Gundersen, Bente Skei, Anne Jorunn Vikdal, et al. 2014. 'Functional Toll-like Receptors in Primary First-Trimester Trophoblasts'. *Journal of Reproductive Immunology* 106 (December): 89–99.
<https://doi.org/10.1016/J.JRI.2014.04.004>.
- Tchesnokova, Veronika, Hemantha Kulasekara, Lydia Larson, Victoria Bowers, Elena Rechkina, Dagmara Kisiela, Yulia Sledneva, et al. 2021. 'Acquisition of the L452R Mutation in the ACE2-Binding Interface of Spike Protein Triggers Recent Massive Expansion of SARSCoV- 2

- Variants'. *Journal of Clinical Microbiology* 59 (11). https://doi.org/10.1128/JCM.00921-21/SUPPL_FILE/JCM.00921-21-S0007.PDF.
- Temgoua, Mazou Ngou, Francky Teddy Endomba, Jan René Nkeck, Gabin Ulrich Kenfack, Joel Noutakdie Tochie, and Mickael Essouma. 2020. 'Coronavirus Disease 2019 (COVID-19) as a Multi-Systemic Disease and Its Impact in Low- and Middle-Income Countries (LMICs)'. *Sn Comprehensive Clinical Medicine* 2 (9): 1377. <https://doi.org/10.1007/S42399-020-00417-7>.
- Tian, Dandan, Yanhong Sun, Huihong Xu, and Qing Ye. 2022. 'The Emergence and Epidemic Characteristics of the Highly Mutated SARS-CoV-2 Omicron Variant'. *Journal of Medical Virology* 94 (6): 2376–83. <https://doi.org/10.1002/JMV.27643>.
- Tian, Fang, Bei Tong, Liang Sun, Shengchao Shi, Bin Zheng, Zibin Wang, Xianchi Dong, and Peng Zheng. 2021. 'N501y Mutation of Spike Protein in Sars-Cov-2 Strengthens Its Binding to Receptor Ace2'. *ELife* 10 (August). <https://doi.org/10.7554/ELIFE.69091>.
- Tobback, Els, Sophie Degroote, Sabine Buysse, Liesbeth Delesie, Lucas van Dooren, Sophie Vanherrewege, Cyril Barbezange, et al. 2022. 'Efficacy and Safety of Camostat Mesylate in Early COVID-19 Disease in an Ambulatory Setting: A Randomized Placebo-Controlled Phase II Trial'. *International Journal of Infectious Diseases : IJID : Official Publication of the International Society for Infectious Diseases* 122 (September): 628–35. <https://doi.org/10.1016/J.IJID.2022.06.054>.
- Troyano-Hernández, Paloma, Roberto Reinoso, and África Holguín. 2021. 'Evolution of SARS-CoV-2 Envelope, Membrane, Nucleocapsid, and Spike Structural Proteins from the Beginning of the Pandemic to September 2020: A Global and Regional Approach by Epidemiological Week'. <https://doi.org/10.3390/v13020243>.
- Tsujimoto, M., and J. Vilcek. 1986. 'Tumor Necrosis Factor Receptors in HeLa Cells and Their Regulation by Interferon-Gamma.' *Journal of Biological Chemistry* 261 (12): 5384–88. [https://doi.org/10.1016/S0021-9258\(19\)57227-1](https://doi.org/10.1016/S0021-9258(19)57227-1).
- Udommethaporn, Sutthirat, Tewin Tencomnao, Eileen M. McGowan, and Viroj Boonyaratanakornkit. 2016. 'Assessment of Anti-TNF- α Activities in Keratinocytes Expressing Inducible TNF- α : A Novel Tool for Anti-TNF- α Drug Screening'. *PLoS ONE* 11 (7). <https://doi.org/10.1371/JOURNAL.PONE.0159151>.
- Uhlén, Mathias, Linn Fagerberg, Bjö M. Hallström, Cecilia Lindskog, Per Oksvold, Adil Mardinoglu, Åsa Sivertsson, et al. 2015. 'Tissue-Based Map of the Human Proteome- Cell Line - ACE2'. *Science* 347 (6220). <https://doi.org/10.1126/SCIENCE.1260419>.
- Valle, Diane Marie Del, Seunghee Kim-Schulze, Hsin Hui Huang, Noam D. Beckmann, Sharon Nirenberg, Bo Wang, Yonit Lavin, et al. 2020. 'An Inflammatory Cytokine Signature Predicts COVID-19 Severity and Survival'. *Nature Medicine* 2020 26:10 26 (10): 1636–43. <https://doi.org/10.1038/s41591-020-1051-9>.
- Verdecchia, Paolo, Claudio Cavallini, Antonio Spanevello, and Fabio Angeli. 2020. 'The Pivotal Link between ACE2 Deficiency and SARS-CoV-2 Infection'. *European Journal of Internal Medicine* 76 (June): 14. <https://doi.org/10.1016/J.EJIM.2020.04.037>.
- Verghese, Michelle, Becky Jiang, Naomi Iwai, Marilyn Mar, Malaya K. Sahoo, Fumiko Yamamoto, Kenji O. Mfuh, et al. 2021. 'A Sars-Cov-2 Variant with L452r and E484q Neutralization Resistance Mutations'. *Journal of Clinical Microbiology* 59 (7).

<https://doi.org/10.1128/JCM.00741-21/ASSET/B885F1C1-167B-41DB-B209-8E4B38E2C272/ASSETS/IMAGES/LARGE/JCM.00741-21-F0001.JPG>.

- Verma, Jyoti, and Naidu Subbarao. 2021. 'A Comparative Study of Human Betacoronavirus Spike Proteins: Structure, Function and Therapeutics'. *Archives of Virology* 166 (3): 697–714. <https://doi.org/10.1007/S00705-021-04961-Y/TABLES/2>.
- Viveiros, Anissa, Jaslyn Rasmuson, Jennie Vu, Sharon L. Mulvagh, Cindy Y.Y. Yip, Colleen M. Norris, and Gavin Y. Oudit. 2021. 'Sex Differences in COVID-19: Candidate Pathways, Genetics of ACE2, and Sex Hormones'. *American Journal of Physiology - Heart and Circulatory Physiology* 320 (1): H296–304. <https://doi.org/10.1152/AJPHEART.00755.2020/ASSET/IMAGES/LARGE/AJ-AHRT200091F004.JPEG>.
- Wang, Lin-Fa, Chee Wah Tan, Wan Ni Chia, Feng Zhu, Barnaby Young, Napaporn Chantasrisawad, Shi-Hsia Hwa, et al. 2022. 'Differential Escape of Neutralizing Antibodies by SARS-CoV-2 Omicron and Pre-Emergent Sarbecoviruses'. *Research Square*, February. <https://doi.org/10.21203/RS.3.RS-1362541/V1>.
- Wang, Mei Yue, Rong Zhao, Li Juan Gao, Xue Fei Gao, De Ping Wang, and Ji Min Cao. 2020. 'SARS-CoV-2: Structure, Biology, and Structure-Based Therapeutics Development'. *Frontiers in Cellular and Infection Microbiology* 10 (November): 724. <https://doi.org/10.3389/FCIMB.2020.587269/TEXT>.
- Wang, Shunxin, Feng Guo, Kangtai Liu, Hongliang Wang, Shuan Rao, Peng Yang, and Chengyu Jiang. 2008. 'Endocytosis of the Receptor-Binding Domain of SARS-CoV Spike Protein Together with Virus Receptor ACE2'. *Virus Research* 136 (1): 8. <https://doi.org/10.1016/J.VIRUSRES.2008.03.004>.
- Wang, Y., K. G. Pringle, Y. X. Chen, T. Zakar, and E. R. Lumbers. 2012. 'Regulation of the Renin-Angiotensin System (RAS) in BeWo and HTR-8/SVneo Trophoblast Cell Lines'. *Placenta* 33 (8): 634–39. <https://doi.org/10.1016/J.PLACENTA.2012.05.001>.
- Wang, Yingjie, Meiyi Liu, and Jiali Gao. 2020. 'Enhanced Receptor Binding of SARS-CoV-2 through Networks of Hydrogen-Bonding and Hydrophobic Interactions'. *Proceedings of the National Academy of Sciences of the United States of America* 117 (25): 13967–74. https://doi.org/10.1073/PNAS.2008209117/SUPPL_FILE/PNAS.2008209117.SD02.TXT.
- Ward-Kavanagh, Lindsay K., Wai Wai Lin, John R. Šedý, and Carl F. Ware. 2016. 'The TNF Receptor Superfamily in Costimulating and Coinhibitory Responses'. *Immunity* 44 (5): 1005. <https://doi.org/10.1016/J.IMMUNI.2016.04.019>.
- Watanabe, Yasunori, Joel D. Allen, Daniel Wrapp, Jason S. McLellan, and Max Crispin. 2020. 'Site-Specific Glycan Analysis of the SARS-CoV-2 Spike'. *Science (New York, N.y.)* 369 (6501): 330. <https://doi.org/10.1126/SCIENCE.ABB9983>.
- WHO. 2023a. 'Tracking SARS-CoV-2 Variants'. World Health Organization SARS-CoV-2 . 15 March 2023. <https://www.who.int/activities/tracking-SARS-CoV-2-variants>.
- WHO. 2023b. 'Weekly Epidemiological Update on COVID-19 - 22 March 2023'. Weekly Epidemiological Update on COVID-19. 22 March 2023. <https://www.who.int/publications/m/item/weekly-epidemiological-update-on-covid-19---22-march-2023>.

- Winstone, Helena, Maria Jose Lista, Alisha C. Reid, Clement Bouton, Suzanne Pickering, Rui Pedro Galao, Claire Kerridge, Katie J. Doores, Chad M. Swanson, and Stuart J. D. Neil. 2021. 'The Polybasic Cleavage Site in SARS-CoV-2 Spike Modulates Viral Sensitivity to Type I Interferon and IFITM2'. *Journal of Virology* 95 (9). <https://doi.org/10.1128/JVI.02422-20>.
- Wise, Jacqui. 2021. 'Covid-19: The E484K Mutation and the Risks It Poses'. *BMJ (Clinical Research Ed.)* 372 (February): n359. <https://doi.org/10.1136/BMJ.N359>.
- Wong, Marty K.S. 2016. 'Angiotensin Converting Enzymes'. *Handbook of Hormones*, 263. <https://doi.org/10.1016/B978-0-12-801028-0.00254-3>.
- Wu, Jing, Yuheng Shi, Xiaoyan Pan, Shuang Wu, Ruixia Hou, Yong Zhang, Tiansheng Zhong, et al. 2021. 'SARS-CoV-2 ORF9b Inhibits RIG-I-MAVS Antiviral Signaling by Interrupting K63-Linked Ubiquitination of NEMO'. *Cell Reports* 34 (7). <https://doi.org/10.1016/J.CELREP.2021.108761>.
- Xiang, Yan, Christian Cambillau, Dimitrios P Vlachakis, Giuseppina Mariano, Julien R C Bergeron, Rebecca J Farthing, and Shamar L M Lale-Farjat. 2020. 'Structural Characterization of SARS-CoV-2: Where We Are, and Where We Need to Be'. <https://doi.org/10.3389/fmolb.2020.605236>.
- Xu, Jiabao, Shizhe Zhao, Tieshan Teng, Abualgasim Elgaili Abdalla, Wan Zhu, Longxiang Xie, Yunlong Wang, and Xiangqian Guo. 2020. 'Systematic Comparison of Two Animal-to-Human Transmitted Human Coronaviruses: SARS-CoV-2 and SARS-CoV'. *Viruses* 12 (2). <https://doi.org/10.3390/V12020244>.
- Xu, Zepeng, Kefang Liu, and George F. Gao. 2022. 'Omicron Variant of SARS-CoV-2 Imposes a New Challenge for the Global Public Health'. *Biosafety and Health* 4 (3): 147. <https://doi.org/10.1016/J.BSHEAL.2022.01.002>.
- Xu, Zhe, Lei Shi, Yijin Wang, Jiyuan Zhang, Lei Huang, Chao Zhang, Shuhong Liu, et al. 2020. 'Pathological Findings of COVID-19 Associated with Acute Respiratory Distress Syndrome'. *The Lancet Respiratory Medicine* 8 (4): 420–22. [https://doi.org/10.1016/S2213-2600\(20\)30076-X](https://doi.org/10.1016/S2213-2600(20)30076-X).
- Xue, Xiaotong, Zihao Mi, Zhenzhen Wang, Zheng Pang, Hong Liu, and Furen Zhang. 2021. 'High Expression of ACE2 on Keratinocytes Reveals Skin as a Potential Target for SARS-CoV-2'. *The Journal of Investigative Dermatology* 141 (1): 206-209.e1. <https://doi.org/10.1016/J.JID.2020.05.087>.
- Yalcin, Huseyin C., Vijayakumar Sukumaran, Mahmoud Khatib A.A. Al-Ruweidi, and Samar Shurbaji. 2021. 'Do Changes in ACE-2 Expression Affect SARS-CoV-2 Virulence and Related Complications: A Closer Look into Membrane-Bound and Soluble Forms'. *International Journal of Molecular Sciences* 22 (13). <https://doi.org/10.3390/IJMS22136703>.
- Yi, Chunyan, Xiaoyu Sun, Jing Ye, Longfei Ding, Meiqin Liu, Zhuo Yang, Xiao Lu, et al. 2020. 'Key Residues of the Receptor Binding Motif in the Spike Protein of SARS-CoV-2 That Interact with ACE2 and Neutralizing Antibodies'. *Cellular & Molecular Immunology*. <https://doi.org/10.1038/s41423-020-0458-z>.
- Yurkovetskiy, Leonid, Xue Wang, Kristen E. Pascal, Christopher Tomkins-Tinch, Thomas P. Nyalile, Yetao Wang, Alina Baum, et al. 2020. 'Structural and Functional Analysis of the D614G SARS-

- CoV-2 Spike Protein Variant'. *Cell* 183 (3): 739-751.e8.
<https://doi.org/10.1016/J.CELL.2020.09.032>.
- Zaim, Sevim, Jun Heng Chong, Vissagan Sankaranarayanan, and Amer Harky. 2020. 'COVID-19 and Multiorgan Response'. *Current Problems in Cardiology* 45 (8).
<https://doi.org/10.1016/J.CPCARDIOL.2020.100618>.
- Zhang, Jun, Yongfei Cai, Christy L. Lavine, Hanqin Peng, Haisun Zhu, Krishna Anand, Pei Tong, et al. 2022. 'Structural and Functional Impact by SARS-CoV-2 Omicron Spike Mutations'. *Cell Reports* 39 (4). <https://doi.org/10.1016/J.CELREP.2022.110729>.
- Zhang, Jun, Tianshu Xiao, Yongfei Cai, and Bing Chen. 2021. 'Structure of SARS-CoV-2 Spike Protein'. *Current Opinion in Virology* 50 (September): 173–82.
<https://doi.org/10.1016/j.coviro.2021.08.010>.
- Zhang, Lingbing, Yandan Zhang, Xia Qin, Xuejun Jiang, Jun Zhang, Lejiao Mao, Ziqi Jiang, et al. 2022. 'Recombinant ACE2 Protein Protects against Acute Lung Injury Induced by SARS-CoV-2 Spike RBD Protein'. *Critical Care* 26 (1): 1–22. <https://doi.org/10.1186/S13054-022-04034-9/FIGURES/10>.
- Zhao, Miao Miao, Wei Li Yang, Fang Yuan Yang, Li Zhang, Wei Jin Huang, Wei Hou, Chang Fa Fan, et al. 2021. 'Cathepsin L Plays a Key Role in SARS-CoV-2 Infection in Humans and Humanized Mice and Is a Promising Target for New Drug Development'. *Signal Transduction and Targeted Therapy* 2021 6:1 6 (1): 1–12. <https://doi.org/10.1038/s41392-021-00558-8>.
- Zhou, Peng, Xing Lou Yang, Xian Guang Wang, Ben Hu, Lei Zhang, Wei Zhang, Hao Rui Si, et al. 2020. 'A Pneumonia Outbreak Associated with a New Coronavirus of Probable Bat Origin'. *Nature* 2020 579:7798 579 (7798): 270–73. <https://doi.org/10.1038/s41586-020-2012-7>.
- Zhou, Ye, Mu Wang, Yunhui Li, Peihui Wang, Ping Zhao, Zixuan Yang, Suyuan Wang, et al. 2021. 'SARS-CoV-2 Spike Protein Enhances ACE2 Expression via Facilitating Interferon Effects in Bronchial Epithelium'. *Immunology Letters* 237 (September): 33–41.
<https://doi.org/10.1016/J.IMLET.2021.06.008>.
- Ziegler, Carly G.K., Samuel J. Allon, Sarah K. Nyquist, Ian M. Mbano, Vincent N. Miao, Constantine N. Tzouanas, Yuming Cao, et al. 2020. 'SARS-CoV-2 Receptor ACE2 Is an Interferon-Stimulated Gene in Human Airway Epithelial Cells and Is Detected in Specific Cell Subsets across Tissues'. *Cell* 181 (5): 1016-1035.e19. <https://doi.org/10.1016/J.CELL.2020.04.035>.